SYNTHESIS, CHARACTERIZATION, AND EVALUATION OF NEW REACTIVE TWO-PHOTON ABSORBING DYES FOR TWO-PHOTON EXCITED FLUORESCENCE IMAGING APPLICATIONS

by

KATHERINE J. SCHAFER
B.S. University of Detroit Mercy, 1997
M.S. University of Central Florida, 1999

A dissertation submitted in partial fulfillment of the requirements
for the degree of Doctor of Philosophy
in the Burnett College of Biomedical Sciences
at the University of Central Florida
Orlando, Florida

Summer Term
2005

Major Professor: Kevin D. Belfield

ABSTRACT

Recent, cooperative advances in chemistry, biology, computing, photophysics, optics, and microelectronics have resulted in extraordinary developments in the biological sciences, resulting in the emergence of a novel area termed 'biophotonics'. The integrative and interdisciplinary nature of biophotonics cuts across virtually all disciplines, extending the frontiers of basic cellular, molecular, and biology research through the clinical and pharmaceutical industries. This holds true for the development and application of the novel imaging modality utilizing multiphoton absorption and its extraordinary contribution to recent advances in bioimaging. Intimately involved in the revolution of nonlinear bioimaging has been the development of optical probes for probing biological function and activity.

The focus of this dissertation is in the area of probe development, particularly conjugated organic probes, optimized for efficient two-photon absorption followed by upconverted fluorescence for nonlinear, multiphoton bioimaging applications. Specifically, π-conjugated fluorene molecules, with enhanced two-photon absorbing (2PA) properties and high photostability, were prepared and characterized. Contemporary synthetic methods were utilized to prepare target fluorene derivatives expected to be highly fluorescent for fluorescence imaging, and, in particular, exhibit high two-photon absorptivity suitable for two-photon excitation (2PE) fluorescence microscopy. The flexibility afforded through synthetic manipulation to integrate hydrophilic moieties into the fluorophore architecture to enhance compatibility with aqueous systems, more native to biological samples, was attempted. Incorporation of functional groups

for direct covalent attachment onto target biomolecules was also pursued to prepare fluorene derivatives as efficient 2PA reactive probes.

Linear and two-photon spectroscopic characterizations on these novel compounds reveal they exhibit high 2PA cross-sections on the order of ~100 GM units, nearly an order of magnitude greater than typical, commonly used fluorophores utilized in nonlinear, multiphoton microscopy imaging of biological samples. Photostability studies of representative fluorene derivatives investigated and quantified indicate these derivatives are photostable under one- and two-photon excitation conditions, with photodecomposition quantum yields on the order of 10^{-5}. Preliminary cytotoxicity studies indicate these fluorene derivatives exhibit minimal cytotoxic effects on proliferating cells. Finally, their ultimate utility as high-performance, 2PA fluorescent probes in 2PE fluorescence microscopy imaging of biological samples was demonstrated in both fixed and live cells. Due to the low cytotoxicity, high photostability, efficient 2PA, and high fluorescence quantum yield, the probes were found suitable for relatively long-term, two-photon fluorescence imaging of live cells, representing a significant advance in biophotonics.

PUBLICATIONS TO DATE FROM DISSERTATION WORK

1. Schafer, K. J.; Belfield, K. D.; Yao. S.; Frederiksen, P. K.; Hales. J. M.; Kolattukudy, P. E. "Fluorene-based fluorescent probes with high two-photon action cross-sections for biological multiphoton imaging applications" *Journal of Biomedical Optics* **2005**, in press.

2. Belfield, K. D.; Bondar, M. V.; Hales, J. M.; Morales, A. R.; Przhonska, O. V.; Schafer, K. J. "One- and two-photon fluorescence anisotropy of fluorene derivatives," *Journal of Fluorescence* **2005**, *15(1)*, 3-11.

3. Belfield, K. D.; Bondar, M. V.; Hernandez, F. E.; Morales, A. R.; Przhonska, O. V.; Schafer, K. J. "Nonlinear transmission and excited-state absorption in fluorene derivatives" *Applied Optics* **2005**, in press.

4. Belfield, K. D.; Bondar, M. V.; Przhonska, O. V.; Schafer, K. J. "Photostability of a series of two-photon absorbing fluorene derivatives" *Journal of Photochemistry and Photobiology A: Chemistry* **2004**, *162*, 489-496.

5. Belfield, K. D.; Bondar, M. V.; Przhonska, O. V.; Schafer, K. J. "Photochemical properties of (7-benzothiazol-2-yl-9,9-didecylfluoren-2-yl)diphenylamine under one- and two-photon excitation" *Journal of Photochemistry and Photobiology A: Chemistry* **2004**, *162,* 569-574.

6. Belfield, K. D.; Bondar, M. V.; Przhonska, O. V.; Schafer, K. J. "One- and two-photon photostability of 9,9-didecyl-2,7-bis-(N,N-diphenylamino)fluorene" *Photochemical and Photobiological Sciences* **2004**, 3, 138-141.

7. Schafer, K. J.; Belfield, K. D.; Yao, S.; Hales, J. M.; Hagan, D. J.; Van Stryland, E. W. "Fluorescent dyes for multiphoton bio-imaging applications" *Proc. SPIE - Int. Soc. Opt. Eng.,* **2004**, *5329*, 201-206.

8. Belfield, K. D.; Schafer, K. J.; Yao, S.; Hales, J. M.; Hagan, D. J.; Van Stryland, E. W. "Reactive two-photon fluorescent probes for biological imaging" *Proc. SPIE - Int. Soc. Opt. Eng.,* **2004**, *5211*, 91-95.

9. Hales, J. M.; Hagan, D. J.; Van Stryland, E. W.; Schafer, K. J.; Morales, A. R.; Belfield, K. D.; Pacher, P.; Kwon, O.; Zojer, E.; Bredas, J.-L. "Resonant Enhancement of Two-Photon Absorption in Substituted Fluorene Molecules" *Journal of Chemical Physics* **2004**, *121 (7)*, 3152-3160.

10. Hernandez, F. E.; Belfield, K. D.; Cohanoschi, I.; Balu, M.; Schafer, K. J. "Three and four-photon absorption of a multiphoton absorbing fluorescent probe" *Applied Optics* **2004**, *43 (28)*, 5394-5398.

This is to my family, especially my husband Joel, who have provided me with years of support, encouragement, and unquestionable love.

ACKNOWLEDGMENTS

I would like to thank my advisor, Dr. Kevin D. Belfield, for providing a great opportunity and environment that made this dissertation possible. His support and guidance was steadfast and purposeful over the years, and I am genuinely grateful for his dedication to excellence and persistence.

This dissertation was the result of a truly interdisciplinary and collaborative effort. I want to express my sincere thanks to Mihaela Balu and Jie Fu of Dr. David J. Hagan's and Dr. Eric Van Stryland's nonlinear optics laboratory for their experimental work on the two-photon absorption measurements. I am deeply indebted to Dr. Pappachan E. Kolattukudy for his encouragement and generous accommodations into his laboratory to perform the cell culture and fixation for the microscopy imaging. I also appreciate and thank Dr. Kiminobu Sugaya and his students, Monowar Hussain and Manny Vrotsos, for their interests and efforts on the live-cell microscopy imaging. All the collaborations have truly been rewarding and contributed to the interdisciplinary nature of this work.

I wish to thank members of Dr. Belfield's research group whom I have had the pleasure of knowing and working with throughout the years. In particular, Dr. Mykhailo Bondar became a great mentor and a wonderful example of dedication and commitment to quality work. He has been inspirational and I am truly fortunate to have made his good acquaintance. I also thank Dr. Peter K. Frederiksen for his efforts on refining the home-built two-photon laser scanning microscope system and imaging, and Dr. Sheng Yao for his comaraderie in synthesis, as well as all the Belfield laboratory members I have known over the years.

Finally, I thank Catherine Hartmann, who has always provided unselfish support and have always been a good friend.

TABLE OF CONTENTS

LIST OF FIGURES

LIST OF SCHEMES

LIST OF TABLES

LIST OF ACRONYMS/ABBREVIATIONS

λ_o	Starting wavelength
λ_{max}	Wavelength of maximum absorption
δ	ppm or 2PA cross section
2PA	Two-photon absorption
3PA	Three-photon absorption
AcOH	Acetic acid
A-D-A	Acceptor-donor-acceptor
A-π-A	Acceptor-π-acceptor
Anal.	Analysis
Ar	Argon or aromatic system
bp	Boiling point
^{13}C	Carbon 13 isotope
Calcd.	Calculated
$CDCl_3$	Deuterated chloroform
cm^{-1}	Wavenumber
d	Doublet
D-A-D	Donor-acceptor-donor
D-π-A	Donor-π-acceptor
EI	Electron impact
eV	Electron volt

fs	Femtosecond (10^{-15} s)
g	Gram
GM	Goppert-Mayer unit for the 2PA cross-section (1 x 10^{-50} cm^4 s $photon^{-1}molecule^{-1}$)
h	Hour
IR	Infrared
L	Liter
lit.	Literature value
m	Multiplet
MHz	Megahertz (10^6 Hz)
min	Minute
mL	Milliliter (10^{-3} L)
mmHg	Millimeters of mercury
mmol	Millimoles (10^{-3} moles)
mp	Melting point
MS	Mass spectrum
NLO	Nonlinear optical
nm	Nanometer (10^{-9} m)
NMR	Nuclear magnetic resonance
ppm	Parts per million
s	Seconds or singlet
t	Triplet
TLC	Thin layer chromotography

TMS	Tetramethylsilane
UV	Ultraviolet
wt%	Weight percent

CHAPTER 1: INTRODUCTION

Advances in scientific technology and development often occur at interfaces of seemingly disparate disciplines. Recent, cooperative advances in chemistry, biology, computing, photophysics, optics, and microelectronics have resulted in extraordinary developments in the biological sciences, resulting in the emergence of a novel area termed 'biophotonics'. The integrative and interdisciplinary nature of biophotonics cuts across virtually all disciplines, extending the frontiers of basic cellular, molecular, and biology research through the clinical and pharmaceutical industries. This holds true for the development and application of the novel imaging modality utilizing multiphoton absorption.

This chapter will introduce the phenomenal concept of a particular nonlinearity known as two-photon absorption, and its extraordinary contribution to recent advances in bioimaging. Intimately involved in the revolution of nonlinear bioimaging has been the development of optical probes for probing biological function and activity. The focus of this dissertation is in this area of probe development, particularly conjugated organic probes, optimized for efficient two-photon absorption followed by upconverted fluorescence for nonlinear, multiphoton bioimaging applications. Section 1.1 begins with a brief account of the development of two-photon absorption and two-photon excited fluorescence, with a discussion of the unique and salient features associated with this process. How this process is exploited, particularly in the application of two-photon excited fluorescence bioimaging, will be presented. Section 1.2 provides the dissertation statement and the concluding section provides an outline for this work.

1.1 Background and Significance

The theoretical concept of two-photon absorption (2PA) was first proposed by physicist Maria Göppert-Mayer in 1931 [1]. The seminal paper described this process as the near simultaneous absorption of two photons to achieve a real transition within an atom or a molecule. Neither photon has sufficient energy to complete this transition on its own but if the sum of the combined photon energies involved is equivalent to the energy difference between the initial and final states, the completion of that transition would be possible. Hence, organic molecules can be excited into transitions upon absorption of two photons whose combined energies match those for single-photon excitation of the same transition. The photons do not necessarily need to be of the same energy (nondegenerate 2PA), and typically, nonlinear, multiphoton microscopy imaging employs two photons of the same energy (degenerate 2PA).

The absorption of two photons to induce a transition, equivalently performed by single photon absorption, requires both of their absorption to be within ~10^{-15} seconds from each other [14b]. This 'near simultaneous' nonlinear absorption process requires a large photon density to produce any appreciable probability for 2PA induced transition to occur. Hence, it was not until after the invention of the laser that the experimental observation of 2PA was demonstrated by Kaiser and Garret in a $CaF_2:Eu^{2+}$ crystal [2], some 30 years after the theoretical description of 2PA. Tremendous developments and subsequent commercialization of high peak-power, tunable laser sources have generated new applications exploiting the principles of two-photon absorption, predominantly by the fields of chemistry and physics [3,4,5]. Only recently, with the invention of the two-photon laser scanning microscope system (also called two-photon excitation (2PE)

fluorescence microscopy) in 1990, have the biological sciences embraced multiphoton excitation to image live cells [6]. Since then, biological uses of multiphoton microscopy have been pervasive and persistent, and highlights of its use have been reviewed [7].

Biological applications based upon 2PA reside upon two salient features of this nonlinear process. As mentioned above, the probability of 2PA correlates with high photon density, or high intensity radiation. For one-photon absorption (1PA), the likelihood of absorption depends linearly on the excitation irradiance, I., while the rate of 2PA is quadratically dependent upon I. This nonlinear dependence ensures high spatial selectivity when an intense laser beam is focused into a two-photon absorbing medium. Practically, this means 2PA occur only the focal volume, where there is sufficiently high photon density, and the probability of 2PA falls off rapidly away from this point, providing the optical-sectioning (confocality) ability of multiphoton imaging. For a fluorescent molecule, the resulting fluorescence emission upon 2PA (and consequently, two-photon excitation (2PE) of the absorbing area) is then proportional to I^2, and fluorescence is practically localized to the focal spot, and unlike in 1PA, there is essentially no out-of-focus light to reject. This is pictorially represented in Figure 1.1, with a focused laser beam demonstrating 1PA and 2PA into a fluorescent medium.

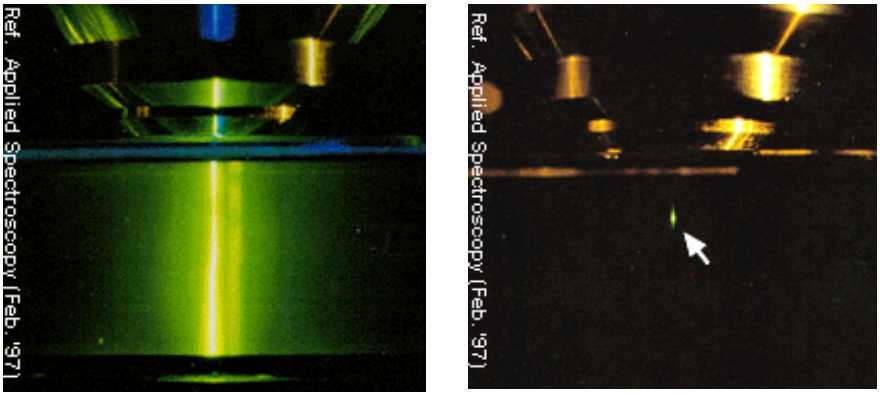

A. 1PE **B.** 2PE

Figure 1.1 Photographs demonstrating the spatial selectivity of one-photon excitation (A) versus two-photon excitation (B) in a fluorescent solution.

Due to the highly localized excitation obtained in 2PA, some major advantages accrue, mainly that photobleaching of precious fluorophores are minimized as are photodamaging/phototoxic effects on living specimens. Additionally, two-photon excitation spectra of many organic fluorophores are much broader than for one-photon excitation, so multiple fluorophores with distinct emission wavelengths may result from a single multiphoton excitation wavelength [8]. Finally, the highly confined nature of 2PE also confines any physical or chemical reactions activated by 2PA to a three-dimensional volume, essentially the same as the focal volume. Hence, highly localized photo-induced chemical reactions as site-specific photodynamic cancer therapy [9] and photoinduced uncaging of bioeffector molecules [10], in addition to nonlinear spectroscopy-based bioimaging, are among emerging technologies which exploit this nonlinear absorption effect.

The second feature of 2PA is the employment of near-infrared (near-IR) excitation wavelengths, typically in the range of ~ 700-1000 nm, provided by tunable femtosecond (fs) laser systems. This excitation range coincides particularly well with the

decreasing absorption range of biological tissues to longer wavelengths of light, shown in Figure 1.2. In the ultraviolet (UV), the absorption increases with shorter wavelength due primarily to proteins and DNA. The existence of the "optical window" [11] between ~ 600-1300 nm, coupled with the use of longer excitation wavelengths, offers greater penetration depths into highly scattering biomaterials than the equivalent blue light used for 1PE [7]. Finally, near-IR light causes negligible photodamage to fluorophores and phototoxicity to live cells, relative to higher energy ultraviolet wavelengths.

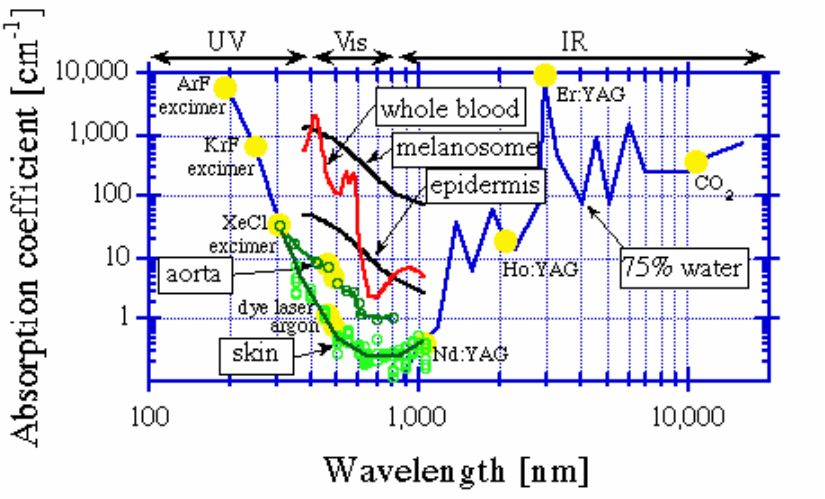

Figure 1.2 Primary absorption spectra of biological tissues along with their absorption coefficients at some common laser wavelengths [11].

Multiphoton absorption/excitation is relatively new in the biological sciences and one can expect developments to improve its utility and overcome some existing shortcomings. Aside from improvements expected from contributing areas of physical optics, computing, and microelectronics, the development and introduction of fluorescent compounds that possess enhanced nonlinearities is an essential area for advancing the utility of two- and multiphoton absorption processes in the biological sciences. In

particular, compounds which exhibit large two-photon absorptivities can reduce the tolerances on devices employing 2PA by increasing their sensitivity. This would allow one to reduce the intensity of the excitation source thereby minimizing the possibility of optical damage to the irradiation area.

Organic molecules are promising candidates as efficient compounds possessing enhanced two-photon absorptivities. Sophisticated synthetic methods of probe development has progressed to a level where hundreds of light-emitting molecules exist to probe the inter- and intracellular activities of living cells and organisms. However, current use of common fluorophores for 2PE fluorescence imaging depends largely on optical properties more suitable for one-photon excitation. Furthermore, only a very limited number of commonly used fluorophores have been spectroscopically characterized to yield their two-photon absorptivities [8], and they exhibit woefully unoptimized optical properties for nonlinear excitation. The lack of knowledge of two-photon absorption cross-sections (δ) and two-photon excitation spectra for fluorophores used in biological studies has been a significant obstacle to the use of 2PE fluorescence microscopy. As such, organic molecules may be synthetically manipulated such that their optical properties may be tailored to possess enhanced nonlinear optical (NLO) properties. Additionally, most commercially available fluorescent probes have limited photostability, often undergoing photobleaching during bright-field and confocal fluorescence microscopic imaging. This is an extremely important aspect for two-photon fluorescent probes, particularly in consideration of the high irradiance necessary for multiphoton excitation. It is expected that novel organic compounds designed with

optimized 2PA properties will likely improve the utility of multiphoton microscopy for the biological sciences.

1.2 Dissertation Statement

The purpose of this dissertation is to prepare π-conjugated fluorene molecules with enhanced 2PA properties and high photostability for nonlinear bioimaging applications. Choice of target structures was based upon extensive NLO studies performed on a series of fluorene molecules whose chemical structures have been systematically altered [12,33]. Independent NLO characterization methods were used to correlate variation of chemical structure to the strength and location of their 2PA spectra and determine whether the π-conjugated fluorene derivatives possess desirable 2PA properties. Contemporary synthetic methods will be utilized to prepare fluorene derivatives expected to be highly fluorescent for fluorescence imaging, and, in particular, exhibit high two-photon absorptivity suitable for 2PE fluorescence microscopy. The flexibility afforded from synthetic manipulation will attempt to integrate hydrophilic moieties into the fluorophore architecture to enhance compatibility with aqueous systems, more native to biological samples. Incorporation of functional groups for direct covalent attachment onto target biomolecules will be pursued to prepare fluorene derivatives as efficient 2PA reactive probes. Linear and two-photon spectroscopic characterization of these novel compounds will be performed and facilitate assessment of their optical nonlinearities. Photostability studies of representative fluorene derivatives will be investigated and quantified. Finally, their utility as high-performance 2PA fluorophores

for 2PE fluorescence microscopy imaging of biological samples under *in vitro* conditions will be demonstrated.

1.3 Dissertation Outline

This work is structured as follows: The concept of two-photon absorption and some motivation for optical probe design for 2PE bioimaging is introduced in the first Chapter. A summary of the current status of optical probe development tailored for 2PE is presented in Chapter 2. The chapter will also highlight key properties of fluorene derivatives studied to date, providing the case of these derivatives as promising candidates for 2PE applications. This will lead into Chapter 3, which provides details of the synthetic methods used to prepare target fluorene derivatives with enhanced hydrophilic properties more amenable for biological systems. Characterization details to unambiguously confirm their structure are also included in this Chapter. The linear and two-photon absorption properties of the prepared compounds will be presented in Chapter 4, followed by additional spectroscopic studies on their photostability under one- and two-photon excitation in Chapter 5. Preliminary cytotoxicity studies indicate fluorene derivatives exhibit minimal cytotoxic effects on proliferating cells and their utility as high-performance, 2PA fluorescent probes in 2PE fluorescence microscopy imaging of biological samples is presented in Chapter 6. Finally, Chapter 7 provides a synopsis of results and suggests some future directions which might be taken to refine fluorene derivatives as efficient 2PA fluorescent probes compatible with living biological systems.

CHAPTER 2: BACKGROUND

The development of the two-photon laser scanning microscope (2PLSM) [6] has propelled this novel imaging modality as one of the fastest growing techniques in biological imaging. Since the first demonstration of the 2PLSM in 1990, much progress has been made in identifying important fundamental parameters and addressing technological problems to create effective instrumentation of 2PLSM systems. Comprehensive reviews on the physical principles underlying two- and multiphoton microscopy are described by those intent on exploring and developing nonlinear microscopy to its full potential [7a,13] particularly for multi-dimensional (x, y, z, time, emission wavelength, and intensity) imaging of biological samples.

Hence, this chapter will only focus on pertinent details of fluorescent optical probes used for 2PE, predominantly concentrating on organic compounds. Section 2.1 defines relevant optical parameters of 2PA compounds and presents relative magnitudes of the two-photon absorptivities of commonly used fluorophores for nonlinear bioimaging. Section 2.2 presents a summary of the current state-of-the-art status on optical probe development tailored for 2PE bioimaging and how their NLO properties compare to the common fluorophores presented in the previous section. Indication of some of their shortcomings for bioimaging will also be discussed. The final section introduces the fluorene derivatives along with highlights of their two-photon absorption properties. A summary of the extensive NLO data collected on these π-conjugated compounds will be presented, based upon which the impetus for continual development of fluorene derivatives as efficient 2PA fluorophores for 2PE microscopy bioimaging is proposed.

2.1 General Optical Properties of 2PA Fluorophores

The criteria for choosing or designing fluorophores for 2PLSM are essentially the same as for any fluorophore used for conventional imaging. They should possess a large absorption cross-section at convenient excitation wavelengths, have a high fluorescence quantum yield, low rate of photobleaching, and minimal chemical or photochemical toxicity to living cells. The common practice in 2PLSM has been to use fluorophores that have proven useful under epi-fluorescence or conventional confocal laser scanning microscopy (both using one-photon excitation) conditions. In many cases, two-photon excitation of these conventional (usually commercially available) fluorophores has sufficed, and in some cases, 2PE fluorescence corresponding to twice the energy of their one-photon absorption wavelengths was possible. However, this "twice wavelength" rule should be regarded as only a rough approximation because one- and two-photon absorption processes have different quantum mechanical selection rules [14]. For centrosymmetric molecules, a transition allowed for one-photon absorption is strictly forbidden for two-photon absorption and vice versa. Such a strict exclusion does not necessarily apply to larger, more complex molecules where their molecular symmetries are relaxed. Moreover, theoretical calculations to determine two-photon absorption cross-sections (δ) for complex molecules are extremely difficult, as are the experimental measurements to determine absolute absorptivities [14,15]. The two-photon absorption cross-section is a measure of the strength of 2PA by a molecule (a more detailed description of the δ parameter as well as factors contributing to this nonlinear process can be found in references 12, 14, and 15). Two-photon absorption cross-section values are often expressed in units of 1×10^{-50} cm^4 sec $molecule^{-1}$ $photon^{-1}$, where this absorptivity

value is known as 1 Göppert-Mayer (GM) unit, in honor of the pioneering contributions of Maria Göppert-Mayer in describing and predicting the two-photon absorption phenomenon.

The problem remains then, that knowledge of the one-photon excitation spectra does not necessarily allow quantitative predictions of the two-photon excitation spectra of complex molecules, as many optical probes used for fluorescence imaging are. However, for molecules that are fluorescent, whose fluorescence quantum yields (η) are known, the two-photon cross-section can be determined by detecting their emitted fluorescence photons generated by 2PA [8a]. Hence, measurements of the two-photon excitation spectra where the fluorescence from the compound to be studied is compared, using the same experimental setup, to that from a compound with a known excitation cross-section, allows for determination of the compound's two-photon absorption cross-section. The values obtained from the two-photon fluorescence signal is termed the two-photon *action* cross-section and is the product of the 2PA cross-section δ and the fluorescence quantum efficiency η, of the fluorophore ($\delta_{2PF} = \eta\delta$). The fluorescence quantum efficiency (or quantum yield, η) is a measure of the "efficiency" of fluorescence (for an excellent discussion on fluorescence spectroscopy, see reference [16]), which can be calculated absolutely, from measurements of fluorescence intensity, or relatively, by comparison with standard compounds of known quantum yield. It is defined as a ratio of the number of photons emitted to the number of photons absorbed, and values range from unity (1) indicating 100% efficiency for highly fluorescent compounds, to zero for compounds that are essentially nonfluorescent. It is intuitive then, that efficient fluorophores for two-photon excited fluorescence imaging should exhibit high two-photon absorption cross-

sections *and* high fluorescence quantum yield, preferably coinciding with the output of the tunability range of Ti:sapphire lasers.

Using the two-photon fluorescence excitation method, the 2PE spectra and absolute δ values for several commonly used organic fluorophores and some green fluorescent proteins (GFPs), excited in the Ti:sapphire tuning range, was compiled to provide a reliable database for the selection of appropriate fluorophores for 2PLSM [8]. The maximum two-photon absorptivity values of some common fluorophores that were measured are displayed in Table 2.1.

Table 2.1. 2PE cross-sections of common fluorophores at selected wavelengths (from 8).

Dyes	**Wavelength, λ (nm)**	**ηδ (10^{-50}cm^{4}s/photon)**	**δ (10^{-50}cm^{4}s/photon)**
Rhodamine B	840	-	210
Fluorescein (pH~11)	782	-	38
Indo-1 (free)	700	4.5	12
Indo-1 (high Ca)	700	1.2	2.1
Bis-MSB	691	6.0	6.3
DiI	700	95	
Coumarinn 307	776	19	
Cascade Blue	750	2.1	
Lucifer Yellow	860	0.95	
DAPI	700	0.16	
Bodipy	920	17	
wtGFP	800	6	

Compilation of qualitative two-photon excitation spectra of additional fluorophores relevant for cellular imaging using a pulsed Ti;sapphire laser over the excitation range from 580-1150 nm are also available [17].

A general observation in the measured 2PE spectra is that a fluorophore's two-photon excitation spectrum, scaled to half the wavelength, can be very different from its

one-photon excitation spectrum, although the emitted fluorescence is typically independent of the excitation condition. This is due to the different quantum mechanical selection rules for one- and two-photon absorption. Moreover, the values of the 2PE cross-sections of common fluorophores are woefully low and, in general, available dyes exhibit absorptivity values, typically in the range of ~10 GM units. Additionally, while the 2PE cross-section is an indication of the efficiency of 2PA at a given wavelength, this does not necessarily correspond to an expectedly bright fluorescence signal, a phenomenon which depends upon the efficiency of the fluorophore's fluorescence quantum yield. Finally, the brightest two-photon induced fluorescence signal may not necessarily be obtained at the predicted 2PE peak, but at the point where the excitation peak and the output power peak of the laser overlap. For tunable Ti:sapphire lasers, the peak output corresponds to ~800 nm, (Figure 2.1) with decreasing output power produced at lower and higher wavelengths.

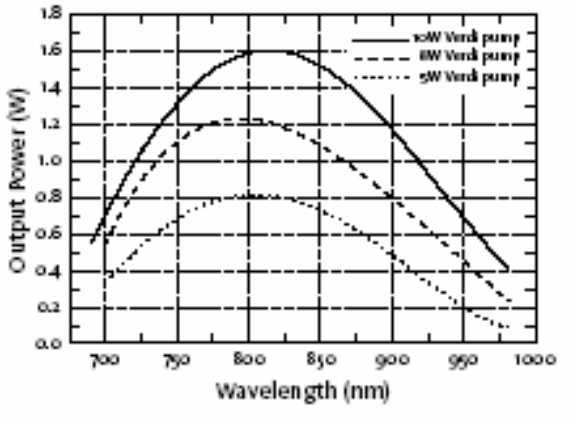

Figure 2.1. Typical tuning curves of a Ti:sapphire laser [18].

Consequently, it is possible to excite a particular fluorophore at a nonoptimal wavelength by increasing the output power, although by doing so, one may inadvertently invoke

phototoxic effects in living samples or rapidly photobleach the fluorescent probe [19].

Phototoxicity in cells is poorly understood in general, and one can expect some extent of cell damage associated with fluorescence microscopy, whether under one- or two-photon excitation conditions. Infrared light is lower in energy than ultraviolet-visible light used in conventional fluorescence imaging and, hence, can be found to be less biologically invasive. However, two-photon induced fluorescence from UV-absorbing endogenous chromophores, as tryptophan and tyrosine in proteins [20] has been demonstrated, as well as from reduced nicotinamide adenine dinucleotide (NADH) [21], and the neurotransmitter, serotonin [22]. Fluorophore-induced effects are not well documented, and potential damage may arise from chemical interactions between the sample and the optically excited fluorophore, whether from intrinsic chromophores or extrinsic fluorophores. Considering the viability of biological samples is the most important constraint on live-cell imaging, assessment of photodamage appears to be difficult and certainly not well documented. For 2PLSM imaging, the general practice for minimizing live-cell damage is to reduce the excitation light intensity to the lowest possible power level using efficient optics and sensitive detectors. Often, the mechanism of photodamage is difficult to ascertain and this remains an elusive area of study.

Up to this point, the major optical properties of an efficient 2PA fluorophore are identified as their two-photon absorption cross-section and fluorescence quantum yield. Certainly, fluorophores with higher values in both would expect improvements in its nonlinear response than a fluorophore exhibiting correspondingly lower values in each parameter. However, if the molecule cannot withstand the intense radiation which nonlinear excitation requires, the compound's enhanced optical properties may be

depreciated. Plainly stated, the photostability or rate of photodegradation under two-photon excitation of a fluorophore is just as important a parameter to define to capitalize on the full utility of the fluorophore for nonlinear imaging.

Part of the benefits of 2PA is that excitation is essentially restricted to the focal volume, and, hence, photobleaching is greatly minimized. However, the irreversible photochemical side effects, such as photobleaching of the fluorophore or photodamage to the specimen, does occur under 2PE and sets limits on the useful duration of observation for 2PLSM. The photodestruction of fluorophores is inherent in any fluorescence microscopy. However, the photodegradation mechanisms of fluorophores are not well understood even under one-photon excitation conditions [23], and detailed photobleaching properties for fluorescence microscopy appear to be restricted to fluorescein [23b-c]. Much less is known about the photodegradation mechanism of fluorophores under two-photon excitation. In fact, the limited studies appear to indicate the photobleaching rates with 2PE are significantly enhanced with respect to 1PE in many dye systems [24]. Measurement of the 2PE photobleaching rates of several fluorophores did not follow an intensity-squared dependence on power, rather revealed a dependence on higher (>3) orders of the excitation power. Some mechanistic possibilities were proposed (radical formation or excited singlet state reactions) but these remain mainly speculative.

The enhanced photobleaching rates of common fluorophores, coupled with their relatively low two-photon absorption cross-sections, may be a serious detriment to imaging thin samples (<5 μm) [24a]. This should not eliminate the development of novel fluorophores with optimized two-photon absorption properties, however. Rather, this

provides greater inspiration for continual development of optical fluorphores with enhanced nonlinearities *and* photostability to function as high-performance 2PA fluorophore for 2PLSM imaging.

2.2 Current Status of Probe Development for 2PE

A major impediment to optimizing 2PLSM imaging is the limited amount of knowledge available about the two-photon absorption cross-sections for potential fluorophores. Selecting the optimal fluorophore is critical, and databases of the two-photon absorption and emission spectra for commonly used fluorophores and bio-indicators have been generated to facilitate the selection process [8,17]. Despite this tremendous effort, many of these compounds are conventional UV-excitable fluorophores, and exhibit low two-photon absorption cross-sections (δ), on the order of ~10 GM units with a few exhibiting ~200 GM units. As stated previously, knowledge of the one-photon excitation spectra does not necessarily allow quantitative predictions of the two-photon excitation spectra of complex molecules, and one-photon probes are not necessarily optimized for two-photon excitation. Recognizing the shortcomings of existing fluorophores, an intense focus on developing novel molecules and materials with enhanced two-photon absorbing properties has received increased attention from a growing number of researchers. Two major, disparate areas of probe development are worth mentioning, but a greater focus on optical probe development based on organic compounds, will be presented.

One of the most important recent innovations in molecular biology is the development of fluorescent protein technology based upon the green fluorescent protein

(GFP) as a powerful tool to monitor specific gene expression [25]. After the first introduction of the GFP, enhanced GFP and fluorescent proteins emitting a variety of colors, ranging from blue, cyan, yellow, and red, were developed [26]. More importantly, the two-photon imaging parameters of a number of these fluorescent protein variants have been recorded [27]. An alternative to the marine based fluorescent proteins are the plant-derived highly fluorescent phytofluors, exhibiting a relatively good two-photon cross-section of 20-30 GM at 792 nm [28]. It is likely that these, and additional intrinsically fluorescent proteins, will play a greater role as fluorescent markers for gene expression *in vitro* and *in vivo*, visualized with 2PLSM.

Another area holding great promise as efficient 2PA fluorphores for 2PLSM bioimaging are semiconductor nanocrystals termed quantum dots (QD). The photophysical properties of cadmium selenide-zinc sulfide quantum dots are intriguing; they are characterized as extremely bright and photostable fluorophores that have a broad excitation range but a narrow emission at wavelengths ranging from 400 nm to 2 μm depending upon their particle size. Water-soluble QDs were prepared and much of the initial problems with biocompatibility appear to be solved. Some QDs are available coated with various substrates allowing them to be conjugated to biomolecules [29]. Reports of enhanced photostabilities (see example, reference 29a) relative to organic compounds, and very large two-photon absorption cross-sections on the range of several 1000s have been estimated, although these values are often difficult to determine [29c,30]. These attractive features of QDs are not without some problems, mainly, residing in controlling and isolating relatively homogeneous particle size. Despite the

difficulty in particle size preparation, the popularity of quantum dots for some 2PLSM imaging applications will likely grow.

At the heart of fluorescence imaging is optical probes, an overwhelming majority of which are organic compounds. The sophistication of probe development has progressed to a level where dozens of compounds exist to act as probes for the study of biological systems. Databases of compiled spectroscopic information on the most common fluorophores can be found in such resources as the *Handbook of Fluorescent Probes and Research Chemicals* [31], such references as 23a, and online interactive fluorescence dye databases (as those of Carl Zeiss' Bio-Rad fluorescence dye database [32]), all of which exist to assist with the selection of very specific probes on the basis of their spectral property and specificity for a particular cellular activity. Keeping in mind that this impressive volume of data mainly exists for fluorophores that are used for conventional fluorescence imaging applications, such comprehensive databases identifying efficient 2PA fluorophores are just being compiled [8,17].

The continuing development of fluorescent probes possessing enhanced nonlinearities, in conjunction with the strong emergence of multiphoton microscopy, will be a major contributor to our understanding of dynamic processes in biology. Much of the synthetic efforts have focused on preparing new organic dyes with the expectation that molecules specifically engineered for two-photon excitation will significantly outperform standard fluorophores optimized for single photon excitation. Initial efforts to prepare a diversity of organic probes tailored for multiphoton imaging applications have focused predominantly on highly hydrophobic, aromatic organic compounds [33,34,35,36]. Measurements of 2PA cross-sections were typically performed in organic

solvents, and it is unclear how the cellular environment will affect the performance of a particular fluorophore. More current efforts are being directed towards developing and evaluating organic compounds with greater compatibility or relevance to biological environments, such as increasing hydrophilicity [37,38,39] and specificity for, e.g., important cellular ions such as Ca^{2+} and Mg^{+2}, zinc, and H^{+} [40,41,42,43,44,45,46].

However, the identification and availability of optimized 2PA fluorophores specifically tailored for direct, covalent labeling of biomolecules for two-photon induced fluorescence imaging studies are limited [29,47,48]. To date, *reactive* fluorescent *organic* probes exhibiting high 2PA cross-section and sufficient action cross-section, specifically to covalently label biomolecules for bioconjugation techniques are rare, and appears to be limited to the dipyrrylmetheneboron difluoride dyes [49]. Hence, the need to incorporate reactive, efficient 2PA organic fluorophores with high action cross-sections ($\eta\delta$) for covalent attachment onto biomolecules within the fluorophore design strategy is timely. Refining organic optical probe design to integrate high nonlinearities, increased hydrophilicity, coupled with reactive functional groups for specific targeting of biomolecules to take advantage of bioconjugation techniques will likely advance 2PLSM imaging experiments.

Characterization of novel organic fluorophores exhibiting enhanced two-photon absorptivities was established essentially through empirical methods. Typically, a series of analogous compounds would be synthetically prepared and their two-photon absorbtion cross-sections would be characterized employing the two-photon fluorescence method. Most recently, quantum chemical calculations are being utilized concurrently with spectroscopic data acquired from organic compounds whose structures are

systematically varied. Strong qualitative and quantitative correlation between theoretical and experimental results have been found for some organic compounds exhibiting very high two-photon absorptivities on the order of >1000 GM units from synthesized bis(styrly)benzene derivatives [50], more recently on aza-crown ether substituted electron donor (D)-acceptor (A)-donor (D) distyrylbenzenes exhibiting $\eta\delta$ on the order of ~ 400 GM units [40], on substituted fluorene derivatives exhibiting 2PA cross-sections >400 GM units [51], and on multibranched dipolar chromophores extending from a triphenylamine electron donating core exhibiting cross-sections on the order of ~ 200 GM units [52]. Although far from definitive, efforts toward quantitative predictions about the behavior of two-photon absorption may well be an integral part of optical probe development possessing enhanced nonlinear optical properties. Computational methods are increasing in their sophistication and it would be expected that quantum-chemical calculations will play a significant role in establishing quantitative predictions about the behavior of two-photon absorption in complex molecules.

2.3 Fluorene Compounds as Efficient 2PA Fluorophores

The δ parameter is an indicator of the two-photon absorption efficiency, and only recently has research been reported on the design and development of very efficient 2PA dyes on the order of >100 and >1000 GM units. Synthetic efforts focused on preparing new nonlinear optical probes specifically engineered to exhibit higher nonlinearities are expected to outperform standard fluorophores currently in use for 2PLSM imaging. Previous studies from our laboratory have reported on the design and development of fluorene-based organic dyes with very efficient two-photon absorption and fluorescence

emission properties [12,33,51,53]. Some aspects of the fluorene derivatives are worth mentioning, as the motivation for tailoring these derivatives for nonlinear bioimaging derives largely from the extensive spectroscopic data obtained on a group of these derivatives prepared in our laboratory.

Fluorene is an aromatic ring system, characterized by two benzene rings fused together by a five-member ring, providing high electron delocalization through good overlap of π molecular orbitals between the rings. The π-conjugated system allows for facile synthetic manipulation as it can be functionalized at the 2, 4, 7, and/or 9 positions as shown in Figure 2.2. Consequently, the acidic, 9-position protons can readily react with electrophilic agents, such as aliphatic bromides, and have been utilized to increase the solubility of complex fluorene derivatives in organic solvents such that very high concentrations ranging from 10^{-4} – 10^{-2} M can be prepared. The chemical reactivity of positions 2 and 7, and to a certain extent position 4, provides the means to integrate different functional substituents on the fluorene core.

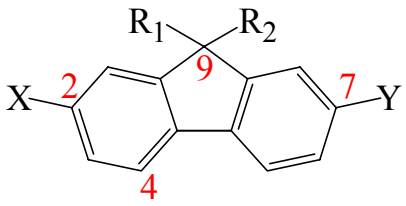

Figure 2.2. The core, fluorene chromophore with positions 2, 4, 7, and 9 of the ring structure indicated in red. Chemical structure variation is accomplished by introduction of various groups X, Y, R_1, and R_2.

Hence, one-dimensional, relatively planar, highly efficient 2PA chromophores have been prepared, and, more recently, was extended to two-dimensional, branched analogues [53]. Exploiting this synthetic versatility, fluorene derivatives with

systematically altered structural motifs were prepared and various electron-acceptor (A) and/or electron-donating (D) groups, with some separated by linking (L) groups, were incorporated into the design architecture. As a result, >20 different series of fluorene derivatives were synthesized to study the relationships between chemical structure and their two-photon absorbing properties, with some of these derivatives exhibiting high fluorescence quantum yields approaching unity [12,33,51,53]. Structures of some of the fluorene derivatives are shown in Table 2.2, with blue representing electron-donating (D) groups, red representing electron-withdrawing groups (A), and green indicating π-conjugated linking groups (L).

Table 2.2. Representative fluorene derivatives characterized as highly efficient 2PA materials.

<table>
<tr>
<td> 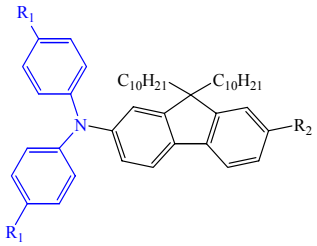

R1 = H; R2 = NO2
R1 = H; R2 = CN
R1 = H; R2 = 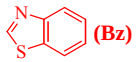 (Bz)
R1 = CH3; R2 = 
Representative dipolar derivatives of the (D-π-A) construct.</td>
<td> 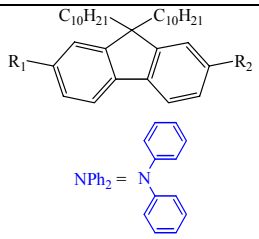

R1 = R2 = NPh2
R1 = R2 = 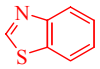 (Bz)
R1 = R2 = CN
R1 = CN; R2 = NO2
Representative symmetrical derivatives of the (D-π-D or A-π-A) construct.</td>
</tr>
<tr>
<td> 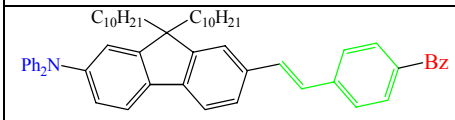
</td>
<td> 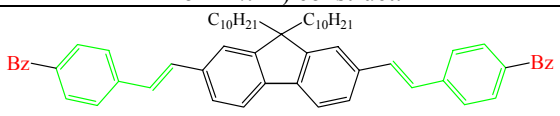
</td>
</tr>
<tr>
<td> 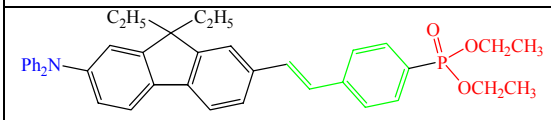
</td>
<td> 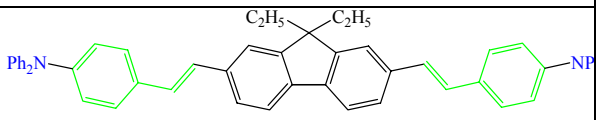
</td>
</tr>
</table>

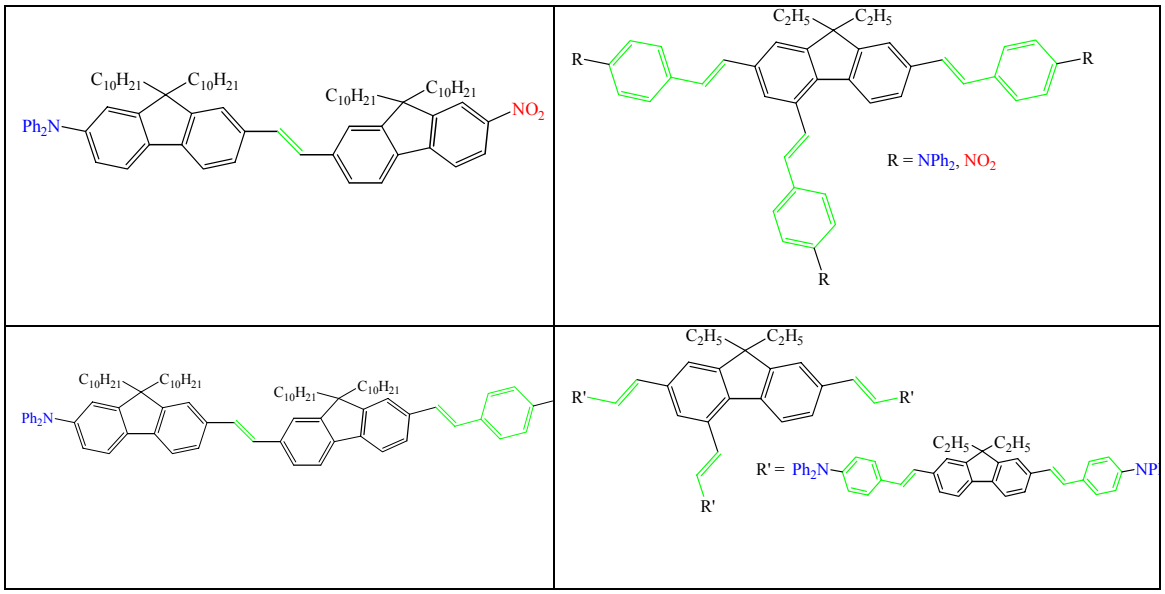

The systematic alteration of these molecules gave rise to a myriad of factors which affected the nonlinearity, and effects of structural symmetry, solvent polarity, strengths of electron donating and/or withdrawing end-groups, and π-conjugation extensions were thoroughly analyzed under one- and two-photon excitation. Three completely independent nonlinear spectroscopic techniques, two-photon fluorescence spectroscopy, white-light continuum pump-probe spectroscopy, and the Z-scan technique were employed (details of these spectroscopic techniques can be found in references 12 and 51) to ensure the measured two-photon absorptivities of these molecules (maximum of ~7000 GM), and consequently the structure-nonlinear optical property relationships were reliable. Additionally, quantum-chemical methods were employed to obtain other critical molecular properties that might impact the optical nonlinearity.

Some plausible explanation correlating the optical properties of these molecules and their structural modifications with their two-photon absorbing capabilities were proposed, and a complete discussion on the analysis may be found in reference 12. An

abbreviated summary highlighting pertinent results from the chemical structure-nonlinear optical properties of fluorene derivatives is as follows:

- Symmetrically substituted fluorene derivatives exhibit negligible 2PA into the first excited state (S1) but strong absorption into the first two-photon allowed state, reminiscent of true centrosymmetric systems. Unsymmetrical derivatives clearly indicate that significant 2PA is possible into nearly any excited state. Since these trends follow for nearly all the derivatives studied here, spectral locations of 2PA can be predicted via linear absorption spectra and excitation anisotropy.

- The study of dipolar molecules reveal compounds with optimal charge transfer character, which maximizes its change in state (or permanent) dipole moments as well as its transition dipole moment, enhances δ into S1. Dipolar fluorene systems benefit from a more polar environment, with an increase in δ into S1 as the polar character of the solvent is raised.

- Extending the π-conjugation length, as for instance with a styryl linking bridge, in dipolar and in symmetric systems shows a considerable improvement in peak nonlinearities, particularly for some symmetric systems (of the A-$\pi\pi$-A and D-$\pi\pi$-D), exhibiting up to 24 times enhancement in its nonlinearity compared to its shorter counterpart (of the A-π-A and D-π-D). Styryl groups also extend the two-photon absorption activity out to longer wavelengths.

- Multi-branched fluorene derivatives do not necessarily exhibit greater charge transfer which would lead to more effective nonlinearities. Nonetheless, they still hold two distinct benefits: an increase in the overall magnitude of two-photon activity as well as an increased spectral band of useable nonlinear absorption (>1000 GM over entire spectral band).

The extensive spectroscopic analysis on these fluorene derivatives supports the contention that fluorene derivatives can be designed to be highly efficient 2PA, highly fluorescent compounds. Moreover, the synthetic flexibility afforded through

manipulation of the chemically labile positions on the core fluorene ring system facilitates the selection of fluorene architectures, whether one of symmetrical or dipolar structure, depending upon particular applications. Additionally, a substantial amount of information correlating variability in fluorene chromophore chemical structure with its nonlinear optical properties has commenced. This database may serve as a guide for the development of particular fluorene derivatives in specific nonlinear optical applications, e.g., development of fluorene derivatives as efficient two-photon absorbing probes for nonlinear fluorescent bioimaging. The remaining chapters of this dissertation are, hence, devoted to the presentation of details relating the development of relatively simple fluorene derivatives optimized for multiphoton microscopy applications.

CHAPTER 3: SYNTHESIS OF 2PA HYDROPHILIC FLUORENE DERIVATIVES

The synthetic details of the fluorene derivatives tailored for multiphoton bioimaging will be discussed in this chapter. A description of the synthetic methods utilized to prepare a model hydrophobic amine-reactive probe, its adduct product with *n*-butyl amine, followed by a description of its reaction with bovine serum albumin (BSA) to prepare a model bioconjugate will be detailed. The synthetic details and structural characterizations of hydrophilic two-photon absorbing fluorescent contrast agents will be presented, followed by the synthetic steps employed towards the preparation of a hydrophilic two-photon absorbing amine-reactive reagent. A discussion on the results of these synthetic methods and structural characterization obtained on the fluorene derivatives will conclude this chapter.

3.1 General Comment on Materials, Methods, and Instruments.

Reactions were conducted under N_2 or Ar atmospheres. Benzothiazole and triethyl phosphate was distilled under reduced pressure prior to use. THF was distilled over $NaBaH_4$ followed by sodium before use. All solvents and reagents were used as obtained from commercial sources unless specified. ^{1}H NMR spectra were recorded on a Varian Mercury-300 NMR (300 MHz) spectrometer using TMS (δ = 0.0 ppm) as the internal standard. ^{13}C NMR spectra were recoded on the same spectrometer (75 MHz) using the carbon signal of the deuterated solvent ($CDCl_3$ δ = 77.4 ppm) as the internal standard. Chemical shifts (δ) of all NMR spectra are reported in parts per million (ppm) and the respective spectra of fluorene compounds prepared in this project can be viewed

in Appendix A. Elemental analyses were performed by Atlantic Microlab, Inc. Norcross, GA. FT-IR spectra were recorded on a Perkin-Elmer Spectrum One spectrometer. Mass spectrometry (MS) analysis was performed by the Department of Chemistry, University of Florida, Gainesville, FL. Additional details of both linear and nonlinear spectroscopic techniques on the fluorene derivatives will be presented in Chapter 4 and in Appendix B. Fluorene compounds utilized for fluorescent microscopy imaging under linear and two-photon irradiation conditions will be discussed in Chapter 5. Additional details of protocols used for cell preparation and imaging techniques and conditions will also be presented in Chaper 5 and Appendix C.

Fluorene (**5**) is commercially available (Sigma-Aldrich) and was recrystallized in hexanes prior to use. Synthesis of (7-benzothiazol-2-yl-9,9-didecylfluoren-2-yl)-diphenyl-amine (**A**), 7-benzothiazol-2-yl-9,9-didecylfluoren-2-ylamine (**1**), 2-nitrofluorene (**6**), 2-iodo-7-nitro-fluorene (**7**), and 2-(tri-*n*-butylstannyl)benzothiazole (**10**) were previously prepared and characterized [33]. These compounds were freshly prepared and characterized following established procedures but a brief description on the preparation of compounds **6**, **7** and **10** will be presented.

3.2 Hydrophobic Amine-Reactive Fluorene Derivative

3.2.1 Synthesis of amine-reactive fluorene probe (2)

The synthesis of the amine-reactive fluorene probe, (2-(9,9-didecyl-7-isothiocyanato-fluorenyl)benzothiazole) (**2**) was prepared following a literature procedure [54]. Briefly, compound **1**, (0.48 g, 0.807 mmol) previously prepared and reported [33],

was dissolved in $CHCl_3$ to which $CaCO_3$ (0.21g, 2.11 mmol) dissolved in H_2O was added to the mixture. Thiophosgene (0.068 mL, 0.892 mmol) was added dropwise to the vigorously stirring mixture in an ice bath. After ~10 min. the starting material was completely consumed as determined via TLC (silica, 2:1 hexanes/CH_2Cl_2), and appeared to have gone to near quantitative conversion. After an additional 20 min. 10% HCl_{aq} was added until no gas generation was observed. The reaction mixture was poured into H_2O, extracted with CH_2Cl_2, dried over $MgSO_4$ and upon filtration and concentration, resulted in an orange oil. Purification was accomplished via flash chromatography (silica, 2:1 hexanes/CH_2Cl_2 eluent). A pale-yellow, viscous oil was isolated (91% yield). FT-IR spectrum of isolated compound revealed the characteristic strong –NCS stretch at 2093 cm^{-1}; no signal at 3600 cm^{-1} from the $–NH_2$ group was observed. ^1H NMR (300 MHz, $CDCl_3$) δ: 8.01 (s, 1H, ArH), 8.07 (s, 1H, ArH), 8.04, 8.01 (dd, 1H, ArH), 7.90 (d, 1H, ArH), 7.72 (d, 1H, ArH), 7.68 (d, 1H, ArH), 7.49 (t, 1H, ArH), 7.38 (t, 1H, ArH), 7.23 (d, 1H, ArH), 7.20 (d, 1H, ArH). ^{13}C NMR (75 MHz, $CDCl_3$) δ: 166.0, 154.0, 152.9, 151.5, 142.4, 139.1, 134.7, 134.5, 132.6, 130.1, 127.1, 126.2, 125.0, 124.7, 122.9, 121.4, 121.3, 120.9, 120.3, 120.2. Anal. Calcd. for $C_{41}H_{52}N_2S_2$: C, 77.31; H, 8.23; N 4.40. Found: C, 77.11; H, 8.45; N, 4.31.

3.2.2 Synthesis of the reactive probe adduct (3)

A mixture of amine-reactive probe **2** (0.85 g, 1.43 mmol) and *n*-butylamine (1.0 ml) was stirred at room temperature for 30 min. The excess butylamine was removed in *vacuo*, and the residue purified by column chromatography using CH_2Cl_2/hexane (2/1 (v/v)) as eluent. Solvent removal and recrystallization from *n*-hexane afforded 0.67g of

white solid (66% yield). m.p. 121-122 °C; ^{1}H NMR (250 MHz, CD_2Cl_2-D_2) δ: 7.99 (m, 3H), 7.85 (d, J = 6.0 Hz, 1H), 7.72 (d, J = 6.5 Hz, 2H), 7.58 (s, 1H, NH), 7.42 (t, J = 7.0 Hz, 1H), 7.31 (t, J = 6.9 Hz, 1H), 7.13 (m, 2H), 5.96 (s, 1H, NH), 3.53 (m, 2H), 1.96 (m, 4H), 1.46 (m, 2H), 1.28 (m, 2H), 1.01 (m, 28H), 0.85 (t, J = 3.9 Hz, 3H), 0.73 (t, J = 3.8 Hz, 6H), 0.56 (m, 4H). ^{1}H NMR (300 MHz, $CDCl_3$) δ: 8.11 (s, 1H, ArH), 8.10 (d, 1H, ArH), 8.04 (s, 1H, ArH), 7.92 (d, 1H, ArH), 7.79 (m, 1H, ArH), 7.72 (s, 1H, NH), 7.50 (t, 1H, ArH), 7.38 (t, 1H, ArH), 7.20 (s, 1H, ArH), 7.17 (d, 1H, ArH), 5.99 (1H, NH), 3.67 (m, 2H), 2.10 (m, 4H), 1.54 (m, 2H), 1.36 (m, 2H), 1.15 (m, 28H), 0.91 (t, 3H), 0.83 (t, 6H), 0.65 (m, 3H). ^{13}C NMR (75 MHz, $CDCl_3$) δ: 180.72, 168.29, 154.25, 153.85, 151.75, 142.73, 139.50, 135.54, 133.01, 127.44, 126.53, 125.35, 124.26, 123.24, 121.95, 121.77, 121.72, 120.49, 120.12, 56.08, 45.83, 40.59, 32.25, 31.46, 30.40, 29.99, 29.91, 29.78, 29.66, 24.46, 23.05, 20.57, 14.52, 14.23. Anal. Calcd. for $C_{45}H_{63}N_3S_2$: C, 76.11; H, 8.94; N, 5.92. Found: C, 76.28; H, 9.19; N, 5.90.

3.2.3 Preparation and characterization of BSA-fluorene bioconjugate (4).

Bovine serum albumin (BSA) (Sigma, Fraction V, ~99 %) was used as received. The bioconjugation reaction was adapted from reference 55. Briefly, a stock solution of BSA (1 mg/mL) in freshly prepared $NaHCO_2$ (0.1 M, pH 9) solution was used. A stock solution of the amine-reactive probe (**2**) dissolved in anhydrous DMSO (5.23×10^{-3} M) was freshly prepared and aliquots slowly added dropwise into the gently stirring BSA solution (1 mL of stock). The concentration of the probe solution was varied such that a 1:10 and a 1:5 mol ratio of protein to probe were prepared to establish a degree of labeling (DOL) for the probe. The reaction was covered from light and allowed to stir at

r.t. for 1 - 2 h, after which the mixture was passed through a Sephadex G-25 fine column (12 cm length, Fluka) equilibrated in and eluted with phosphate buffered saline (PBS, pH 7.2; Gibco). Fractions containing the bioconjugate were identified spectrophotmetrically by monitoring both the protein fraction at 280 nm and the dye at 360 nm. The BSA protein concentration was approximated in the BSA-fluorene bioconjugate via a BSA calibration curve using the Beer-Lambert law. The molar absorptivity (ε_{278}) of BSA in PBS (pH 7.2) was determined to be 39.4 x 10^3 $Lmol^{-1}cm^{-1}$ and corresponds well to the literature value [56] of ε_{278} = 44 x 10^3 $Lmol^{-1}cm^{-1}$ (in 0.1 M Tris-Cl, pH 8.2). Calculation of the DOL was approximated from the product information page provided by Molecular Probes on amine-reactive probes and from reference 55.

3.3 Hydrophilic Fluorene Intermediates and Fluorescent Contrast Agents.

3.3.1 Synthesis of fluorene (6)

Fluorene (**5**) (30g, 180.48 mmol) and glacial acetic acid were added together into a three-neck round bottom flask and heated to 85 °C. Nitric acid (60%, 40 mL) was slowly added, maintaining the temperature. The reaction was cooled down to rt, resulting in a thick yellow precipitate which was filtered, washed with 65 g potassium acetate dissolved in 50 mL of acetic acid. The solid was transferred into 1000 mL of distilled H_2O, stirred and vacuum filtered. The yellow product was dissolved in absolute EtOH and pale orange crystals were collected, washed with cold EtOH and dried. m.p. 152-153 °C (lit 157 °C).

3.3.2 Synthesis of fluorene (7)

2-Nitrofluorene (**6**) (12 g, 56.87 mmol) and acetic acid were placed into a three-neck flask fitted with a condenser, N_2 inlet and thermometer. I_2 (7.23 g, 28.49 mmol) was added and the reaction mixture was stirred for 30 min turning the orange, inhomogeneous solution to a dark orange-brown in coloration. $NaNO_2$ (4.4 g, 63.77 mmol), followed by concentrated H_2SO_4 (37.5 mL) was added and the reaction heated to 120 °C fro 2 h. A pale yellow precipitate resulted. The suspension was cooled down to rt, poured into 500 g of ice, filtered and dried in a vacuum oven. The crude was recrystallized in a mixture of 1/1 (v/v) of EtOH/THF (1000 mL) resulting in the collection of yellow crystals. m.p. 245-246 °C (lit 244-245 °C). ^{1}H NMR (300 MHz, $CDCl_3$) δ: 8.34 (s, 1H, ArH), 8.30 (d, 1H, ArH), 7.97 (s, 1H, ArH), 7.85 (d, 1H, ArH), 7.79 (d, 1H, ArH), 7.61 (d, 1H, ArH), 3.99 (s, 2H, ArH).

3.3.3 Synthesis of fluorene (9)

2-Iodo-7-nitro-fluorene (**7**) (1.5 g, 4.44 mmol), 1-bromo-2-(2-methoxy-ethoxy)ethane (1.89 g, 10.3 mmol), and KI (0.075 g, 0.45 mmol) were placed into DMSO at rt. To the stirring solution, freshly powdered KOH (1.05 g, 18.75 mmol) was slowly added, turning the yellow reaction mixture dark green. The reaction was followed to completion via TLC (1/1 (v/v) hexanes/diethyl ether. The reaction mixture was poured into distilled water and its organic components extracted with CH_2Cl_2, and dried over $MgSO_4$. The resulting filtered and concentrated dark orange oil was purified via silica gel column chromatography using the same eluent system used to monitor the reaction on TLC. Two fractions, identified via NMR spectroscopy and elemental analysis, were

isolated as the mono-substituted fluorene compound **8** and the di-substituted fluorene compound **9**. The major product, compound **9**, was obtained as a pale yellow oil which solidified into a waxy solid (1.3 g, 62% yield). ^{1}H NMR (300 MHz, $CDCl_3$) δ: 8.26 (s, 1H, ArH), 8.24 (d, 1H, ArH), 7.82 (s, 1H, ArH), 7.76 (d, 1 H, ArH), 7.73 (1H, ArH), 7.51 (d, 1H, ArH), 3.26 (s, 6H, OCH_3), 3.23 (m, 4H, OCH_2), 3.15 (m, 4H, OCH_2), 2.80 (m, 4H, OCH_2), 2.43 (m, 4H, CH_2). ^{13}C NMR (75 MHz, $CDCl_3$) δ: 152.92, 150.11, 147.59, 145.90, 137.85, 137.01, 133.25, 123.79, 122.81, 120.19, 119.22, 95.73, 71.98, 70.28, 67.06, 59.37, 52.61, 39.59. Anal. Calcd. for $C_{23}H_{28}INO_6$: C, 51.03; H, 5.21; N 2.59. Found: C, 50.96; H, 5.23; N, 2.59.

3.3.4 Synthesis of 2-(tri-*n*-butylstannyl)benzothiazole (10).

Freshly distilled benzothiazole (9.9 g, 73.23 mmol) was added under N_2 via syringe into freshly prepared anhydrous THF in a three-neck flask fitted with a low-temperature thermometer. The clear solution was cooled down to -72 °C and *n*-BuLi (5.76 g, 88.5 mmol) was slowly added into the cooled solution, gradually turning the solution a deep orange in coloration. *n*-Bu_3SnCl (30.18 g, 92.72 mmol) was slowly added through an addition funnel into the cooled reaction mixture. Upon complete addition, the reaction was gradually allowed to warm up to -10 °C and stirred for 1 h turning the mixture green in coloration. After ~1 h, the reaction was gradually warmed to 0 °C and aqueous KF (3%, 50 mL) was gradually added, turning the solution bright yellow, which was then stirred at 10 °C for 1 h. The organic layer was separated, dried over $MgSO_4$, filtered, and concentrated to give an orange oil. A light pale yellow liquid

was collected under vacuum distillation at 144-146 °C/0.1 mm Hg (lit. 144-146 °C/0.15 mm Hg).

3.3.5 Synthesis of fluorene (11)

2-Iodo-9,9-di-[2-(2-methoxy-ethoxy)-ethyl]-7-nitro-fluorene, compound **9** (0.695 g, 1.46 mmol) and 2-(tri-*n*-butylstannyl)benzothiazole **10** (0.797 g, 1.88 mmol) were dissolved in toluene, degassed, and placed under Ar. To the clear, yellow solution, $Pd(PPh_3)_4$ (0.0428 g, 0.037 mmol) was added and degassed. The reaction was heated to reflux under Ar and allowed to stir overnight, turning the reaction dark orange in coloration. Upon completion (TLC: 1/1.5 (v/v) cyclohexane/ethyl ether), the reaction was passed through a silica gel plug and concentrated, resulting in an orange oil purified via silica column chromatography using 2/1/1 (v/v) CH_2Cl_2/cyclohexanes/diethyl ether as eluent. The resulting bright yellow solution solidified upon standing (0.41 g, 51% yield). ^{1}H NMR (300 MHz, $CDCl_3$) δ: 8.33 (s,1H, ArH), 8.30 (d, 1H, ArH), 8.22 (s, 1H, ArH), 8.15 (d, 1H, ArH), 8.11 (d, 1H, ArH), 7.94, (d, 1H, ArH), 7.88 (d, 1H, ArH), 7.86 (d, 1H, ArH), 7.52 (t, 1H, ArH), 7.41 (t, 1H, ArH), 3.22 (m, 4H, OCH_2), 3.21 (m, 6H, OCH_3), 3.15, (m, 4H, OCH_2), 2.90 and 2.82 (m, 4H, OCH_2), 2.55, (t, 4H, CH_2). ^{13}C NMR (75 MHz, $CDCl_3$) δ: 167.37, 154.17, 151.70, 151.37, 147, 67, 145.78, 140.89, 135.18, 134.59, 127.81, 126.71, 125.66, 123.76, 123.47, 122.60, 121.90, 121.85, 120.60, 119.37, 71.94, 70.25, 67.16, 59.29, 52.77, 39.67. Anal. Calcd. for $C_{30}H_{32}N_2O_6S$: C, 65.67; H, 5.88; N 5.11. Found: C, 65.73; H, 5.98; N, 4.96.

3.3.6 Synthesis of fluorene (12)

Fluorene compound, 2-{9,9-di-[2-(2-methoxy-ethoxy)-ethyl]-7-nitro-fluoren-2-yl}-benzothiazole, **11** (0.218 g, 0.4 mmol) was dissolved into a mixture of 1/1 (v/v) EtOH/THF mixture after which 10% Pd/C (0.019g) was added. The reaction was heated to 70 °C under N_2 and hydrazine monohydrate (0.124 g, 2.48 mmol) was added dropwise and the reaction mixture was allowed to stir overnight. Upon completion (TLC: 9.5/0.5 (v/v) ethyl ether/MeOH), the reaction was passed through a silica gel plug washed with 1/1 (v/v) ethyl ether/MeOH, concentrated, and purified via silica gel column chromatography using 9.5/0.5 (v/v) ethyl ether/MeOH eluent. A bright yellow solid was isolated (0.192 g, 93% yield). m.p. 137-139 °C . ^{1}H NMR (300 MHz, $CDCl_3$) δ: 8.08 (s, 1H, ArH), 8.06 (d, 1H, ArH), 8.02 (d, 1H, ArH), 7.91 (d, 1H, ArH), 7.60 (d, 1H, ArH), 7.50 (d, 1H, ArH), 7.45, (t, 1H, ArH), 7.36 (t, 1H, ArH), 6.74 (s, 1H, ArH), 6.68, (d, 1H, ArH), 3.87 (s, 2H, NH_2), 3.29 (m, 4H, OCH_2), 3.25, (s, 6H, OCH_3), 3.21 (m, 4H, OCH_2), 2.79 (m, 4H, CH_2), 2.49 and 2.38 (m, 4H, OCH_2). ^{13}C NMR (75 MHz, $CDCl_3$) δ: 168.59, 154.27, 151.75, 148.70, 147.34, 144.15, 135.0, 131.02, 130.49, 127.51, 126.39, 125.05, 123.01, 121.89, 121.70, 121.61, 118.92, 114.67, 109.88, 72.02, 70.22, 67.30, 59.31, 51.41, 40.27.

3.3.7 Synthesis of fluorene (13)

Fluorene compound, 7-benzothiazol-2-yl-9,9-di-[2-(2-methoxy-ethoxy)-ethyl]-fluoren-2-ylamine, **12** (0.118 g, 0.23 mmol), 18-crown-6 (0.018 g, 0.068 mmol), K_2CO_3 (0.256 g, 1.85 mmol), and Cu-bronze (0.076 g, 1.2 mmol) were added together into 1,2-dichlorobenzene (1,2-DCB) at rt. Into the degassed mixture, iodobenzene (0.187 g, 0.917

mmol) was added under N_2, and the reaction mixture was heated to 180 °C and stirred overnight. Upon completion (TLC: 5/1 (v/v), CH_2Cl_2/ethyl ether), the hot reaction mixture was passed through a short silica gel plug which was then washed with 9/1 (v/v) ethyl ether/MeOH. The organic solution was concentrated, with the high boiling solvent (1,2-DCB) and excess iodobenzene removed under vacuum, resulting an a viscous, orange oil which was purified via silica gel column chromatography (same eluent use for monitoring TLC). A bright yellow-green oil was isolated which crystallized upon standing to yield a bright yellow solid (Fluorene compound **13**: {7-benzothiazol-2-yl-9,9-di-[2-(2-methoxy-ethoxy)-ethyl]-fluoren-2-yl}-diphenyl-amine). (0.11 g, 73% yield). m.p. 156-157 °C. ^{1}H NMR (300 MHz, $CDCl_3$) δ: 8.09 (s, 1H, ArH), 8.07 (d, 1H, ArH), 7.91 (d, 1H, ArH), 7.67 (d, 1H, ArH), 7.57 (d, 1H, ArH), 7.48 (t, 1H, ArH), 7.37 (t, 1H, ArH), 7.26 (t, 1H, ArH), 7.24 (s,1H, ArH), 7.14-7.01 (m, 3H, ArH), 3.32 (m, 4H, CH_2), 3.26 (s, 6H, CH_3), 3.25 (m, 4H, CH_2), 2.87 (m, 4H, CH_2), 2.40 and 2.32 (m, 4H, CH_2). ^{13}C NMR (75 MHz, $CDCl_3$) δ: 168.34, 154.26, 151.17, 149,76, 148.51, 147.71, 143.37, 135.04, 133.89, 131.79, 129.47, 127.52, 126.44, 125.16, 124.63, 123.33, 123.15, 122.10, 121.73, 121.29, 119.65, 118.43, 72.04, 70.226, 67.50, 59.33, 51.70, 39.75. Anal. Calcd. for $C_{42}H_{42}N_2O_4S$: C, 75.19; H, 6.31; N 4.18. Found: C, 75.42; H, 6.34; N, 4.18.

3.3.8 Synthesis of fluorene (14)

Fluorene compound, 7-benzothiazol-2-yl-9,9-di-[2-(2-methoxy-ethoxy)-ethyl]-fluoren-2-ylamine, **12** (0.073 g, 0.141 mmol) and freshly distilled triethyl phosphate was added under N_2. The reaction mixture gradually turned from yellow, to a dark, orange-red, solution upon reflux at 205 °C. After ~1 h, the reaction appeared to be complete as

determined via TLC (3/1 (v/v) CH_2Cl_2/ethyl ether). NaOH (4.16 M) addition to the reaction turned the reaction mixture bright green and the reaction was allowed to continue to reflux for ~1.5 h after which it was cooled to rt. The organic components were extracted with CH_2Cl_2, dried over $MgSO_4$, filtered, and concentrated. The bright green oil was purified via flash silica gel column chromatography (3/1 (v/v) CH_2Cl_2/ethyl ether) resulting in a bright green, viscous, oil (Fluorene compound **14**: {7-benzothiazol-2-yl-9,9-di-[2-(2-methoxy-ethoxy)-ethyl]-fluoren-2-yl}-diethyl-amine). (0.056 g, 69% yield). ^{1}H NMR (300 MHz, $CDCl_3$) δ: 8.05 (s, 1H, ArH), 8.02 (d, 1H, ArH), 7.98 (s, 1H, ArH), 7.89 (d, 1H, ArH), 7.57 (d, 1H, ArH), 7.54 (d, 1H, ArH), 7.46 (t, 1H, ArH), 7.35 (t, 1H, ArH), 6.67 (s, 1H, ArH), 6.67 (d, 1H, ArH), 3.44 (q, 4H, NCH_2), 3.31 (m, 4H, OCH_2), 3.25 (s, 6H, OCH_3), 3.23 (m, 4H, OCH_2), 2.38 (m, 4H, OCH_2), 2.51 and 2.80 (m, 4H, CH_2), 1.22 (t, 6H, CH_3). ^{13}C NMR (75 MHz, $CDCl_3$) δ: 168.81, 154.32, 151.70, 148.74, 148.60, 148.09, 144.65, 134.97, 130.28, 127.51, 127.40, 126.33, 124.91, 122.96, 121.83, 121.66, 121.61, 118, 44, 111.42, 105.99, 72.05, 70.19, 67.46, 59.30, 51.41, 45.05, 40.35, 13.11. Anal. Calcd. for $C_{34}H_{42}N_2O_4S$ (574.29): C, 71.05; H, 7.37; N 4.87. Found: C, 70.79; H, 7.65; N, 4.39. HR-MS (EI): *m/z* = 574.2873 (M+).

3.4 Hydrophilic Amine-Reactive Fluorene Reagents

3.4.1 Synthesis of fluorene (8)

2-Iodo-7-nitro-fluorene (**7**) (1 g, 2.96 mmol), 1-bromo-2-(2-methoxy-ethoxy)ethane (0.674 g, 3.68 mmol), and KI (0.109 g, 0.657 mmol) were placed into

DMSO at rt. To the stirring solution, freshly powdered KOH (0.994 g, 17.72 mmol) was slowly added, turning the yellow reaction mixture dark green. The reaction was followed to completion via TLC (1/1 (v/v) hexanes/ethyl ether. The reaction mixture was poured into distilled water and its organic components extracted with CH_2Cl_2, dried over $MgSO_4$, filtered, and concentrated resulting in a dark orange oil which was purified via silica gel column chromatography using the same eluent system used to monitor the reaction on TLC. Two fractions, identified via NMR spectroscopy and elemental analysis, were isolated as the mono-substituted fluorene compound **8** and the di-substituted fluorene compound **9**. The minor product, compound **8**, was obtained as a pale, yellow oil which solidified into a waxy solid (0.38 g, 29% yield). ^{1}H NMR (300 MHz, $CDCl_3$) δ: 8.38 (s, 1H, ArH), 8.28 (d, 1H, ArH), 7.95 (s, 1H, ArH), 7.81, (d, 1H, ArH), 7.77 (d, 1H, ArH), 7.56 (d, 1H, ArH), 4.22 (t, 1H, CH), 3.56-3.47 (m, 6H, OCH_2), 3.38 (s, 3H, OCH_3), 2.27, (m, 2H, CH_2). ^{13}C NMR (75 MHz, $CDCl_3$) δ: 150.95, 147.73, 147.36, 146.38, 138.28, 136.84, 134.47, 123.60, 122.83, 120.41, 120.18, 109.50, 95.28, 72.22, 70.58, 68.48, 59.49, 45.20, 32.98. Anal. Calcd. for $C_{18}H_{18}INO_4$: C, 49.22; H, 4.13; N 3.19. Found: C, 49.50; H, 4.22; N, 3.19.

3.4.2 Synthesis of fluorene (15)

2-iodo-9-[2-(2-methoxy-ethoxy)-ethyl]-7-nitro-fluorene, compound **8** (0.376 g.0.856 mmol), 3-(BOC-amino)propyl bromide (0.611 g 2.57 mmol), and KI (0.02 g, 0.172 mmol) were added and dissolved in DMSO under N_2. Freshly powdered KOH (0.2 g, 3.56 mmol) was slowly added into the stirring solution, turning the reaction mixture from clear yellow into dark green in coloration. After about 30 h, most of the starting

compound **8** was consumed and distilled water was added to the reaction mixture. The organic components were extracted with CH_2Cl_2, dried over $MgSO_4$, filtered, and concentrated, resulting in an orange oil. The crude mixture was passed through a silica gel column using 5/1 (v/v) CH_2Cl_2/ethyl ether eluent, resulting in isolation of a pale yellow residue (0.27 g, 53% yield). ^{1}H NMR (300 MHz, $CDCl_3$) δ: 8.28 (d, 1H, ArH), 8.21 (s, 1H, ArH), 7.77 (s, 1H, ArH), 7.75 (d, 1H, ArH), 7.73 (d, 1H, ArH), 7.51 (d, 1H, ArH), 4.29 (1H, NH), 3.26 (s, 3H, OCH_3), 3.25 – 3.23 (m, 2H, OCH_2), 3.14 (m, 2H, OCH_2), 2.90–2.77 (m, 4H, CH_2), 2.41 (2H, CH_2), 2.05 (m, 2H, CH_2), 1.38 (s, 9H, CH_3), 0.76 (m, 2H, CH_2). ^{13}C NMR (75 MHz, $CDCl_3$) δ: 155.79, 153.09, 150.22, 147.68, 146.20, 138.10, 137.16, 132.88, 123.87, 122.91, 120.29, 118.76, 95.91, 79.54, 71.98, 70.27, 67.29, 59.37, 54.00, 40.63, 39.36, 37.58, 28.78, 24.75. Anal. Calcd. for $C_{26}H_{33}IN_2O_6$: C, 52.36; H, 5.58; N 4.70. Found: C, 52.49; H, 5.53; N, 4.66.

3.4.3 Synthesis of fluorene (16)

Fluorene compound, (3-{2-iodo-9-[2-(2-methoxy-ethoxy)-ethyl]-7-nitro-fluoren-9-yl}-propyl)-carbamic acid tert-butyl ester, **15** (0.12g 0.202 mmol) and 2-(tri-*n*-butylstannyl)benzothiazole 10 (0.13 g, 0.306 mmol) were dissolved in toluene, degassed, and placed under Ar. To the clear, yellow solution, $Pd(PPh_3)_4$ (0.008 g, 0.007 mmol) was added and degassed. The reaction was heated to reflux under Ar, and after ~4 h, appeared complete (TLC: 5/1 (v/v) CH_2Cl_2/ethyl ether). The reaction was passed through a silica gel plug which was washed with 1/1 (v.v) CH_2Cl_2/ethyl ether and concentrated. The resulting orange oil was purified via silica column chromatography using 5/1 (v/v) CH_2Cl_2/ethyl ether as eluent and a yellow residue was obtained (Fluorene compound **16**:

of (3-{2-benzothiazol-2-yl-9-[2-(2-methoxy-ethoxy)-ethyl]-7-nitro-fluoren-9-yl}-propyl)-carbamic acid tert-butyl ester). (0.089g, 77% yield). ^{1}H NMR (300 MHz, $CDCl_3$) δ: 8.31, (d, 1H, ArH), 8.27 (s, 1H, ArH), 8.20 (s, 1H, ArH), 8.12 (d, 1H, ArH), 8.10 (d, 1H, ArH), 7.94 (d, 1H, ArH), 7.88 (d, 1H, ArH), 7.82 (d, 1H, ArH), 7.51 (t, 1H, ArH), 7.41 (t, 1H, ArH), 4.30 (s, 1H, NH), 3.23 (m, 2H, OCH_2), 3.21 (m, 3H, OCH_3), 3.15 (m, 2H, OCH_2), 2.93 (m, 2H, OCH_2), 2.85 (m, 2H, CH_2), 2.53 (t, 2H, CH_2), 2.19 (t, 2H, CH_2), 1.34 (s, 9H, CH_3), 0.82 (m, CH_2). ^{13}C (75 MHz, $CDCl_3$) δ: 167.35, 155.76, 154.16, 151.89, 151.48, 147.75, 146.09, 141.11, 135.18, 134.70, 127.91, 126.72, 125.68, 123.86, 123.47, 122.19, 121.98, 121.84, 120.72, 118.90, 79.46, 71.95, 70.25, 67.40, 59.30, 54.20, 40.67, 39.41, 37.69, 28.73, 24.80.

3.4.4 Synthesis of fluorene (17)

Fluorene compound, (3-{2-iodo-9-[2-(2-methoxy-ethoxy)-ethyl]-7-nitro-fluoren-9-yl}-propyl)-carbamic acid tert-butyl ester, **15** (0.089 g, 0.15 mmol) was dissolved into a mixture of 1/1 (v/v) EtOH/THF mixture after which 10% Pd/C (0.011g) was added. The reaction was heated to 70 °C under N_2 and hydrazine monohydrate (0.0457 g, 0.91 mmol) was added dropwise. The reaction was allowed to stir overnight til completion (TLC 5/1 (v/v) ethyl ether/CH_2Cl_2) and was passed through a silica gel plug which was washed with 4/1 (v/v) CH_2Cl_2/MeOH. The resulting bright green solution was concentrated to yield a yellow powder which was passed through a silica gel column using 8/1/1/ (v/v) CH_2Cl_2/ethyl ether/MeOH mixture as eluent. A pale, yellow powder was obtained (Fluorene compound **17**: (3-{2-amino-7-benzothiazol-2-yl-9-[2-(2-methoxy-ethoxy)-ethyl]-fluoren-9-yl}-propyl)-carbamic acid tert-butyl ester). (0.073 g, 84% yield). ^{1}H

NMR (300 MHz, $CDCl_3$) δ: 8.06 (d, 1H, ArH), 8.04 (s, 1H, ArH), 7.99 (d, 1H, ArH), 7.90 (d, 1H, ArH), 7.60 (1H, ArH), 7.51 (d, 1H, ArH), 7.48 (t, 1H, ArH), 7.36 (t, 1H, ArH), 6.69 (q, 1H, ArH), 6.66 (1H, ArH), 4.22 (s, 1H, NH), 3.88 (s, 2H, NH_2), 3.31 (m, 2H, OCH_2), 3.28 (s, 3H, OCH_3), 3.20 (m, 2H, OCH_2), 2.86 and 2.81 (m, 4H, CH_2), 2.46 and 2.36 (m, 2H, CH_2), 2.20 and 1.99 (m, 2H, CH_2), 1.35 (s, 9H, CH_3), 0.82 (m, 2H, CH_2). ^{13}C (75 MHz, $CDCl_3$) δ: 168.65, 155.8, 154.26, 152.08, 149.11, 147.37, 144.52, 134.98, 131.02, 130.83, 127.61, 126.40, 125.06, 123.04, 121.68, 121.64, 118.93, 114, 67, 109.68, 79.29, 72.03, 70.21, 67.61, 59.31, 53.03, 40.94, 39.91, 38.24, 28.78, 24.68.

3.4.5 Attempted synthesis of fluorene (18)

Fluorene compound **16** (0.123 g, 0.212 mmol), 18-crown-6 (0.023 g, 0.0848 mmol), K_2CO_3 (0.236 g, 1.70 mmol), and Cu-bronze (0.071 g, 1.06 mmol) were added together into 1,2-DCB at rt. Into the degassed mixture, iodobenzene (0.190 g, 0.848 mmol) was added under N_2, and the reaction mixture heated to 180 °C. The reaction was monitored via TLC (3/1 (v/v), CH_2Cl_2/ethyl ether) and became progressively very complex with many components being observed. After about 48 h, no obvious product formation was identified and the reaction was stopped by passing through a silica gel plug while hot. The plug was washed with 5/1 (v/v) ethyl ether/MeOH, the organic solution concentrated, and the high boiling solvent (1,2-DCB) and excess iodobenzene removed under vacuum, resulting an a viscous, dark brown oil. Repeated attempts to isolate individual components via flash column chromatography were unsuccessful. Repeated synthesis was attempted under the same reaction conditions, resulting in an unsuccessful isolation of the expected product.

3.5 Results and Discussion on the Preparation of Fuorene Derivatives.

3.5.1 Hydrophobic amine-reactive fluorene derivative, adduct, and bioconjugate.

The details of how the hydrophobic probe (**2**) was prepared and used to prepare a model adduct **3**, along with a model bioconjugate **4**, will be discussed [57]. The synthesis and structural characterization of fluorene derivative **1** was previously reported [33]. Compound **2** was prepared as an amine-reactive fluorescent label (Scheme 1), and contains the isothiocyanate (-NCS) functionality for covalent bond formation with primary amine groups. Generation of the isothiocyante functionality utilized the highly reactive thiocarbonyl insertion reagent, thiophosgene. Though toxic, careful handling of this reagent resulted in the reaction being over in <15 min with high conversion of 90% isolated yield of compound **2**.

FT-IR spectrum of the isolated compound revealed the characteristically strong -NCS stretch at 2093 cm^{-1}; no signal at 3600 cm^{-1} from the $–NH_2$ group was observed. Further confirmation of the target compound was achieved via NMR spectroscopy. The ^1H NMR spectrum of compound **1** displays the primary amino group (1° $–NH_2$) protons as a broad singlet at 3.57 ppm in $CDCl_3$. This peak is not observed in compound **2** as the 1° $–NH_2$ is replaced by the –NCS group. Furthermore, there is a noticeable downfield shift of the aromatic protons *ortho* to the $–NH_2$ group in compound **1** from ~ 6.54 ppm to 7.20 and 7.23 ppm. The ^{13}C NMR spectrum of compound **2** revealed a weak, new peak for the –NCS carbon observable at ~ 134.55 ppm that is not present in its precursor. Final structural confirmation for the amine-reactive probe, **2** was verified through its

CHN elemental analysis, in which the largest deviation of weight percent was for H = 0.22%. This is within the acceptable error limits of ± 0.3% placed on elemental results.

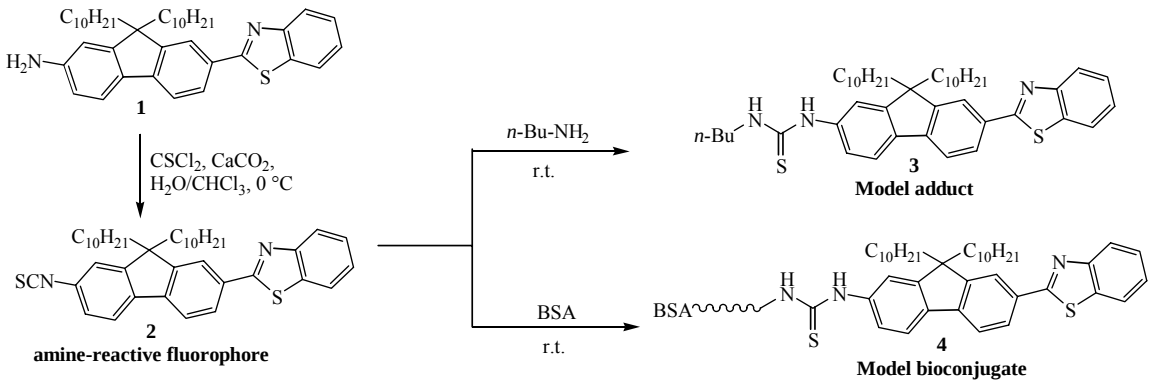

Scheme 1. Preparation of the model adduct (3) and bioconjugate (4) with the amine-reactive fluorenyl reagent (2).

A simple reaction of *n*-butylamine with the compound **2** allowed for the preparation and isolation of model adduct compound **3** (Scheme 1). This verifies reactivity of compound **2** as an amine-reactive fluorescent label for covalent bond formation with, e.g. lysine residues, of protein molecules. Furthermore, preparation of this model adduct allowed for facile single- and two-photon spectroscopic characterizations which more closely resembles the bioconjugate than that of the amine-reactive probe alone. The spectral properties of these compounds will be discussed to further detail in Chapter 4.

The reaction of compound **2** with *n*-butylamine was quick, being over in ~ 30 min at room temperature. The expected thiourea group was evident in the ^{1}H NMR spectrum, where the thiourea –NH protons were observed at 7.71 and 5.99 ppm in $CDCl_3$. Furthermore, the methylene protons α to the thiourea group was observed at 3.67 ppm, with the internal methylene protons observed at 1.54 and 1.36 ppm. Finally, the terminal

methyl protons of butylamine were observed at 0.91 ppm. Additional evidence for the formation of the model adduct was found in the ^{13}C NMR spectrum, where the thiocarbonyl carbon signal was observed at 180.72 ppm. Furthermore, the aliphatic carbons from the butyl group were also observed at 45.83, 31.46, 20.57, and 14.52 ppm, and were not observed in the precursor compound. Final confirmation of adduct, **3** was verified through its elemental analysis, where the greatest deviation of weight percent from CHN elemental analysis was for H = 0.25%.

Upon structural confirmation and reactivity of compound **2** as an amine-reactive label, a bioconjugate was prepared with bovine serum albumin (BSA), a well- known and well-characterized protein molecule. The bioconjugation reaction was adapted as presented in reference 55 and 58 and is a typical condition for labeling protein molecules with a reagent containing an isothiocyante reactive group, such as fluorescein isothiocyante (FITC). The conjugation reaction was stopped by loading the completed reaction mixture directly onto an equilibrated Sephadex G-25 column, and the bioconjugate collected into fractions were identified and characterized spectrophotometrically.

Furthermore, the mol ratios of protein to probe were varied to establish a degree of labeling (DOL) for the probe. The equations used to calculate the DOL can be found in Appendix B. This parameter is important for any reactive probe and is typically performed for each protein that is being labeled to establish an average number of fluorophores covalently attached to the particular protein. Knowledge of the DOL then allows for optimizing the number of fluorophores attached onto the protein for sufficient fluorescence signal, without unduly compromising the protein's bioactivity. Hence, a

1:10 and a 1:5 mol ratio of protein to probe allowed for an estimated DOL ranging from 2.2 to 3.4 (Table 1), a typical range for amine-reactive probes [55]. Interestingly, increasing the time of reaction up to 2 hours under the 5:1 mol ratio did not seem to increase the DOL of the fluorophore attached onto the protein. A higher DOL was achieved with the 10:1 mol ratio of fluorophore to protein under half the time used for the 5:1 mol ratio. The resultant DOL of 3.4 obtained under this condition may be more desirable, to reduce deleterious effects on the protein during its conjugation, as the reaction occurs at a high pH of ~9. High pH levels may be detrimental to the tertiary conformation of a protein structure, but is necessary to generate free amino groups of lysine residues targeted for conjugation. Minimizing the time requirement needed for sufficient amount of fluorophore attachment may reduce potentially detrimental effects the high pH may have on protein structure.

Table 3.1. Variable degree of labeling (DOL) obtained upon altering molar ratios of the amine-reactive probe **2** to the BSA protein.

BSA	**Reactive fluorophore**	**Dye/Protein Mol ratio**	**Reaction time**	**DOL (mol dye/mol protein)**
1.53E-8 mol	1.53E-7 mol	10:1	1 h	3.4
1.53E-8 mol	7.7E-8 mol	5:1	1 h	2.4
1.53E-8 mol	7.7E-8 mol	5:1	2 h	2.2

The amine-reactive probe **2** was shown to form covalent bonds with primary amines, as demonstrated through its reaction with *n*-butylamine followed by isolation of the resulting adduct compound **3**. Utilizing typical reaction conditions of isothiocyante-containing regents for labeling proteins, compound **2** was attached onto BSA, a common protein. The degree of labeling can be controlled by varying the molar ratios of the

reactive reagent to the protein of interest. The final DOL may depend on additional factors, such as the fluorescence quantum yield and photostability, of the fluorophore. For instance, one can imagine wanting a greater DOL for a fluorophore of a low fluorescence quantum yield to achieve a higher fluorescence signal. However, if the DOL is too high, the number of fluorophore linked onto the protein molecule may interfere with the protein activity by, for instance, binding to critical recognition or activity sites on the protein [16,58]. Alternatively, overlabeling a protein with a fluorophore of a sufficiently high fluorescence quantum yield may also lead to a 'self-quenching' effect, resulting in a reduced fluorescence signal being observed [16].

Parameters as the linear- and two-photon absorption properties, fluorescence quantum yields, fluorescence lifetimes, photostability, and additional spectroscopic details of the amine-reactive probe **2**, the model adduct **3**, bioconjugate **4**, and subsequent hydrophilic fluorene compounds will be discussed in further details in Chapters 4 and 5.

3.5.2 Hydrophilic fluorene intermediates and fluorescent contrast agents.

Organic compounds tailored for bioimaging applications are beset with the unique challenge of compatibility with aqueous environments that is more native to living cells and biological specimen. However, many highly-fluorescent organic compounds are comprised of extended π-conjugated systems in which large hydrophobic forces are an integral property of the fluorophore. If the hydrophobic character of the fluorophore is dominant, the compound is unlikely to be soluble in aqueous solvents or in very polar co-solvents as DMSO, rendering them unsuitable or difficult for introduction into biological systems. Hence, many methods have been developed to integrate or enhance the

hydrophilic character into a fluorescent compound without compromising their desirable fluorescent properties. Perusing the chemical structures of organic compounds commonly used in fluorescence microscopy imaging reveals integration of certain functional groups which enhances their hydrophilicity. Many contain carboxylic acids, hydroxyl groups, quaternary ammonium salts, and/or a variety of additional ionized salts, all functionalities which enhance the hydrophilicity of the compound to allow for solubility in very polar and/or aqueous solvents.

The compounds prepared and studied in this project have the aromatic, or π-conjugated, fluorene ring structure as its common base chromophore. The fluorene ring system can be readily functionalized from the 2, 7, and 9 positions as shown in Figure 3.1. The versatility of this synthetic opportunity enables preparation of key intermediates, such that target compounds of varying electronic properties may be obtained. Hence, various electronic acceptor (A) and/or donating (D) groups have been systematically incorporated, allowing for the elucidation of how chemical structure, i.e., electronic variation, on the fluorene ring structure affects its nonlinear properties, specifically, two-photon absorption and two-photon excited fluorescence [12]. Based upon these structure-property studies, a simple D-π-A fluorene-based derivative was identified as possessing key properties and was targeted for development as efficient, two-photon absorbing fluorescent contrast agents for two-photon induced imaging applications.

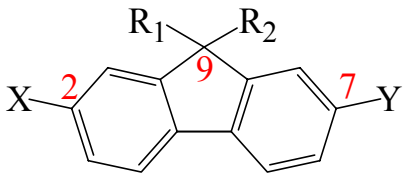

Figure 3.1. The base fluorene chromophore with positions 2, 7, and 9 of the ring structure indicated in red. Structural variation is accomplished by introduction of variable chemical groups X, Y, R_1 and R_2.

Increasing the hydrophilicity of the fluorene derivatives was achieved by substitution of linear alkyl groups, typically present on the 9-position of the base fluorene chromophore prepared for the structure-property studied, with ethylene-oxy or ether groups. This substitution should have minimal perturbation to the π-conjugation responsible for fluorescence. Ethers can act as a hydrogen-bond acceptor but not as a donor. As a result, they may be less soluble in water than an alcohol with the same molecular weight, but are more soluble in water than linear alkyl hydrocarbons of the same molecular weight. Furthermore, they are essentially inert to chemical reactions, do not undergo oxidation or reduction readily, and are relatively stable to most acids and bases at ambient temperatures. The following discussion will entail the synthetic methodology utilized to prepare the hydrophilic, relative to the linear alkyl-containing fluorene analogues, fluorene intermediates and hydrophilic fluorene fluorescent contrast agents. For sake of brevity, the fluorene derivatives will be indicated by their compound number established in the previous section detailing their synthetic conditions. ^{1}H and ^{13}C NMR spectra of the respective compounds can be found in Appendix A.

Preparation of key intermediates was efficient from readily available fluorene (**5**). Regiospecific nitration with nitric acid yielded 2-nitrofluorene (**6**) (Scheme 2) following a literature procedure. The melting point obtained on the purified crystals (152-153 °C)

was in good agreement with that of the literature value (157 °C). This was followed by the regiospecific iodination of **6**, using literature procedure, to yield a key intermediate compound **7**. Again, the melting point of the purified yellow crystals (245-246 °C) was consistent with that of the literature value (244-245 °C). The ^{1}H NMR in $CDCl_3$ clearly showed the 9-position fluorene protons as a strong singlet at 3.99 ppm. Additionally, the protons on the fluorene ring system at positions 8 and 1 were observed as clear singlets at 8.38 and 7.91 ppm, respectively.

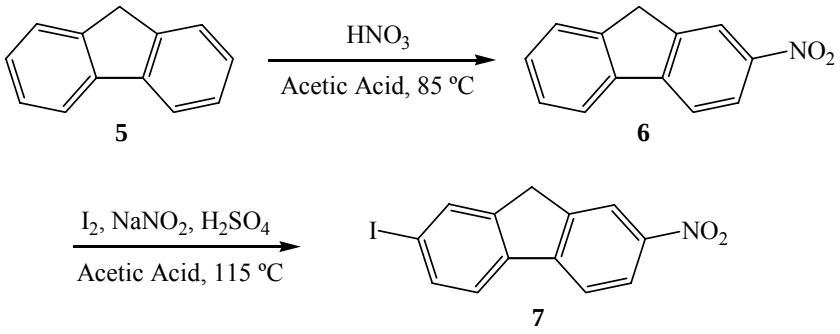

Scheme 2. Preparation of key intermediates.

Introduction of the ether groups into compound **7** was accomplished upon generation of the fluorenyl anion with KOH in DMSO with subsequent addition of excess molar amounts of 1-bromo-2-(2 methoxy-ethoxy)ethane (Scheme 3). The di-substituted compound **9** was obtained as a pale yellow liquid which solidified into a waxy solid in 62% yield. Depending upon the stoichiometry used under the reaction condition, mono-substituted compound **8** was also obtained, although to a lower yield (Scheme 3). Compound **8** will be discussed in the next section entailing efforts toward a hydrophilic amine-reactive probe. Evidence of the di-substitution at the 9-position of the fluorene ring was shown in the ^{1}H NMR spectrum of compound **9**, where no peak was observed at

3.99 ppm. The ethylene-oxy or ethylene protons were observed as complex multiplets at 3.23, 3.15, 2.80, and 2.43 ppm, while the terminal methoxy ($–OCH_3$) protons as a strong singlet at 3.26 ppm. These peak positions will be characteristic for all compounds containing the ether group, whether mono- or di-substituted. The aromatic region remained relatively unperturbed by the di-substitution, with minor shifts observed in the peak positions with splitting patterns of the aromatic protons remaining the same. The ^{13}C spectrum for compound **9** clearly showed carbon 7 attached to the nitro group and carbon 2 attached to iodine at 152.9 and 95.7 ppm, respectively. Additonally, carbon 9 was characteristically observed at ~39.6 ppm, with the ethylene-oxy carbons observed at 17.9, 70.2, 67.1, and 52.6 ppm. The terminal methoxy carbon was observed at 59.3 ppm. These positions remain nearly constant in all compounds comprising the ether group at the 9-position of fluorene. Final structural confirmation was obtained through the CHN elemental analysis, where the greatest deviation in weight percent composition was for C = 0.07%.

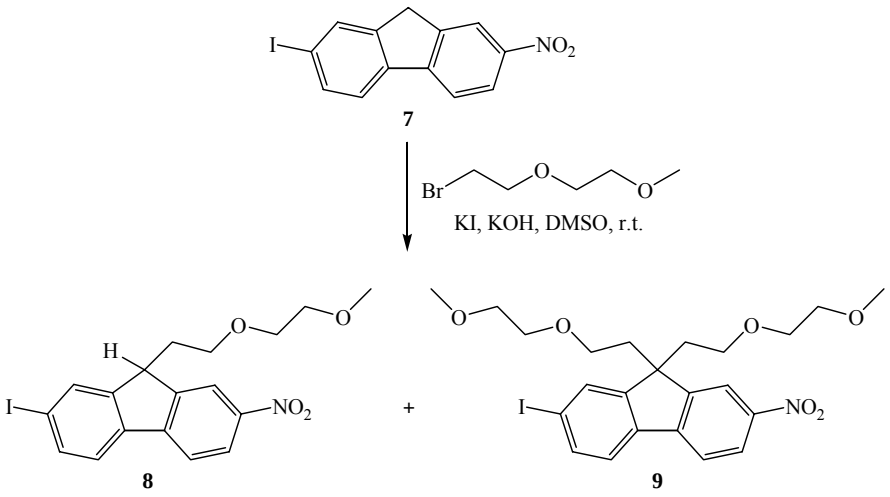

Scheme 3. Introduction of a hydrophilic group into the fluorene architecture.

A Stille coupling procedure was employed to prepare compound **11** as shown in Scheme 4. (2-Tri-*n*-butylstannyl)benzothiazole (**10**) was prepared by treating freshly distilled benzothiazole with *n*-BuLi in dry THF at -75 °C, followed by addition of tri-*n*-butyltin chloride [59]. The purified product collected under reduced pressure (144-146 °C/0.1 mm Hg) agreed well with that of the literature value (144-146 °C/0.15 mm Hg). Pd-catalyzed Stille coupling was subsequently performed between compound **9** and **10** in refluxing toluene with tetrakis(triphenyl phosphine)palladium 0 [60], resulting in isolation of a yellow solid in 51% yield. The ^{1}H NMR spectrum for compound **11** immediately displayed a downfield slight of the aromatic protons, relative to those observed in compound **9**, indicative of the influence of the weakly electronic withdrawing benzothiazole group on the aromatic protons. Hence, the shift of the *ortho* proton at fluorene ring position 1 was observed from 7.82 to 8.22 ppm from compound **9** to **11**, respectively. Furthermore, additional aromatic proton peaks due to the benzothiazole group was observed. Most notable is the pair of triplet signals observed at 7.52 and 7.41 ppm, due to the two outer aromatic protons of the benzothiazole group, remaining as relatively constant signatures of these benzothiazole protons. Further confirmation of the benzothiazole group was found in the ^{13}C spectrum for compound **11**. The bridge carbon of the benzothiazole group joining fluorene (N=C-S) was observed at 167.4 ppm, the α-carbon to the benzothiazole nitrogen at 154.2 ppm, and the corresponding number of carbon peaks due to the benzothiazole aromatic ring were all observed. Final structural confirmation was verified through its CHN elemental analysis, where the greatest deviation of weight percent composition was for N = 0.15%.

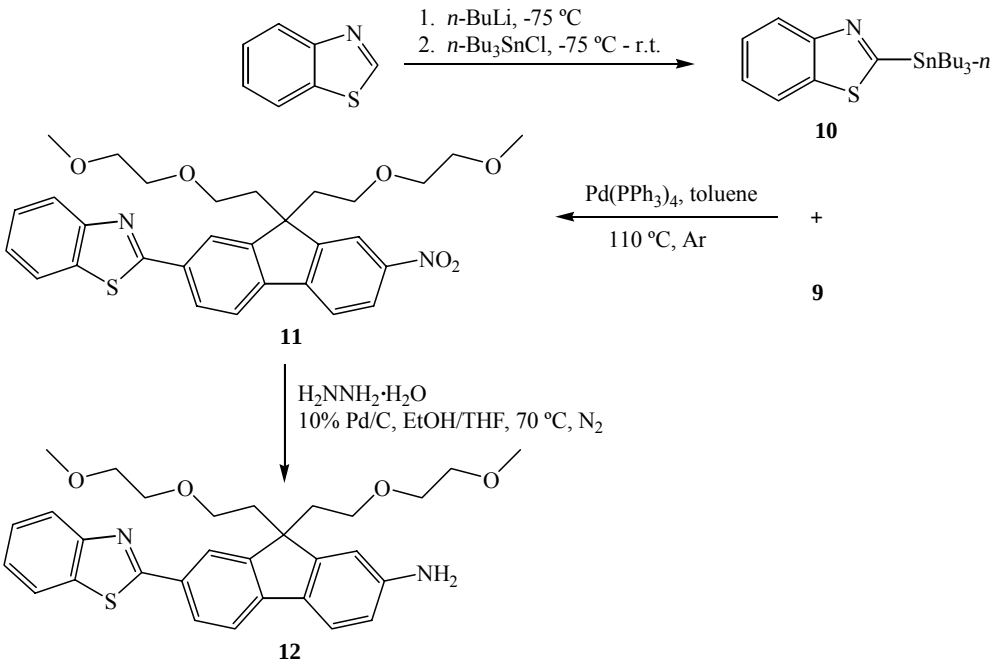

Scheme 4. Stille coupling to introduce the benzothiazole group, followed by nitro reduction conditions.

Fast, nearly quantitative, reduction of compound **11** was achieved with hydrazine monohydrate and 10% Pd/C in a 1/1 (v/v) mixture of EtOH/THF (Scheme 4). Compound **12** was obtained in 93% yield as a bright, yellow solid, with a relatively narrow melting range (137-139 °C). Immediately evident in the ^{1}H NMR spectrum were the primary amine (-NH_2) protons at 3.87 ppm as a slightly broad singlet. Additionally, positions of the two *ortho* protons to the -NH_2 group on fluorene shifted upfield to a singlet observed at 6.74 and a doublet at 6.68 ppm. Similarly, the ^{13}C spectra for compound **12** showed the *ortho* carbons to the –NH_2 group on fluorene upfield at 114.7 and 109.9 ppm.

Compound **12** was immediately used, to minimize potential oxidation of the primary amine, to prepare two new fluorescent dyes conforming to the A-π-D electronic architecture. Hence, compound **13** was attained via a copper-mediated Ullmann condensation of compound **12** with iodobenzene in *o*-DCB using K_2CO_3 as base and 18-

crown-6 ether at 180 °C (Scheme 5), and a bright yellow solid was obtained in 73% isolated yield. The ^{1}H NMR spectrum of compound **13** clearly showed the disappearance of the primary amino protons that were observed in compound **12** at 3.87 ppm. The *ortho* protons on the fluorene ring system to the -NH_2 also shifted downfield to where the new, electron-donating diphenylamine protons were observed from 7.29 – 7.01 ppm. The ^{13}C NMR spectrum of compound **13** revealed the downfield shift of the *ortho* carbons to the diphenylamine group on fluorene at 119.65 and 118.43 ppm. In addition to the increase in the number of carbon peaks observed due to the presence of the diphenylamine group, a notable appearance of the *para* carbon of the diphenylamine at 129.5 ppm was observed. Finally, structural verification was secured through its CHN elemental analysis, where the greatest deviation in the weight percent composition for compound **13** was for C = 0.23 %. The linear- and two-photon spectroscopic characterization of this compound was expected to and was found to be similar to a well-characterized analogue, compound **A** (Scheme 5). Further details of the spectroscopic properties of compound **13** and **14**, and comparisons to the analogue compound **A**, will be presented in Chapter 4.

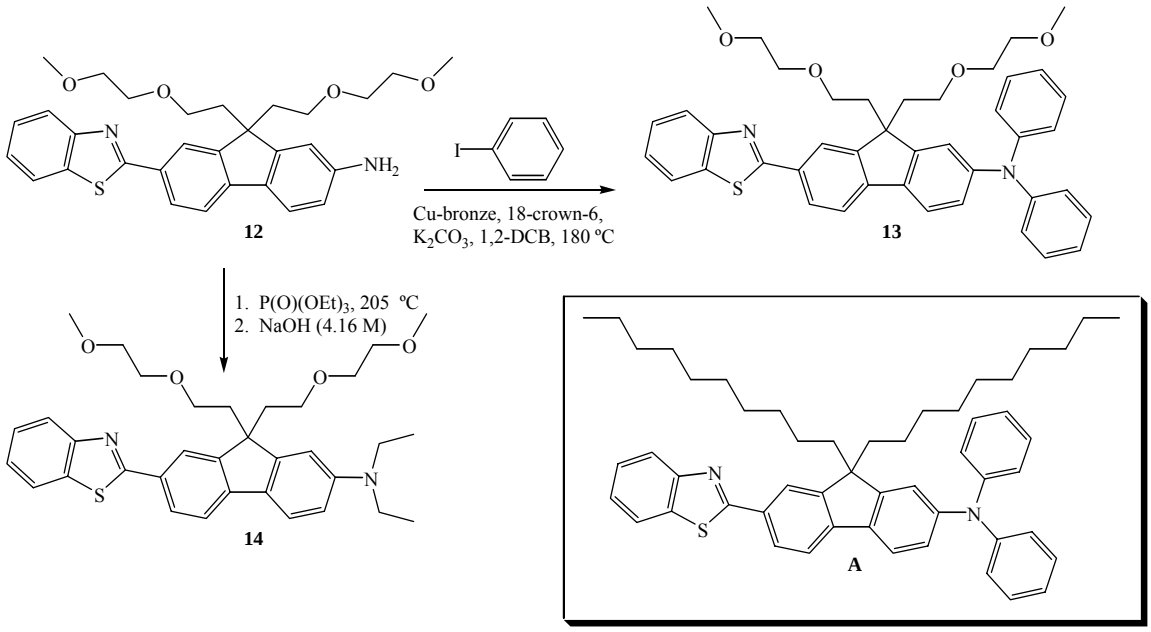

Scheme 5. Preparation of two, 2PA fluorescent contrast agents of the D-π-A electronic architecture.

Compound **12** was a useful intermediate, allowing for facile preparation of another potential contrast agent similar to that of compound **13**. Hence, N-alklyation of the primary amine in compound **12** with freshly distilled triethyl phosphate [61] yielded compound **14** as a bright green, viscous, oil in 69% isolated yield. The diethyl protons were clearly visible in the ^{1}H NMR spectrum, with the methylene (CH_2) protons observed as a quartet at 3.44 ppm and the terminal methyl protons as a triplet at 1.22 ppm. More compelling evidence for the diethyl substitution was supported by the ^{13}C NMR spectrum, with the methylene and the terminal methyl carbons observed at 45.1 and 13.1 ppm, respectively. The CHN elemental analysis provided the greatest deviation in the weight percent composition for N = 0.48%. A possible reason for this deviation may perhaps be due to presence of unacceptable levels of moisture being present. As this value resides outside the acceptable confidence limit for this type of analysis, a second, independent method to confirm the structure was obtained. Hence, high-resolution mass

spectroscopy (EI) identified the molecular ion (M+) of *m/z* = 574.2873, which corresponds to the exact mass analyzed for compound **14** composed of $C_{34}H_{42}N_2O_4S$ (574.29). Combined with the data obtained from the NMR spectra along with the results obtained from the HR-MS, verification of this structure was satisfied.

As a final note, the purification of compound **14** was tedious, requiring multiple purifications via flash column chromatography. A contributing factor to the purification problem may be due to the relative oxidative sensitivity of amino substituents, with aromatic amines being known to be more stable than aliphatic amines. Nevertheless, compound **14** was an attractive target, as the substitution of the diphenyl group with that of the diethyl group was expected to reduce the hydrophobicity of the fluorophore, and perhaps, contribute towards a more favorable compatibility with aqueous environments. Furthermore, the substitution of the diphenyl with that of the diethyl group does not appear to perturb the main π-π^* transition responsible for absorption and fluorescence, as will shown in Chapter 4.

This completes the discussion on the preparation of intermediates and hydrophilic fluorene-based dyes for potential use in two-photon excited fluorescence microscopy. Pertinent linear- and two-photon spectroscopic details of compound **13** and **14** will be presented in the next chapter. Demonstrated use of these dyes as fluorescent contrast agents in two-photon excited fluorescence microscopy in both glutaraldehyde-fixed cells and of live cells under *in vitro* conditions will be presented in Chapter 6.

3.5.3 Hydrophilic amine-reactive fluorene derivatives.

Fluorescent contrast agents serve their purpose in fluorescence imaging but do not provide the opportunity to specifically label a particular molecule or a protein of interest. Fluorescent compounds containing reactive functionalities for covalent bond formation with protein molecules to form a bioconjugate provide the distinctive advantage of specificity over general contrast agents. Bioconjugation involves the linking of two or more molecules to form a novel compolex having the combined properties of its individual components [58]. The ability to chemically attach a fluorescent molecule to proteins or other biomolecules of interest is a technology ubiquitously utilized, and the extent to which this has affected the research and practice of the life sciences is both pervasive and persistent. Many efforts have been developed to continuously develop and/or improve the current technology of bioconjugation. The advent and development of two-photon fluorescent microscopy systems provide new benefits for imaging, particularly in the area of live-cell imaging, that extends beyond what epi-fluorescent or linear confocal fluorescent microscopy systems provide. Hence, while the infrastructure for imaging have advanced to generate sophisticated techniques, probe development, particularly reactive reagents for bioconjugation, suitable for these imaging systems have progressed relatively slowly. This section will detail the attempt to address a particular need in two-photon fluorescence microscopy, specifically, the need for efficient two-photon absorbing and fluorescent compounds containing a reactive functionality, and in particular, an amine-reactive functional group, for covalent attachment onto protein molecules.

The goal towards an efficient two-photon absorbing fluorene-based fluorophore containing an amine-reactive functional group required maximal utilization of synthesis available from the key intermediate, compound **7**, shown in Scheme 2. Incorporation of the same ethylene-oxy group for enhanced hydrophilicity into the fluorophore architecture was performed using the same 9-alklyation conditions shown in Scheme 3. Controlling the reaction stoichiometry allowed for the isolation of the desired mono-substituted compound **8**, although the di-substituted compound **9** was always produced as well.

Nevertheless, compound **8** was isolated as a pale yellow oil which solidified into a waxy solid in ~ 30% yield. An obvious need for this reaction is an improved synthetic methodology that targets the mono-substitution product to increase its overall yield. The mono-substitution compound is desirable as the proton remaining on the 9-position of fluorene is chemically labile for introducing additional functional groups. Structural verification for compound **8** was validated in the ^{1}H NMR spectrum, where the 9-position proton on the fluorene ring was clearly visible as a triplet observed at 4.22 ppm. The terminal methyl protons were observed as a strong, clear singlet at 3.38 ppm, the internal methylene protons as complex multiplets from 3.56 – 3.47 ppm, and the methylene protons α to the 9-position of fluorene on the ethylene-oxy group was observed as a multiplet at 2.27 ppm. The aromatic proton positions and splitting patterns were nearly the same as those of observed for compound **7**. Likewise, the ^{13}C NMR spectrum for compound **8** was nearly identical to that of compound **9**. The positions of the observed resonance peaks were nearly the same, with the noted observation that the ethylene-oxy carbon signals in compound **8** were less intense than were observed for compound **9**. The

observed signal at 109.5 ppm was unidentifiable and seems to appear randomly in other ^{13}C NMR spectra collected on the fluorene compounds. Final structural verification for compound **8** was obtained through its CHN elemental analysis, where the greatest deviation in weight percent composition was found for C = 0.28%.

As stated above, the remaining proton on the 9-position of fluorene is available for additional chemical transformations. This flexibility was utilized to introduce a protected primary amine, which may later be transformed into an isothiocyante group. Hence, a commercially available *t*-butyloxycarbonyl (*t*-BOC) protected aminopropane was selected for inclusion into the fluorene architecture. The *t*-BOC protected aminopropyl group was expected to survive the subsequent transformation conditions for the construction of the target fluorophore. Standard conditions using trifluoroacetic acid (TFA) could then be employed to deprotect and generate the primary amine. The free amine could then easily be transformed into the isothiocyante reactive group, an amine-reactive reagent, as was demonstrated for the preparation of compound **2**.

The same alklyation condition to generate the fluorenyl anion with KOH was employed to incorporate the *t*-BOC protected aminopropyl group. Hence, compound **15** was obtained as a pale yellow residue in 53% isolated yield. The ^{1}H NMR spectrum was notably more complex than its precursor compound **7**. However, the amide proton was observed as a broad singlet at 4.29 ppm and the terminal methyl protons from the *t*-butyl group as a strong singlet at 1.38 ppm. The methylene protons from the propyl group were observed as multiplets at 0.76, 2.05, and 2.80 ppm. The singlet observed at 5.30 ppm is due to presence of the solvent, CH_2Cl_2, with the quartet at 3.48 and triplet at 1.21, also due to presence of the solvent, diethyl ether. More compelling evidence for the

inclusion of the *t*-BOC protected aminopropyl group was obtained through the ^{13}C NMR spectrum for compound **15**. In particular, the amide carbonyl carbon was observed downfield at 155.8 ppm, and the quaternary carbon of the *t*-butyl group as a weak signal at 79.5 ppm. These two positions are benchmark signals indicating the presence of the *t*-BOC protected aminopropyl group. Additionally, the terminal methyl carbons of the *t*-butyl group were observed as a strong signal at 28.8 ppm with the remaining propyl carbons at 54.0, 39.4, and 24.8 ppm. Finally, structural confirmation was secured from the CHN elemental analysis for compound **15**, where the greatest deviation in weight percent found was for C = 0.13%.

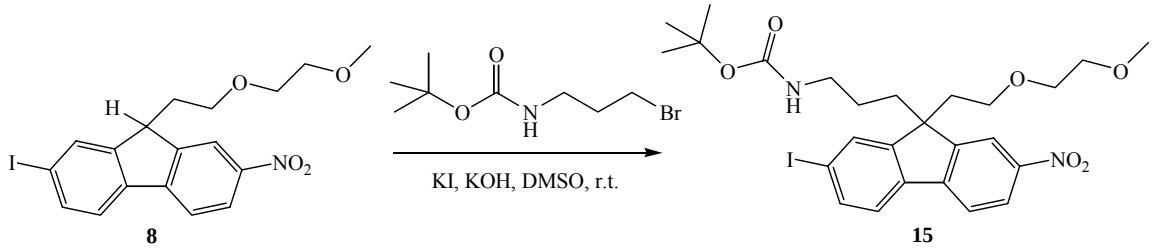

Scheme 6. Intermediates for a 2PA fluorescent amine-reactive reagent.

The same, Pd-mediated, Stille coupling conditions were employed to append the benzothiazole group onto the tentative amine-reactive fluorene conjugation system. Hence, compound **16** (Scheme 7) was isolated as a pale yellow residue in 84% yield. The aliphatic region of the ^{1}H NMR spectrum for compound **16** was nearly identical to that of compound **15**, with the amide proton was still clearly visible as a broad singlet at 4.30 ppm, along with the strong singlet for the methyl protons of the *t*-butyl group at 1.34 ppm. The aromatic region displayed marked differences from that of compound **15**, with the characteristic pair of triplet resonance signals from the outer benzothiazole aromatic

protons observed at 7.51 and 7.41 ppm. The ^{13}C NRM spectrum for compound **16** verified the presence of the bridge carbon joining the benzothiazole group to fluorene at its signature position observed at 167.4 ppm. The *t*-BOC protected aminopropyl group was preserved; the carbonyl carbon from the *t*-BOC protected aminopropyl group was observed at 155.8 and the terminal *t*-butyl carbons at 28.8 ppm. The CHN elemental analysis for this compound will need to be performed for final structural verification, although the NMR spectra appear to support the structure of the expected product.

The same nitro-reduction condition used to obtain compound **12** was used to obtain the primary amine group of compound **17** (Scheme 7). Hence, hydrazine mono-hydrate and 10% Pd/C was used to reduce the nitro to the amine to obtain a pale yellow powder in 84% yield. The primary amine protons were clearly observed as a broad singlet at 3.88 ppm, upfield to the amide proton at 4.22 as a broad singlet. Consequently, the *ortho* protons to the amino group on the fluorene ring system were shifted upfield to 6.69 and 6.66 ppm. That the *t*-BOC group was unaffected by the reduction conditions was further confirmed by the observation of the terminal methyl protons at 1.35 ppm. The ^{13}C NMR spectrum supported the nitro conversion to the amine, and consequently displayed the *ortho* carbons to the amino group on fluorene upfield to 114.67 and 109.68 ppm. The integrity of the *t*-BOC protected aminopropyl group was again verified upon the observed signals for the carbonyl carbon at 155.8 ppm and that of the quaternary carbon of the *t*-butyl group at 79.3 ppm.

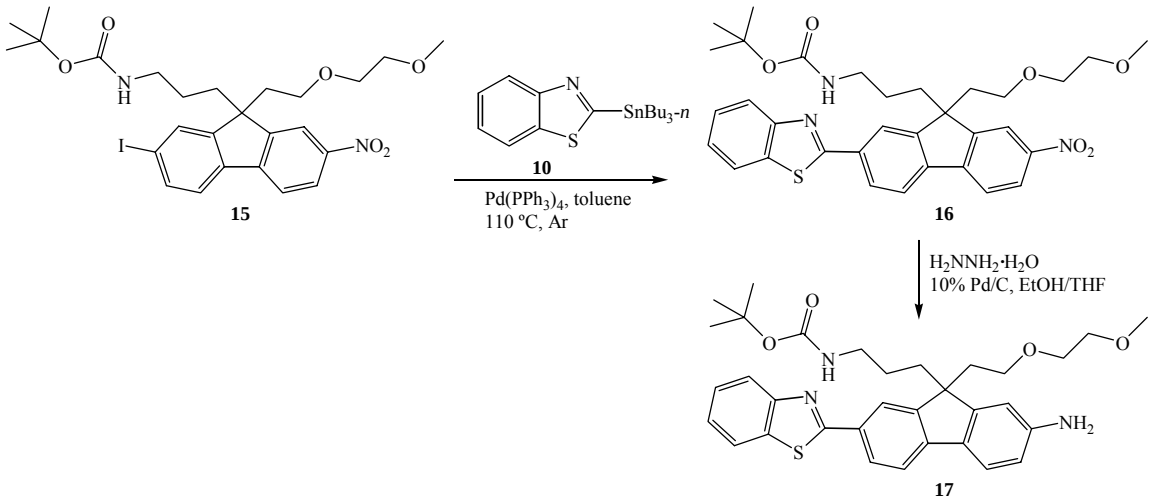

Scheme 7. Stille coupling to introduce the benzothiazole group followed by nitro reduction conditions on route towards a 2PA fluorescent amine-reactive reagent.

Compound **17** was subsequently subjected to the same copper-mediated Ullmann condensation with iodobenzen (Scheme 8) as was used to prepare the fluorescent contrast agent, compound **13**. However, this reaction proved very problematic for this compound. For instance, generation of compound **13** was relatively easy to observe utilizing thin-layer chromatography (TLC) techniques. As the reaction progressed, the gradual disappearance of the starting reagent over time correlated with that of a gradual increase in a fluorescent compound that was the expected product. While the reaction condition for compound **18** was identical to that employed for compound **13**, the expected product was not obviously identifiable as the reaction progressed. Monitoring the reaction via TLC revealed a very complex reaction mixture that increasingly became more so over time as evidenced by the generation of many observed components. Hence, after ~48 hours, the reaction was stopped, and after removal of the high-boiling solvent under reduced pressure, an attempt to isolate an identifiable compound via repeated flash

chromatographic efforts were unsuccessful. The reaction was repeated with similar results, and therefore, compound **18** was not isolated.

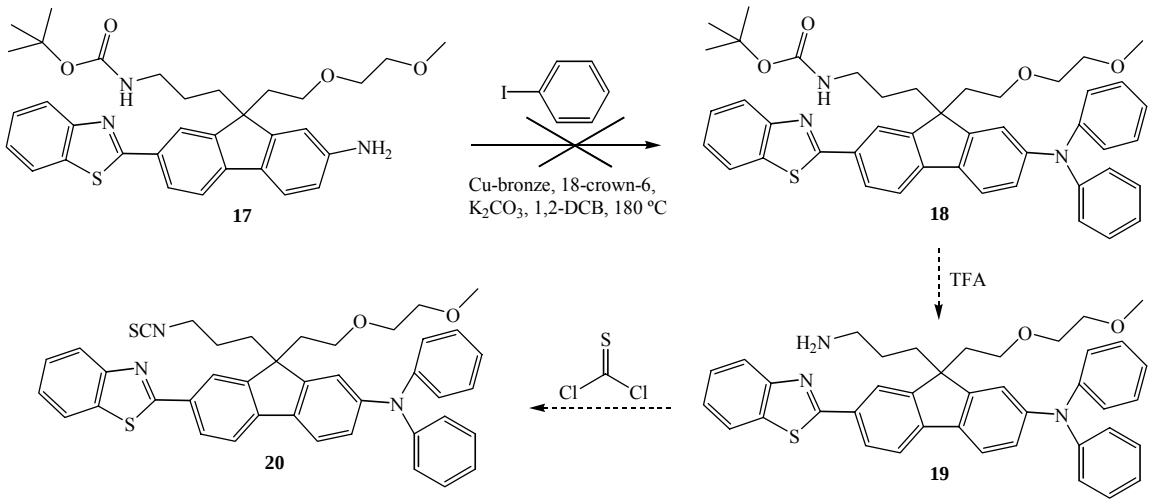

Scheme 8. Attempted synthesis towards a 2PA fluorescent amine-reactive reagent.

This untimely impasse was unfortunate, as the anticipated product was expected to possess key fluorescent properties ideal for two-photon excited fluorescence imaging. Furthermore, the incorporation of an amine-reactive functional group would have made compound **18** invaluable for bioconjugation techniques for two-photon fluorescence based applications. For instance, the *t*-BOC deprotection of the aminopropyl group with trifluoroacetic acid (TFA) to generate the free amine would have been ideal to incorporate the isothiocyante group (Scheme 8, compounds **19** and **20**) as was demonstrated for compound **2**. The placement of the reactive functional group at the 9-position of the fluorene ring system was expected to have minimal impact on the π-conjugation system predominantly responsible for efficient 2PA and upconverted fluorescence.

The anticipated importance that compounds with optimized nonlinear absorption and fluorescent properties may have in the area of two- and multi-photon fluorescence imaging applications is a strong impetus for persistent development of fluorescent agents. Efficient two-photon absorbers that are also photostable under high irradiation conditions required in two-photon based imaging applications are a premium, although incompatibility with aqueous environments will render them less useful for nonlinear bioimaging applications. The fluorescent compounds **13** and **14** are expected to be efficient two-photon absorbers that were sufficiently hydrophilic and were readily soluble in the polar solvent, DMSO, a miscible solvent with water. The properties detailing their linear- and two-photon absorption and fluorescence properties will be discussed in the following chapter. That they were also utilized as fluorescent contrast agents in two-photon excited fluorescence microscopy imaging of both fixed and live cells in *in vitro* conditions will be presented in Chapter 6.

The ultimate utility of an efficient two-photon absorbing reactive fluorophore resides in the versatility of its function as a photostable fluorophore and its specificity to target a compound of interest. Such targeting may be achieved if the fluorophore contains reactive functional groups amenable to bioconjugation techniques. A major effort of this project was to employ conventional synthetic methods to secure a fluorene-based fluorophore containing an amine-reactive functional group for covalent attachment onto protein molecules. While the synthetic method utilized was efficient in procuring sufficiently hydrophilic fluorescent contrast agents **13** and **14**, these methodologies to secure the amine-reactive fluorophore composed of the same fluorene base chromophore was unsuccessful. It is worth noting that the synthetic pathway currently utilized towards

target compound **20** is flexible, and alternative methods may be used to arrive at the same compound. For instance, it may have been possible to perform the Stille coupling to append the benzothiazole group, followed by the Ullmann condensation with iodobenzene from compound **8**. The *t*-BOC protected aminopropyl group may then be incorporated after these transformations, perhaps allowing for an alternative pathway towards compound **20**. Synthetic methods to develop such functional reagents are a major challenge and achieving this goal to secure compound **20** was met with an unexpected impasse that prevented its creation. New synthetic methodologies and alternative pathways can be used to secure this compound, and worthy efforts await its future development.

CHAPTER 4: SPECTROSCOPIC PROPERTIES OF FLUORESCENT FLUORENE DERIVATIVES

Details and discussions from the previous chapter highlighted the flexibility of the synthetic methods employed for the preparation of the fluorene derivatives targeted for this project, and how those structures were verified. Verification of compound structure allows confident studies of their spectral properties as discrete compounds. Hence, each isolated compound of interest may be studied to probe their properties, such as efficiency of photon absorption, fluorescence, their photostability under various excitation conditions, etc. This chapter will focus on key fluorene compounds and some aspects of their spectral properties in solution. The highlights of the linear- and two-photon absorption properties in solution of the hydrophobic amine-reactive fluorene compound **2**, and the model adduct product **3**, will be presented. Furthermore, demonstrated use of the amine-reactive probe **2** as a reagent to label BSA to generate a model bioconjugate 4 will also be presented. Subsequently, a discussion of the linear- and nonlinear spectroscopic properties of the more hydrophilic fluorene compounds, **13** and **14**, will be presented. A final discussion on anticipated spectroscopic properties of the putative, hydrophilic amine-reactive fluorene derivative **20** will be mentioned. Instrumental details and pertinent equations used for calculation of general spectroscopic properties can be found in Appendix B.

4.1 Hydrophobic Amine-Reactive Fluorene Compound and Its Adduct

The normalized UV-visible absorption and steady-state fluorescence emission spectra of the free amine-reactive probe (**2**) and the dye adduct (**3**) in DMSO are shown

in Figure 4.1 [57]. The free reactive fluorophore exhibits two absorption maxima at 357 and 375 nm, along with two emission maxima at 384 and 404 nm. Reaction of compound 2 with *n*-butylamine to form adduct **3**, produced a single absorption maximum at 363 nm with an emission maximum at 403 nm, that is well resolved, with minimal spectral overlap, from its absorption spectrum. The fluorescence quantum yield of the reactive reagent in DMSO was 0.02, virtually non-fluorescent, while that of the dye adduct in DMSO increased significantly to 0.74, indicating the fluorescence of the reactive tag is restored upon conjugation.

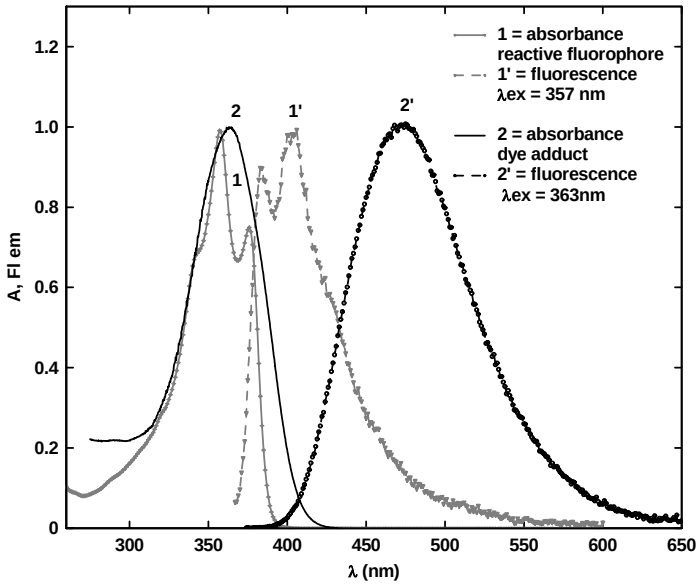

Figure 4.1. Normalized UV-visible absorbance (1, 2) and fluorescence emission (1', 2'; excitation line indicated) spectra of the amine-reactive compound 2, and dye adduct 3 in DMSO.

The two-photon absorption cross section for the dye adduct in DMSO was obtained using the two-photon induced fluorescence method (2PF) under femtosecond, near-IR irradiation conditions [57]. In the 2PF method, a strong, tunable pump beam excites the fluorophore via two-photon absorption, and the subsequent induced

fluorescence is monitored as a function of the excitation wavelength. The 2PF results obtained for the fluorophore under investigation are calibrated against well-known reference standards. Furthermore, the quadratic dependence of 2PF on the pump irradiance is verified for multiple excitation wavelengths. A more detailed explanation of this experimental setup can be found in Reference 12.

The linear absorption and fluorescence emission spectra of the model adduct (line and dashed profiles, respectively) and the two-photon induced fluorescence excitation spectrum measured at wavelengths twice that of the linear absorption (data points) are displayed in Figure 4.2. The 2PF measurements of the model adduct were performed in DMSO (1.6×10^{-3} M), and exhibited a 2PA cross-section of ~25 GM units at the linear absorption maximum of 370 nm. With its fluorescence quantum yield of ~0.74, the action cross-section for the model adduct is ~19 GM units. This is higher than most commonly used amine-reactive dyes. More importantly, additional hydrophilic fluorenyl derivatives, analogous in structure to compound **2**, are being developed and are expected to exhibit higher action cross-sections.

Interestingly, while the linear absorption spectrum for the compound does not display any significant absorption at the shorter wavelengths, the value of the 2PA cross-section increases, possibly accessing higher excited-state transitions of the fluorophore. To ensure the dye adduct is undergoing two-photon absorption, a log-log plot of the fs pump power to that of the integrated fluorescence was constructed. As can be seen from Figure 4.3, the slopes from the measurements (inset of graph) confirm the quadratic dependence of fluorescence obtained from a two-photon absorption process.

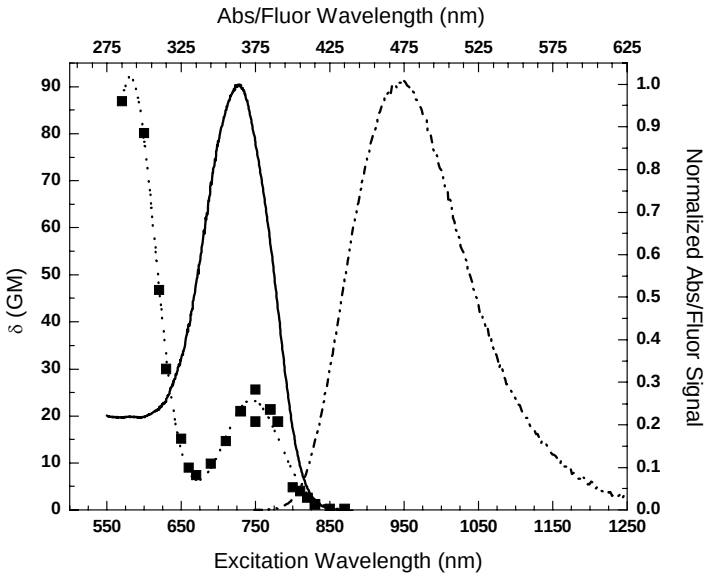

Figure 4.2. Linear and nonlinear spectra of adduct 3 in DMSO. The solid line is the normalized one-photon absorption spectrum; the dashed line is the normalized one-photon fluorescence spectrum. The two-photon induced fluorescence excitation spectrum is represented by filled symbols and the dotted line is a two-peaked Gaussian fitting function. The y-axis (left) denotes 2PA cross-sections in GM units (1 x 10^{-50} cm^4 sec $photon^{-1}$ $molecule^{-1}$) and the x-axis (bottom) represents the two-photon excitation wavelength.

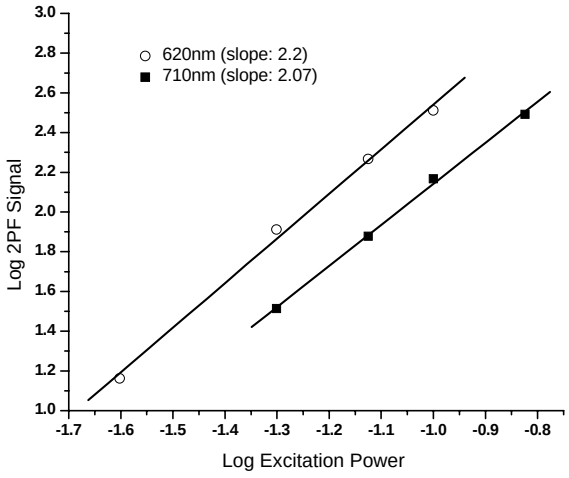

Figure 4.3. Log-log plot of two-photon induced fluorescence signal versus excitation power at two different excitation wavelengths extracted from the data shown in Figure 4.2. The solid lines are linear fitting functions whose slopes are indicated in the inset of the graph. The slopes show a quadratic dependence indicative of a two-photon induced process.

4.2 Characterization of a Model Bioconjugate

The amine-reactive fluorenyl reagent (**2**) was used to label bovine serum albumin (BSA) protein, a model biomolecule [57]. The use of BSA, an inexpensive protein that has been extensively characterized, is ideal for establishing optimal conditions to obtain a model bioconjugate, facilitating subsequent spectroscopic characterization. The isothiocyanate functionality reacts with aliphatic amine groups, including the N-terminus of proteins and the ε-amino groups of lysines (pKa ≈ 10.5). A typical protocol for conjugation was followed in an amine-free buffer under basic pH (pH = 9.0) conditions. The conjugate was identified spectrophotometrically and its steady-state fluorescence emission spectra subsequently obtained. Two different molar ratios of the reactive dye to protein under different reaction times were performed to assess the reactivity of the dye for its degree of labeling (DOL). The DOL was estimated using standard equations obtained from reference 55 and was tabulated in Chapter 3. The DOL is a key parameter to establish, as over-labeling of a fluorescent tag may interfere with the biological activity of a particular protein, and a DOL range of ~2.2 – 3.4 was obtained with the amine-reactive tag, a typical range for amine-reactive probes.

The normalized absorption and steady-state fluorescence emission spectra of the BSA-dye conjugate (**4**) in phosphate buffered saline (PBS) buffer (pH 7.2) are shown in Figure 4.4. For reference, the absorption spectrum of the free BSA protein in PBS solution is also shown. The conjugate displays absorption peaks corresponding to that of the BSA protein in the shorter wavelength range (λ_{max} = 280 nm), as well as that of the fluorescent tag in the longer absorption range (λ_{maxima} = 360 nm and 380 nm). The fluorescence emission of the bioconjugate is broad and exhibits an appreciable Stokes

shift. A bathochromic shift in the fluorescence emission was observed in the BSA-dye conjugate, relative to that of the free reactive fluorophore. Similar to the broadening observed in the absorption profile, the fluorescence emission of the model conjugate was also broader than that of the free fluorophore. The observed Stokes shift in the free dye was about 45 nm, while that of the BSA-dye conjugate was much greater (Stokes shift = 73 nm upon λ_{ex} = 360 nm, and 53 nm upon λ_{ex} = 380 nm). The fluorescence emission profile of the BSA-dye conjugate upon excitation at λ_{ex} = 360 nm and λ_{ex} = 380 nm yielded similar fluorescence intensities. The spectral profile of the model conjugate indicates the electronic property of the fluorene label is perturbed upon binding and may additionally be affected by the proximity of the protein. The di-decyl groups on the 9-position of the fluorene ring system in compound **2** is quite long and hydrophobic, potentially interacting with the protein to influence the local environment surrounding the π-conjugated fluorene ring system.

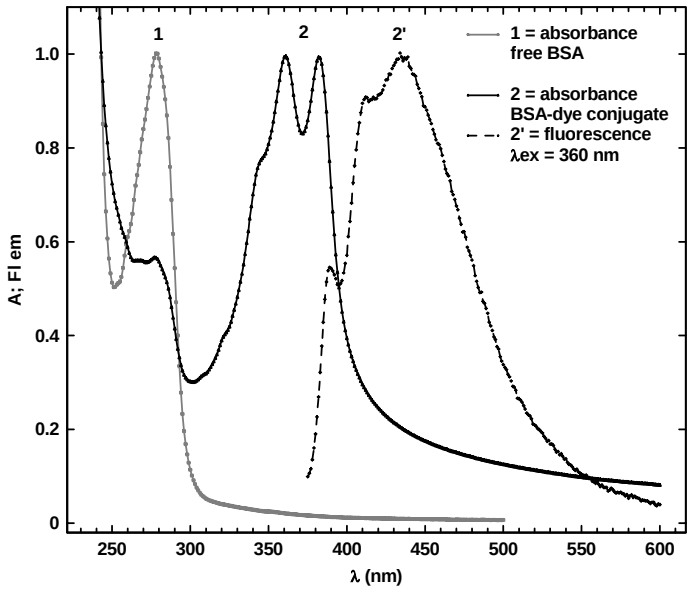

Figure 4.4. Normalized absorption spectra of the free BSA protein (1), BSA-fluorene conjugate (2), and steady-state fluorescence emission spectrum of the BSA-fluorene conjugate (2') in PBS solution.

The amine-reactive fluorene compound **2** is effective for covalent bond formation with a small molecule as *n*-butylamine. The fluorophore underwent sufficient two-photon absorption, as demonstrated by the quadratic dependence observed on its fluorescence signal to fs excitation pump power. However, the utility of this compound as a label for practical use in multiphoton bioimaging applications with bioconjugates is not without its shortcomings. The presence of the two large alkly substituents begs the question of compatibility with biomolecules and whether they may interfere with successful targeting of reactive sites available for conjugation. Additionally, while the fluorene chromophore was shown to undergo relatively efficient two-photon absorption, its two-photon absorption cross-section is far from optimal. That a relatively hydrophobic fluorene-based compound containing an amine-reactive functional group was effective in its reactivity towards a primary amine and was shown to undergo two-photon absorption followed by upconverted fluorescence, was strong motivation for the pursuit of more rationally designed fluorene-based fluorophores. Hence, fluorene compounds containing more hydrophilic pendent groups were pursued. The improvements in the two-photon absorption and fluorescent properties, relative to those of compound **2**, obtained on the hydrophilic fluorene derivatives, will be presented in the following section.

4.3 Hydrophilic Fluorene Compounds.

The linear- and two-photon absorption and fluorescence properties of compound **A** were extensively studied and provide for reliable comparisons to the spectroscopic properties of the more hydrophilic fluorene analogues [12,33,51]. Spectroscopic data

obtained on Compounds **A** and **13** are displayed in Figures 4.5, A – D. The linear UV-visible absorption spectra are shown in blue and the two-photon induced fluorescence excitation spectrum is represented by filled symbols with the dotted line providing a guide for the eyes. The y-axis (left) denotes 2PA cross-sections in GM units (1 x 10^{-50} cm^4 sec $photon^{-1}$ $molecule^{-1}$) and the x-axis (bottom) represents half the two-photon excitation wavelength.

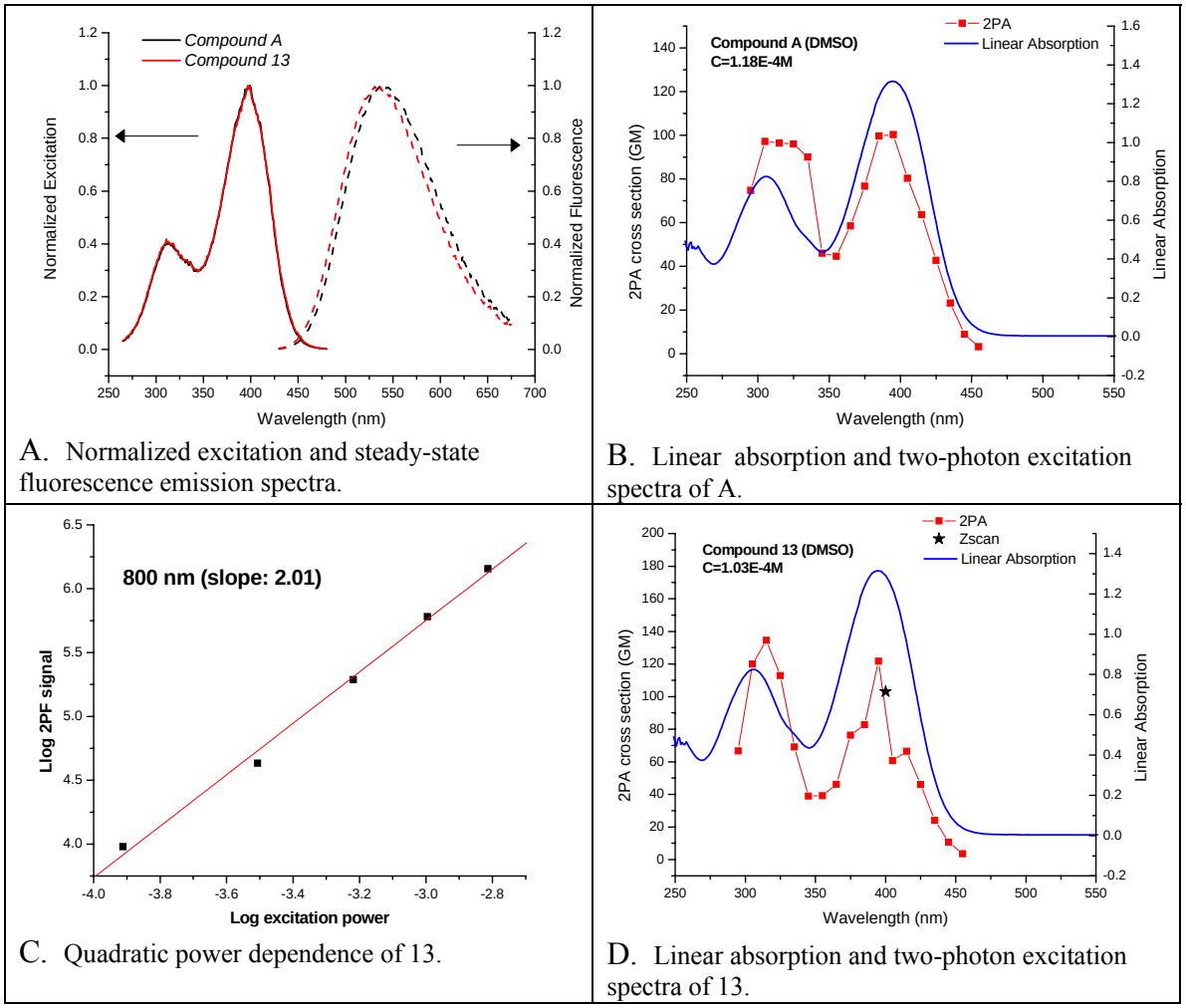

A. Normalized excitation and steady-state fluorescence emission spectra.

B. Linear absorption and two-photon excitation spectra of A.

C. Quadratic power dependence of 13.

D. Linear absorption and two-photon excitation spectra of 13.

Figure 4.5. Spectroscopic data of two analogous fluorene compounds, A and 13 in DMSO solution. A: Normalized excitation spectra and steady-state fluorescence emission spectra of both compounds. B and D: UV-visible absorption spectra are in blue, two-photon excitation spectra are shown as red filled symbols; red line act as guide for eyes only. Z-scan data (star symbol in B) was obtained at 800 nm. C: Steady-state fluorescence spectrum of both compounds was collected upon linear excitation of their absorption maxima. C: Log-log plot of two-photon induced fluorescence signal versus excitation power at 800 nm excitation wavelength for compound 13; slope of fitted line is indicated.

The two compounds are nearly identical in chemical structure, with the only difference arising from the pendent groups at the 9-position of the fluorene ring system. The substitution at the 9-position of the fluorene ring system appears to have minimal perturbation on the electronic properties of the fluorophores. This is apparent upon comparing the two linear excitation and UV-visible absorption spectra (Figures A, B, and D). Despite the substitution from the linear alkly groups of compound **A** to the ether groups of compound **13**, the linear UV-visible absorption and excitation spectra taken in DMSO are nearly identical, both in their profile shapes and range. The lowest excitable energy absorption band for each compound is centered at ~395 nm with the higher energy absorption band centered at ~305 nm. The electronic transitions for both compounds would, therefore, be nearly the same, and this expectation would be satisfied upon collection of additional spectral parameters.

That the 9-position substitution has negligible affect on the electronic properties is further corroborated in the steady-state fluorescence emission spectra collected for each compound in DMSO (Figure 4.5.A). The profiles and fluorescence emission range were found to be independent of excitation wavelength (data not show), and are nearly identical for each compound, with only a 5 nm blue-shift observed for compound **A**. The fluorescence quantum yield (η) for each was determined to be 1.0 in DMSO solvent, the highest achievable of any fluorophore. Furthermore, the energy difference between the linear absorption and the fluorescence emission peaks, the Stokes shift, for each compound was also similar. This indicates the energy difference between the ground state and that of the first electronic excited state of each are also comparable.

The linear, spectral properties of both compounds identify them as desirable candidates for fluorescent imaging applications. The large Stokes shift, coupled with the fluorescence quantum yield of unity, allows emitted photon to be detected against a low background, isolated from excitation photons, which may be suitable for typical linear fluorescent conditions. However, application and utility for multi-photon induced fluorescence imaging requires definition of additional spectral parameters of fluorophores. For a two-photon absorption process, a key parameter to identify would be the two-photon absorption cross-section (δ), in GM units (1 x 10^{-50} cm^4 sec $photon^{-1}$ $molecule^{-1}$), often obtained via the two-photon induced fluorescence method [12]. Much like the molar extinction parameter obtained from the linear UV-visible absorption spectrum of a chromophore, the two-photon absorption cross-section is an indication of efficiency for the indicated nonlinear absorption process across a range of excitation wavelengths. Essentially, the larger the δ value, the greater the probability of the two-photon absorption process at a particular excitation wavelength.

A perusal of δ values compiled on commonly used 'standard' fluorophores for two-photon imaging applications indicates their typical values are on the order of ~10 GM units. Hence, compounds whose δ values are greater than those of 'standard' compounds for nonlinear bioimaging are expected to outperform them. An evaluation of the two-photon excitation spectra for the two fluorene compounds, **A** and **13**, immediately reveals their δ values are nearly an order of magnitude larger than those of 'standard' fluorophores. The values of the two-photon absorption cross-section for both compounds are very similar over the excitation wavelength range and are nearly coincident with the linear absorption range. A foremost observation arises from the

relatively significant two-photon absorption into the first excited energy band, located in the linear absorbance spectra centered at ~ 395 nm for both compounds. This follows characterized trends for other dipolar (of the D-π-A architecture) fluorene compounds of relaxed molecular symmetries in which excited states may be both one- and two-photon allowed. A thorough treatment of one- and two-photon spectroscopic trends and characterizing molecular symmetry with observed transitions under these conditions in fluorene derivatives of varying electronic architecture can be found in references 12 and 51.

Needless to say, the two-photon excitation spectra of compounds **A** and **13** are similar to those observed for dipolar fluorene derivatives previously characterized. A noted exception in both of these compounds to the previously characterized spectra arises from the decreasing trend in the higher excited states for these compounds, located at ~300 nm. Investigation into this deviation observed in the higher energy transitions should be the subject of future studies, and, while interesting, the utility of these compounds for nonlinear fluorescence bioimaging applications resides in the properties obtained upon exciting the lower energy transition band. This restricted interest coincides with the tunability range of Ti:sapphire fs laser sources typically used in multiphoton fluorescence microscopy systems, where the performance of the ultrafast lasers is typically in the output range of ~700-900 nm, equivalent to a ~350-495 nm linear wavelength range. To obtain further confidence in the values of the 2PA cross-sections, an independent nonlinear absorption method, the Z-scan, was employed to collect the absolute value of 2PA at a particular excitation wavelength. While only one Z-scan data point is shown in the spectral data for compound **13** (Figure 4.5.D), the

magnitude of the obtained value at the linear equivalent wavelength of 400 nm coincides well with the values from the 2PF method.

Two-photon absorption by the compounds was further corroborated from the diagnostic, power-dependence studies, obtained from the 2PF method. Here, the irradiation power at a particular excitation pump is varied and the resulting upconverted fluorescence is collected. The integrated area of the two-photon induced fluorescence is plotted as a function of varied irradiation power, and the resulting slope can act as a figure of merit of the undergoing nonlinearity. Hence, the value of the slope (slope ≈ 2) obtained as a function of irradiation power at 800 nm excitation wavelength, verifies 2PA by compound **13** (Figure 4.5.C).

Similar spectral properties were obtained for compound **14**, containing diethyl groups in place of the diphenyl amino groups of compound **13**. Substitution of the small alkyl groups in place of the aromatic rings was expected to enhance the solubility of this compound in solution. Qualitative observation appears to confirm this expectation, as this compound is a viscous oil versus the crystalline solid of compound **13** at ambient temperature. It should be more soluable than the corresponding compound **14** in DMSO.

The linear, UV-visible absorption spectrum showed near-coincident placement of the lower energy transition band at ~405 nm (Figure 4.6 A - D). Interestingly, the higher energy transition band distinctly observed at ~300 nm in compounds **A** and **13** is suppressed in the absorption profile of compound **14**, indicating the contribution of the diethyl groups is less than the diphenyl group in this region. The large Stokes shift of ~140 nm is analogous to those observed for compounds **A** and **13** in DMSO, indicating the lower energy transition is also similar to these compounds. Finally, the two-photon

excitation spectrum of compound **14** is similar in magnitude, profile, and excitation range as those of compounds **A** and **13** in DMSO solution, and the quadratic power dependence verifies 2PA is the dominant process at 790 nm excitation wavelength.

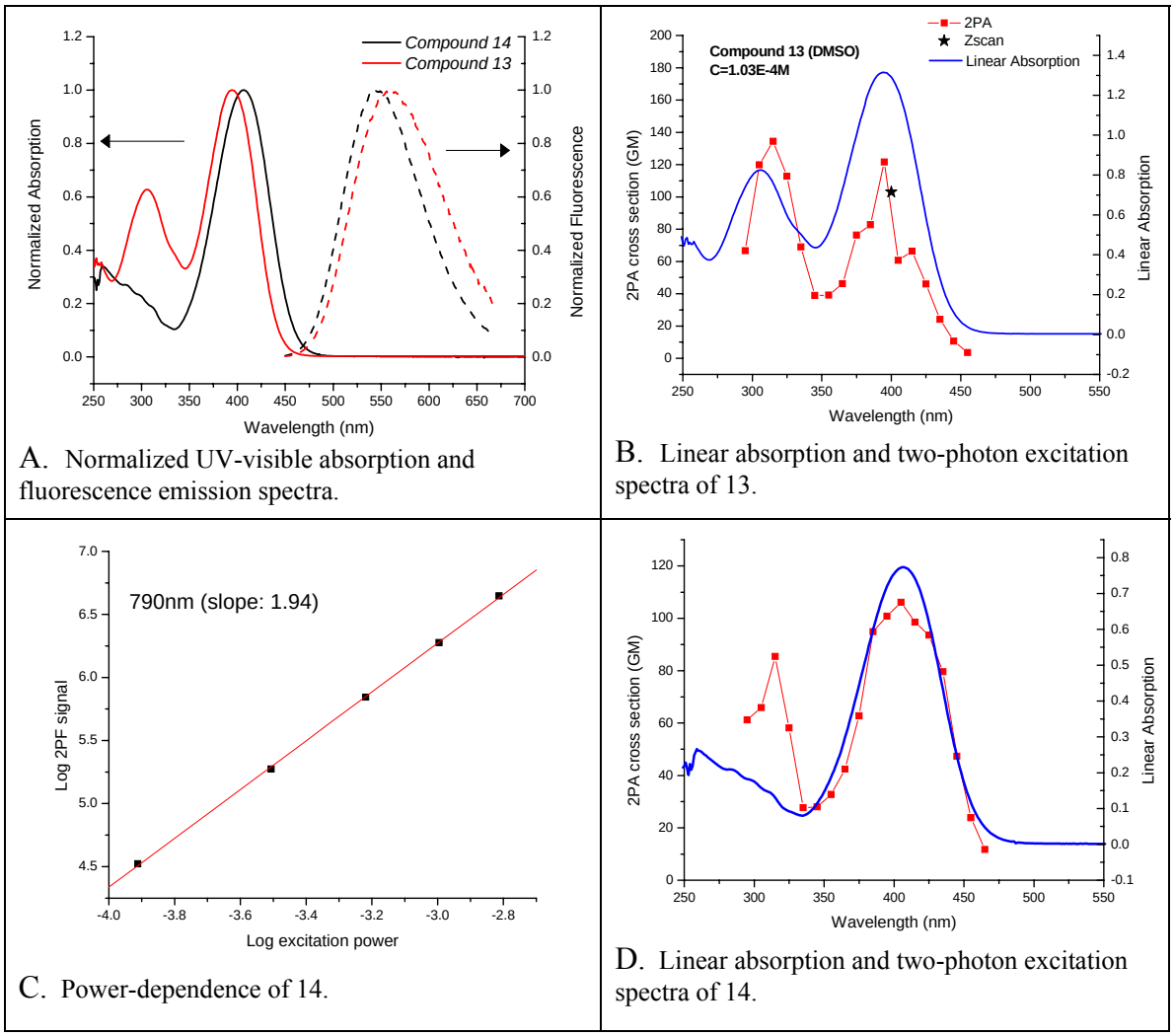

A. Normalized UV-visible absorption and fluorescence emission spectra.

B. Linear absorption and two-photon excitation spectra of 13.

C. Power-dependence of 14.

D. Linear absorption and two-photon excitation spectra of 14.

Figure 4.6. Spectroscopic data of analogous fluorene compound 14 in DMSO solution. A: Normalized UV-visible absorption and steady-state fluorescence emission spectra of both compounds. B and D: UV-visible absorption spectrum is in blue, two-photon excitation spectrum is shown as red filled symbols; red line act as guide for eyes only. C: Log-log plot of the two-photon induced fluorescence signal versus excitation power at 790 nm excitation wavelength for compound 14; slope of the fitted line is indicated with the excitation wavelength.

The summary of the spectral properties of the three compounds are tabulated below (Table 4.1). These compounds were identified as targets expected to exhibit improved spectral properties for two-photon induced fluorescence imaging applications. Certainly additional organic compounds have been prepared and characterized possessing greater nonlinear absorption properties. However, the fluorene compounds presented in this short description are more suitable for multiphoton bioimaging. They contain more hydrophilic pendant groups that enable them to be readily soluble in polar solvents compatible with aqueous environments. Additionally, these hydrophilic pendant groups do not perturb the electronic character responsible for efficient 2PA over the practical tunability range of excitation output of Ti:sapphire laser systems. Finally, exhibiting the most efficient fluorescence quantum yield possible for a fluorophore, the hydrophilic fluorene derivatives are promising candidates as efficient, 2PA fluorescent contrast agents for nonlinear bioimaging that are superior to many conventional 'standard' fluorescent contrast agents currently used. Demonstrated use of these compounds in two-photon induced fluorescence microscopy imaging of animal cells will be presented in subsequent chapters.

Table 4.1. Summary of pertinent linear- and two-photon spectral properties of 2PA fluorene derivatives obtained in DMSO solvent. * Error for the calculation of quantum yield is ±5 %.

Compound	$\lambda_{max\ abs}$ **(nm)**	$\lambda_{max\ fl}$ **(nm)**	$\Delta\lambda_{St}$ **(nm)**	η^*_{fl}	δ **(GM)**	$\eta_{fl}\delta$
A	394	534	140	1	122 (790 nm)	122
13	395	540	145	1	100 (790 nm)	100
14	406	544	138	1	106 (810 nm)	106

The hydrophilic fluorene compounds **13** and **14** have been shown to undergo efficient 2PA over a wide excitation wavelength range of the near-IR. The spectral properties of these compounds are expected to be superior, relative to standard fluorescent contrast agents currently in use. However, full utility of fluorene-base fluorescent agents reside in generating them as compounds integrated with reactive functionalities for specific targeting of biomolecules. Effort to secure an amine-reactive fluorenyl reagent (compound **20**) was met with an untimely synthetic challenge that prevented its isolation. Based upon the spectral properties revealed by the hydrophilic compounds **13** and **14**, it is expected that reactive, functional fluorine-based fluorescent compounds will be superior reagents for two- and mutliphoton fluorescent bioimaging, an expectation that awaits worthy pursuit and development.

CHAPTER 5: SPECTROSCOPIC PROPERTIES OF FLUORESCENT FLUORENE DERIVATIVES

The fluorene derivatives presented in the previous chapters were shown to undergo efficient 2PA over a large bandwidth of fs irradiation. The conjugated π-electron system comprising the fluorenyl chromophores give rise to a relatively strong molecular polarizability for sufficiently strong nonlinear absorption upon excitation. Additionally, the aromatic ring system also affords a high fluorescence quantum yield upon photon energy absorption. These organic molecules with strong nonlinear properties are expected to outperform standard fluorophores currently in use for nonlinear fluorescence imaging applications. However, if the compounds cannot withstand the intense irradiation conditions required for nonlinear excitation, their premium optical properties will be rendered useless for long-term imaging applications. Hence, the photostability of organic compounds is a key parameter to establish, and facilitates their full utility in critical applications in, for instance, nonlinear fluorescent bioimaging. The following discussion will concentrate on photostability studies in solution of some fluorene derivatives. Initial results indicate one- and two-photon photodegradation of these derivatives is low, i.e., they are robust and resilient to high irradiation conditions. Consequently, fluorene-based fluorophores are strong candidates for use in two-photon fluorescence microscopy.

5.1 Photochemical Stability of Substituted Fluorene Derivatives under 1PE

Reports on the effect of solvent and substituent on the photooxidation of fluorene was previously investigated [62]. The results indicated that the rate of photooxidation

was solvent dependent, and mainly due to the difference in the solubility of atmospheric oxygen in the solvent. The presence of -COOH and -CH_2COOH groups at the 9 position of fluorene decreased its photochemical and thermal stability. The photochemistry of fluorene at a silica gel/air interface was also reported [63] and an electron transfer mechanism for the formation of fluorenone by direct photolysis of fluorene was proposed. In general, relatively little is known about the photochemical reactivity of fluorenes. Therefore, the photochemical investigation of new 2PA fluorene derivatives is important to understand their possible applications and limitations.

A comprehensive investigation of the photochemical stability, particularly photooxidative stability, of a series of analogous fluorene derivatives with different electron-donating and electron-withdrawing substituents that also possess both high two-photon absorptivity and high fluorescence quantum yields were investigated in air- and N_2-saturated acetonitrile (ACN) at room temperature [33c-h]. The structures of the fluorene compounds are shown in Figure 5.1. The quantum yields of the photoreactions were determined at various concentrations of the fluorene derivatives, oxygen concentration of the solvent, and linear, UV-visible irradiation wavelength. The absorption and fluorescence spectra of the photoproducts, corresponding to different linear excitation conditions, were analyzed, and full details of the spectroscopic techniques can be found in reference 33c and in Appendix B. A more thorough discussion on the photostability of compound **A** under one- and two-photon excitation conditions will be presented in the subsequent section.

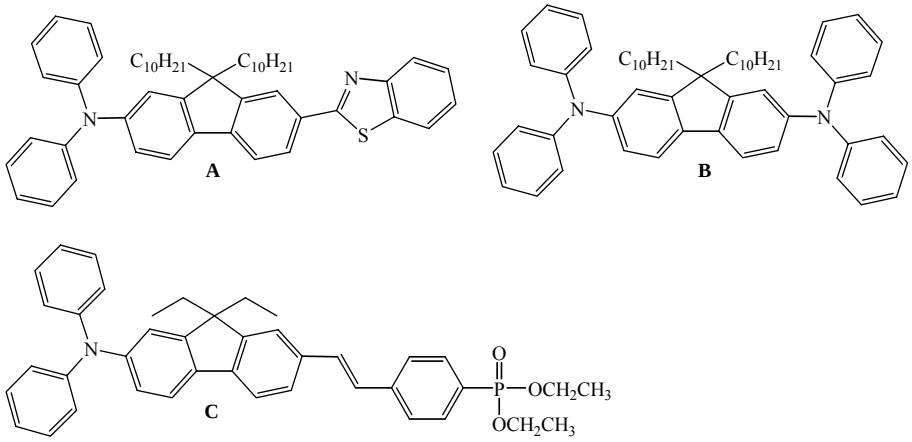

Figure 5.1. Structures of fluorene compounds investigated for photostability studies.

Detailed photophysical characterization of fluorene derivatives **A** - **C** in ACN and other aprotic solvents was described previously [33h]. These compounds are characterized by high fluorescence quantum yields in ACN (0.9±0.08 (**A**), 0.7±0.1 (**B**), and 0.9±0.08 (**C**)), which were nearly independent of the oxygen concentration in the solvent. In order to understand the major factors that contribute to the photodegradation of fluorene derivatives **A** – **C**, the quantum yields of the photoreactions (Φ) were measured at different concentrations, linear irradiation wavelengths, and oxygen concentration, and the results of these data are presented in Table 5.1. For higher concentrations (C ~ 2-5 x 10^{-5} M), the values of Φ were obtained from time-dependent absorption spectra of **A** – **C** upon $\lambda_{irr} \approx 360$ nm, and the corresponding Φ for $\lambda_{irr} \approx 250$ nm are presented in Table 5.1. For lower concentrations, (C ~ 1-3 x 10^{-6} M), the photoreaction quantum yield Φ, was measured by the fluorescence method, as described in detail in reference [33c], for different λ_{irr} in the spectral region 240 nm < λ_{irr} < 400 nm. Thus, the wavelength dependent quantum yields, $\Phi(\lambda_{irr})$ were obtained at low

concentrations for **A** - **C** in ACN, facilitating the photochemical analysis of these compounds under linear UV-visible excitation conditions.

Table 5.1. Quantum yields Φ, of the photoreactions of compounds **A** - **C** at different concentrations, C, excitation wavelength, λ_{exc} , and oxygen content in ACN. C* denotes the solutions were air-saturated; C^{N2} denotes the solutions were N_2-saturated.

Φ, λ excitation, Concentration	Fluorene **A**	Fluorene **B**	Fluorene **C**
Φ, λ_{exc} = 360 nm C* (M)	$(3.5 \pm 0.6) \times 10^{-4}$ 2.4×10^{-5}	$(6.5 \pm 1) \times 10^{-4}$ 4.5×10^{-5}	$(3.9 \pm 0.7) \times 10^{-4}$ 2.5×10^{-5}
Φ, λ_{exc} = 250 nm C* (M)	$(2.3 \pm 0.4) \times 10^{-4}$ 2.4×10^{-5}	$(6.5 \pm 1) \times 10^{-4}$ 4.5×10^{-5}	$(1.7 \pm 0.3) \times 10^{-4}$ 2.5×10^{-5}
Φ, λ_{exc} = 360 nm C^{N2} (M)	$(2.7 \pm 0.4) \times 10^{-6}$ 2.4×10^{-5}	$(1.8 \pm 0.3) \times 10^{-4}$ 4.5×10^{-5}	$(1.6 \pm 0.3) \times 10^{-5}$ 2.5×10^{-5}
Φ, λ_{exc} = 250 nm C^{N2} (M)	$(6.3 \pm 1) \times 10^{-6}$ 2.4×10^{-5}	$(5 \pm 0.8) \times 10^{-4}$ 4.5×10^{-5}	$(5.8 \pm 1) \times 10^{-5}$ 2.5×10^{-5}
Φ, λ_{exc} = 360 nm C* (M)	$(3 \pm 1) \times 10^{-5}$ 1.6×10^{-6}	$(6.5 \pm 1.5) \times 10^{-5}$ 2.4×10^{-6}	$(2.3 \pm 0.6) \times 10^{-4}$ 1.6×10^{-6}
Φ, λ_{exc} = 250 nm C* (M)	$(1.2 \pm 0.5) \times 10^{-5}$ 1.6×10^{-6}	$(3.5 \pm 1) \times 10^{-5}$ 2.4×10^{-6}	$(6 \pm 1.5) \times 10^{-5}$ 1.6×10^{-6}

The analyses of the quantum yields of the photoreactions, in conjunction with analysis of the absorption and fluorescence spectra of the photoproducts, suggested the following mechanisms for the photodegradation of compounds **A** - **C**: 1) singlet oxygen formation via sensitization by excited fluorene molecules, followed by bimolecular reaction between $^1O_2$ and the ground state fluorene derivative; 2) direct molecular oxygen $^3O_2$ reaction with the excited fluorene derivative; and 3) electron transfer processes with the formation of stable cation radicals (or other nonfluorescent photoproducts) with absorption at $\lambda \geq 440$ nm. The photochemical decomposition of **A** was primarily influenced by singlet oxygen formation and decreased by over two orders of magnitude when oxygen was excluded. Symmetrical fluorene derivative **B** exhibited reactivity that

can largely be attributed to photoreaction with singlet oxygen and electron transfer processes. Photostability of **C** was dependent on oxygen concentration in the solvent, suggesting a dominant role of molecular oxygen $^3O_2$ in the photodecomposition processes. Appearance of long wavelength absorbing species also suggested that an electron transfer process occurred in the photodegradation of **C**, resulting in formation of cation radical photoproducts. The low photochemical quantum yield ($\Phi \sim 10^{-4}$ and $\sim 10^{-6}$ in oxygen-reduced environments) suggests the photostability of compounds **A – C** are relatively high under linear excitation conditions, and approximately 1-3 orders of magnitude more photostable than most commonly used fluorescent probes.

5.2 Photochemical Stability of Substituted Fluorene Derivatives Under 2PE

The fluorene derivatives shown above appear to be robust under linear UV-visible irradiation conditions. As stated previously, organic molecules with strong nonlinear properties are expected to outperform standard fluorophores currently in use for nonlinear fluorescence imaging applications, though their full utility is likely dependent upon their photostability under nonlinear excitation conditions. While some of these highly fluorescent fluorene compounds have been shown to be relatively photostable under linear excitation conditions, their photostability under nonlinear excitation conditions are more germane for two-photon fluorescence imaging applications. Hence, comparative photostability studies under one- and two-photon excitation of compounds **A** and **B** (structures shown above) will be presented as representative photochemical properties of substituted fluorene derivatives. These studies reiterate their high photostablity under linear, one-photon excitation, but more importantly, indicate relatively high photostability

under two-photon excitation as well. A summary of these results will be presented below, and a more complete and detailed explanation of the photochemical properties of each of these compounds under one- and two-photon excitation can be found in references 33d and 33e.

Two-photon absorption processes can be conceptualized through considering a simplified electronic state diagram (Figure 5.2) for S_0 (ground state) and S_1 (first excited state). As shown below, both one- and two-photon absorption generally results in the same electronic level from which photoreactions may take place. Photobleaching processes resulting from intense laser irradiation can occur by one- or two-photon absorption, or two-step successive absorption of two photons within one laser excitation pulse. High irradiation intensity can also generate molecules excited to higher electronic states from which photochemical reactions such as photoionization and bond fission may occur [64]. These photoprocesses may be different from reactions of the molecule in its lowest excited state, produced by low intensity excitation. The comparison of one- and two-photon excitation may help to reveal the nature of dominant photobleaching processes of organic dyes and determine the peculiarities of their photochemical behavior. For example, Kao *et al.* recently revealed distinctions between one- and two-photon induced photobleaching processes in protoplasts [65]. It was shown that high intensity, multi-photon excitation impacted the molecules in ways much different than under low intensity, linear irradiation conditions. Hence, one cannot assume organic compounds to behave similarly under linear and nonlinear excitation conditions, and elucidating their photochemical properties will facilitate not only an understanding of

their photochemical reactivity but, ultimately, their usefulness and limitations for emerging nonlinear optical applications.

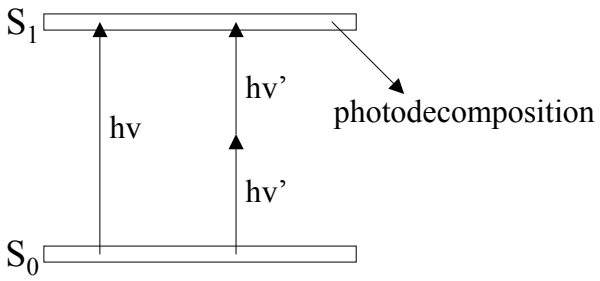

Figure 5.2. Simplified diagram of the one- and two-photon excitation processes.

5.2.1 Fluorene A (D-π-A) under one- and two-photon excitation.

The photochemical properties of fluorene derivative **A** in *n*-hexanes and CH_2Cl_2 were studied under linear (one-photon) and nonlinear (two-photon) excitation at room temperature. Photochemical parameters were measured by the absorption and fluorescence methods, comprehensively described in [33d]. Here, the quantum yields of the photoreactions were determined as a function of dye concentration and solvent polarity. The absorption and corrected fluorescence emission spectra of fluorene **A** in hexanes and CH_2Cl_2 are presented in Figure 5.3. The maxima of the fluorescence spectra of **A** (curves 1', 2') exhibited a strong dependence on solvent polarity. This is in contrast to the solvent insensitive absorption spectra (curves 1, 2). Hence, no specific interactions of **A** with solvent molecules occurred.

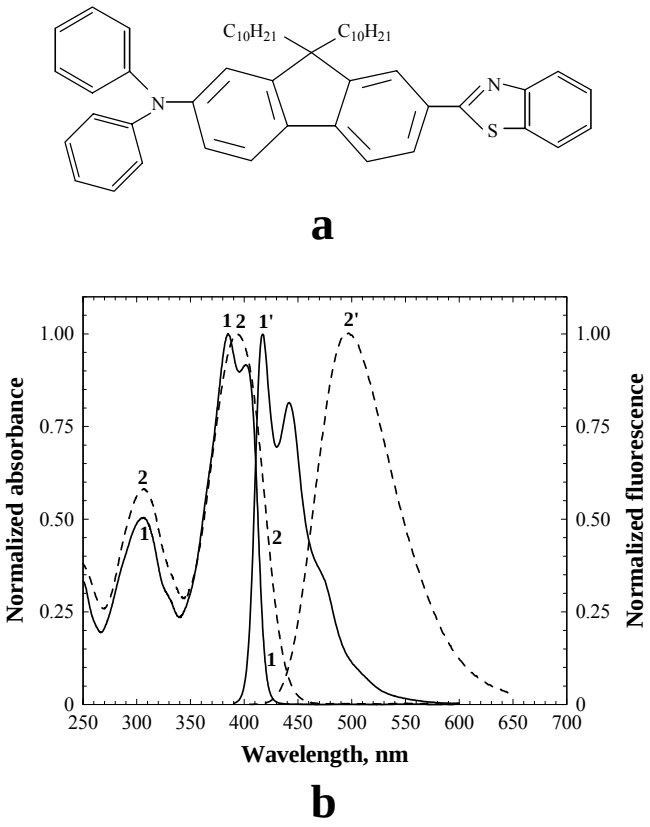

Figure 5.3. (a) Structure of **A**. (b) Normalized absorption (1, 2) and fluorescence (1', 2') spectra for **1** in hexane (1, 1') and CH_2Cl_2 (2, 2').

The absorption method was used for the determination of the photoreaction quantum yields in air-saturated and deoxygenated solutions under one-photon excitation. The changes in the absorption spectra of **A** in hexanes and CH_2Cl_2 under UV irradiation ($\lambda_{exc} \approx 355$ nm) as a function of dye concentration revealed the photobleaching processes of **A** are complex. This was manifested as variable rates of photobleaching occurring upon irradiation, except in low concentration hexanes solution in which the photobleaching rate was essentially constant. Hence, the quantum yields of the photoreactions, Φ_i, were calculated for each small intermediate change in the optical density, ΔD_i, at the corresponding irradiation time, Δt_i = 15 min or 30 min (i = 1 - n, n is the number of measurements). The averaged values of $\Phi = \Sigma\Phi_i / n$ for the entire

irradiation time are given in Table 5.2. The photochemical quantum yield exhibited a weak dependence on dye concentration for both solvents. This suggests that the photochemical processes of **A** in hexanes and in CH_2Cl_2 correspond primarily to first order photoreactions, especially at low concentrations in hexane ($C \leq 10^{-5}$ M), when a constant rate of photobleaching was observed.

Table 5.2. Quantum yields of the photoreactions for **A** in air saturated, Φ, and deoxygenated, Φ^d, solutions with different concentrations, C, under one- (Φ, Φ^d) and two-photon (Φ_{2PA}) excitation.

C (M)	Hexane			CH_2Cl_2		
	$\Phi \times 10^5$	$\Phi^d \times 10^4$	$\Phi_{2PA} \times 10^5$	$\Phi \times 10^5$	$\Phi^d \times 10^4$	$\Phi_{2PA} \times 10^3$
1.3×10^{-3}	5±2	-	5±3	4±1.5	-	2±1
3×10^{-4}	4.5±1.5	1.2±0.4	4.5±2	3.5±1	1.2±0.4	1.5±0.5
8×10^{-5}	4±1.3	1.5±0.5	3±1	4±1.2	1.3±0.4	2±1
2×10^{-5}	5±1.5	1.2±0.4	3.5±1.2	3±1.3	1±0.3	0.8±0.4
3×10^{-6}	3.5±1	1.4±0.4	3±1	2.5±0.8	0.8±0.25	0.9±0.45

As a result of photoreaction, an absorption band of the photoproducts of **A** appeared at ≥ 430 nm in CH_2Cl_2 (data shown in 33d). This is in contrast to what was observed in hexane solutions, where changes occurred mainly in the spectral range corresponding to the main absorption band (< 420 nm). The appearance of the longer wavelength absorption, in the spectral region ≥ 430 nm, is likely due to an electron transfer reaction of **A** (for example, electron transfer from the nitrogen of the diphenylamino group to polar CH_2Cl_2), resulting in the formation of a stable cation radical [66]. In hexane, no long wavelength absorbing photoproducts were observed, consistent with electron transfer only occurring in electron accepting solvents. In this case, photoproducts were generated that only absorbed in the shorter wavelength spectral region ($\lambda \leq 350$ nm). Deoxygenation of the solutions led to an increase in the

photochemical quantum yields of **A** by 2 - 5 times (Table 5.2), i.e. a decrease in photostability. These results suggest an unexpected role of molecular oxygen in the photostability of **A**, possibly quenching a potentially reactive excited state species, e.g., a triplet state leading to efficient return to ground state.

The quantum yields of the photochemical reactions for **A** in hexanes and CH_2Cl_2 under two-photon excitation (λ_{exc} = 760 nm; $\tau_P \approx$ 120 fs; f = 1 kHz) were obtained by the fluorescence method described in detail in reference 33d. The temporal dependences of the fluorescence intensity of **A**, F(t), were measured under two-photon irradiation, and the quantum efficiencies of the photoreactions, Φ_{2PA}, for different dye concentrations are listed in Table 5.2. The analysis of these data reveals a weak dependence of Φ_{2PA} on dye concentration, similar to the photochemical behavior of **A** under one-photon excitation. Thus, a dominant role of first-order photoreactions can also be assumed.

The Φ_{2PA} for **A** in CH_2Cl_2 increased 30-50 times relative to those obtained for low intensity one-photon irradiation, reaching a maximum of $\Phi_{2PA} \approx 2 \times 10^{-3}$. In contrast, nearly the same photochemical quantum yield for **A** was observed for both one- and two-photon excitation in hexane ($\Phi \approx \Phi_{2PA} \approx (3 - 5) \times 10^{-5}$). In order to understand this photochemical behavior, the influence of the excitation intensity, I, on the efficiency of the photobleaching was studied. Figure 5.4 illustrates the temporal changes in the optical density, $\Delta D/\Delta t$, on I^2 for the solutions of **A** in hexane and CH_2Cl_2 under two-photon excitation. For a pure two-photon excitation process, a quadratic dependence of $\Delta D/\Delta t$ on I can be expected. In general, the value of $\Delta D/\Delta t$ can be expressed as:

$$\Delta D/\Delta t \sim \sigma_{2PA} I^2 (k_1 + \sigma_{1n} I k_n \tau_n) \tau_1 \quad (1)$$

where k_1, k_n and τ_1, τ_n are the rate constants of the photochemical decomposition and lifetimes of the first, S_1, and higher excited, S_n, electronic states of **A**, respectively; σ_{1n} is the one-photon absorption cross-section for the transition $S_1 \rightarrow S_n$ at λ_{exc} = 760 nm.

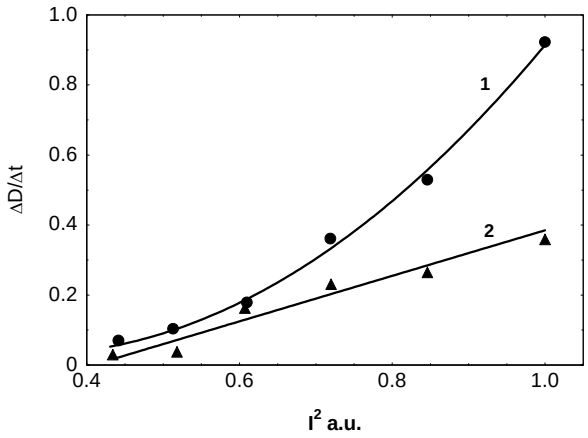

Figure 5.4. Temporal changes in the optical density, $\Delta D/\Delta t$, of **A** as a function of the square of excitation intensity, I^2, in CH_2Cl_2 (1) and hexane (2).

In Figure 5.4, a quadratic dependence of $\Delta D/\Delta t$ on I in hexanes can be seen (i.e. $\Delta D/\Delta t \sim I^2$), suggesting the dominance of photoreaction from the first excited state, S_1, i.e. $k_1 >> \sigma_{1n} I k_n \tau_n$ (since 760 nm radiation is only energetic enough to produce two-photon absorption into S_1 or the longer wavelength absorption band). In contrast, there was a substantial increase in the photochemical decomposition of **A** in CH_2Cl_2, relative to hexane, and corresponded to a cubic dependence $\Delta D/\Delta t \sim I^3$. This dependence can be explained by an additional one-photon absorption processes from S_1 at λ_{exc} = 760 nm, and effective photochemical reaction from the higher excited state S_n, when $k_1 << \sigma_{1n} I k_n$

τ_n. Hence, more efficient photochemical decomposition of **A** was observed from higher excited electronic states.

The photochemical decomposition of fluorene **A** in hexane and CH_2Cl_2 under one-photon (linear) excitation resulted in the quantum yield of the photoreaction $\Phi \approx (2.5 - 5) \times 10^{-5}$. Under these conditions, the photodecomposition was approximately a first order process. In air-saturated solutions, the one-photon photodecomposition of **A** is suppressed 2-5 times relative to that in deoxygenated solutions, revealing an important role of molecular oxygen in the photostability of compound **A**. Under two-photon excitation, the quantum yield of the photodecomposition for **A** in hexane was nearly the same, $\Phi \approx (3 - 5) \times 10^{-5}$ as under single-photon excitation and independent of irradiation intensity. This can be ascribed to a dominant photoreaction occurring from the first excited state of **A**, and to photoprocesses similar to those observed for one-photon excitation. In contrast, the quantum yields of the photochemical reactions of **A** in CH_2Cl_2 under two-photon excitation increased by 30 - 50 times ($\Phi_{2PA} \approx 2 \times 10^{-3}$) relative to single-photon excitation, and exhibited a clear dependence on the irradiation intensity. This behavior can be explained by an additional one-photon absorption from the first excited state, followed by subsequent photoreaction from higher electronically excited states. Overall, **A** exhibited relatively good photostability, making it suitable for use in linear and nonlinear optical applications.

5.2.2 Fluorene B (D-π-D) under one- and two-photon excitation.

Similar linear- and two-photon spectroscopic treatment of the symmetrically substituted fluorene compound **B** was performed in hexanes and in CH_2Cl_2 [33e]. The

UV-visible absorption, corrected fluorescence emission, and anisotropy spectra of **B** are presented in Figure 5.5. The absorption maximum was nearly independent of solvent polarity (curves 1, 2). The fluorescence spectrum exhibited a weak dependence on solvent polarity (curves 1', 2'), indicating **B** undergoes a small change in dipole moment upon excitation. The excitation anisotropy spectrum of **B** in viscous silicon oil (curve 3) revealed the nature of the absorption band. A constant value of anisotropy in the spectral region $\lambda \geq 340$ nm corresponded to the first electronic transition from the ground, S_0, to the first excited, S_1, electronic states. The decrease in anisotropy at $\lambda \approx 300$ nm (short wavelength absorption maximum) corresponded to the second electronic transition $S_0 \rightarrow S_2$ (S_2 = second excited state).

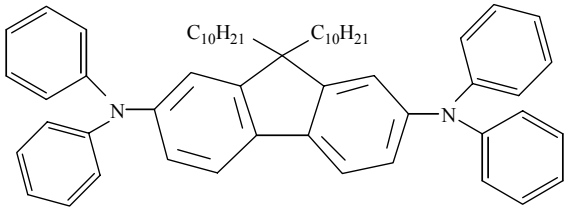

a

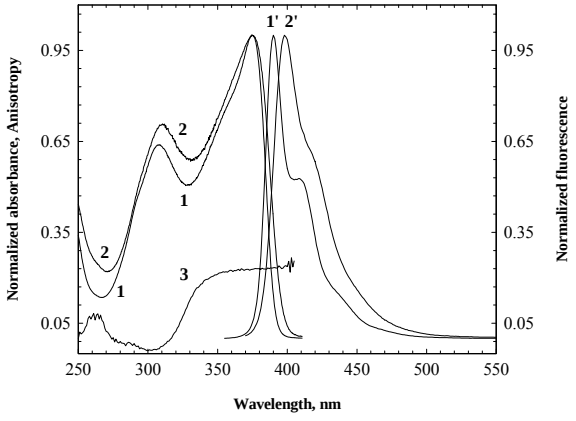

b

Figure 5.5. (a) Structure of fluorene **B**. (b) Normalized absorption (1, 2), fluorescence (1', 2'), and anisotropy (3) spectra of **B** in hexane (1, 1'), CH_2Cl_2 (2, 2'), and silicon oil (3).

Time-dependent absorption spectra of **B** under low intensity UV lamp irradiation ($\lambda_{exc} \approx 360$ nm) in hexanes and CH_2Cl_2 were also performed as was done for fluorene compound **A**. A decrease of the optical density in the absorption maximum was accompanied by absorption due to photochemical products over a broad spectral range. For the nonpolar solvent hexane, photodecomposition processes for small changes in absorbance were characterized by a linear dependence at various wavelengths, indicating direct transformation of **B** into photoproducts without intermediate photochemical reactions. In contrast, quite complex transformations of the photochemical products were observed in CH_2Cl_2. For example, a linear dependence was observed in the spectral region in the main absorption band (near λ_{max}) but a nonlinear dependence was found in the long wavelength spectral region (480 - 490 nm), revealing at least two consecutive photoreactions. The quantum yields of the photoreactions, Φ, determined for different dye concentrations in hexanes and in CH_2Cl_2, are presented in Table 5.3. The values of Φ were independent of dye concentration (first order photoreactions), reached $\approx$ (3.4 - 4.6) x 10^{-4} in hexane and increased up to 1.5 x 10^{-2} in CH_2Cl_2.

Table 5.3. Quantum yields of the photoreactions for **B** in air saturated, Φ, and deoxygenated, Φ^d, solutions at different concentrations, C, under one- (Φ, Φ^d) and two-photon (Φ_{2PA}) excitation.

C (M)	Hexane			CH_2Cl_2		
	Φ x 10^4	Φ^d x 10^4	Φ_{2PA} x 10^4	Φ x 10^2	Φ^d x 10^2	Φ_{2PA} x 10^2
1.3 x 10^{-3}	3.4 ± 0.8	-	3 ± 1.5	1 ± 0.2	-	1.4 ± 0.7
3 x 10^{-4}	4.6 ± 1.2	10 ± 2	2 ± 1	1 ± 0.3	1.3 ± 0.3	0.8 ± 0.4
8 x 10^{-5}	4 ± 1	15 ± 5	2.2 ± 1	1 ± 0.3	1 ± 0.2	1.7 ± 0.8
2 x 10^{-5}	3.4 ± 0.8	6 ± 1.5	2 ± 1	1.2 ± 0.4	1.2 ± 0.4	1 ± 0.5
3 x 10^{-6}	3.5 ± 0.8	5 ± 1	2.3 ± 1	1.5 ± 0.5	1.5 ± 0.5	0.7 ± 0.3

The fluorescence and excitation spectra of the photochemical products of **B** were measured after low intensity irradiation in order to understand the nature of the photoreactions and to determine the main possible mechanisms. Excitation spectra for a hexane solution revealed only three different fluorescent species. One of them can be attributed to unreacted fluorene **B** [33g], and the short and long wavelength fluorescent species were photochemical products that arose from direct transformation of **B** upon irradiation. From the excitation spectra, the long wavelength portion of the photoproducts' absorption band corresponded to nonfluorescent species. These longer wavelength absorbing, nonfluorescent products can be attributed to stable cation radicals obtained by photoinduced electron transfer from the nitrogen atom of the diphenylamino group [66].

Photochemical decomposition of **B** in the more polar solvent CH_2Cl_2 was characterized by a relatively high quantum yield of the photoreaction, $\Phi \sim 10^{-2}$ and appearance of photoproducts over a broad spectral range (300 - 800 nm). The analysis of the fluorescence and excitation spectra of these photoproducts revealed species with overlapping fluorescence spectra formed in CH_2Cl_2 upon UV irradiation. In addition to unreacted **B**, many different fluorescent centers were observed. Finally, a long wavelength part of the photoproduct absorption spectrum ($\lambda \geq 500$ nm) may be assigned to a nonfluorescent, stable aminofluorenyl cation radical species as was proposed in hexanes solution. An increase in quantum yields of the photoreactions by 2 - 4 times (Table 5.3) were observed in deoxygenated hexane solutions of **B** relative to air-saturated ones. These results clearly demonstrate oxygen concentration is a decisive factor in the

photostability of **B** in nonpolar media. In contrast, the photochemical behavior of **B** in the electron-accepting solvent CH_2Cl_2 was independent of oxygen concentration.

High intensity irradiation of fluorene **B**, using the output from an IR femtosecond laser at λ_{exc} = 720 nm, resulted in two-photon excitation of **B** at an energy corresponding to the maximum of the main absorption band (≈ 360 nm). Two-photon absorption cross sections, $\sigma_{2PA}(\lambda_{exc})$, of **B** in hexanes and CH_2Cl_2 were determined by the up-converted fluorescence method [8a,12] and found to be $\sigma_{2PA} \approx 5 \pm 1$ GM and $\sigma_{2PA} \approx 20 \pm 4$ GM, respectively. Temporal changes of the fluorescence intensity of **B**, F(t), under high intensity irradiation, were measured [67]. The quantum yields of the photochemical reactions under two-photon excitation, Φ_{2PA}, were calculated and are presented in Table 5.3. From these it can be seen that the values, Φ_{2PA}, were nearly the same as those obtained for low intensity UV lamp irradiation, i.e. $\Phi_{2PA} \approx \Phi$ for hexane and CH_2Cl_2 solutions of **B**. Therefore, it can be concluded that photodecomposition of **B** in both solvents is independent of the type of excitation (one- or two-photon) though different mechanisms predominated depending on whether irradiation was conducted in hexane or CH_2Cl_2. These results suggest that, in some particular cases, two-photon photochemistry can be assessed for an organic compound through careful investigation of the corresponding one-photon photochemistry.

Photochemical reactions of the two-photon absorbing fluorescent dye **B** in hexanes and CH_2Cl_2 corresponded to first order reactions under one- and two-photon excitation. The quantum yields of the photoreactions under low intensity UV lamp irradiation were (3.4 - 4.6) x 10^{-4} in nonpolar hexane and increased dramatically up to 1.5 x 10^{-2} in polar CH_2Cl_2. The direct transformation of **B** into photoproducts was observed

in hexane solutions without intermediate photoreactions. In this case, two different fluorescent photoproducts were detected, and molecular oxygen played an important role in the photochemical stability of **B**. For the more polar solvent (electron-accepting) CH_2Cl_2 many different photoproducts were observed under low intensity irradiation, exhibiting absorption over a broad spectral region (visible and near-IR). In addition, the photodecomposition was independent of the presence of oxygen in the solution. Two-photon excitation of **B** in hexane and CH_2Cl_2 afforded nearly the same quantum yields of the photoreactions as for low intensity UV lamp irradiation. Thus, the photostability of **B** is independent of the type of excitation (one- or two-photon). The relatively low photochemical quantum yield of **B** in hexane suggests this compound has characteristics favorable for use in linear and nonlinear optical applications.

Photochemical stabilities of the dipolar fluorene compound **A** and symmetrical compound **B** were investigated under one- and two-photon excitation in solvents of disparate polarity. The analyses of the quantum yields of the photoreactions suggest the mechanisms for photodegradation of fluorenyl compounds involve a role of dissolved oxygen in the photostability of these compounds in nonpolar solvents and electron transfer processes with the formation of stable cation radicals (or other nonfluorescent photoproducts) in electron accepting, polar solvents. In nonpolar environments, the quantum yield of the photochemical reaction, Φ, for one-photon excitation was nearly the same as those of two-photon excitation for compounds **A** and **B**. The values of Φ in CH_2Cl_2 increased dramatically under two-photon excitation for fluorene **A**, while that of the symmetric fluorene **B** were similar to those of one-photon excitation. In general, these compounds are relatively photostable under both linear and two-photon excitation

in organic solvents. One may question their photochemical stability in aqueous environments, and these experiments should be performed for the more hydrophilic fluorene compounds **13** and **14**. However, as the more hydrophobic analogues (fluorene compounds **A** and **B**) have been shown to exhibit photostable properties in solvents of disparate polarity, one may expect structurally similar fluorene-based fluorophores to behave similarly. Certainly, photostability studies in DMSO or in aqueous environments will provide more pertinent assessment of the hydrophilic fluorene compounds, but that these fluorene compounds exhibit relatively high photostability under linear and two-photon excitation conditions are promising for two-photon fluorescence bioimaging.

CHAPTER 6: DEMONSTRATION OF FLUORENE DERIVATIVES IN 2PLSM IMAGING.

The previous chapters have focused on the preparation, structural, and spectroscopic characterizations of efficient two-photon absorbing fluorene derivatives. The challenges of preparing and isolating rationally designed compounds targeted for particular applications are satisfied upon their demonstrated utility in those designated applications. Hence, while the design, synthesis, and photophysical properties of isolated hydrophilic fluorene derivatives are important, their full assessment resides in their demonstrated use in two-photon fluorescence microscopy of biological samples. This chapter will focus on aspects of the fluorene derivatives in fluorescence microscopy, in epi-fluorescence and two-photon induced fluorescence imaging, of glutaraldehyde-fixed and live animal cells. Preliminary studies indicate the fluorene derivatives are not cytotoxic to an NT2 cell line and can be used for live-cell imaging of these cells for long imaging times. That these fluorene compounds were used for two-photon excited laser scanning fluorescence microscopy (2PLSM) imaging using relatively low femtosecond near-IR irradiation conditions provide strong incentives for continuous development of these compounds for nonlinear fluorescence imaging applications.

6.1 Fluorene A as a Fluorophore in epi-Fluorescence and 2PLSM Imaging

Previous studies from our laboratory have reported on the design and development of fluorene-based organic dyes with very efficient two-photon absorption and fluorescence emission properties [12,33,51,53]. Use of two-photon excited fluorescence microscopy images of a well-characterized 2PA fluorene dye (**A**) for

staining glutaraldehyde-fixed rat cardiomyoblasts was demonstrated and lends credence to our motivation towards developing fluorene-based reagents for multiphoton fluorescent bioimaging [57]. In particular, efforts directed towards preparing hydrophilic fluorene-based fluorescent contrast agents have been initiated with the synthesis of compounds **13** and **14**, both of which appear to exhibit improved optical properties more amenable for nonlinear excitation, relative to standard fluorophores currently in use. Efforts directed towards preparing, fluorene-based reactive fluorescent reagents have been initiated with the synthesis of compound **2**, though obvious improvements in its structure and hence, its optical properties await its realization. Demonstration of these fluorene derivatives as suitable compounds for fluorescence microscopy imaging of animal cells was performed with compound **A**. The fact that this hydrophobic derivative was effectively used in epi-fluorescence and two-photon induced fluorescence imaging bodes well for the application of the more hydrophilic fluorene derivatives in similar applications.

6.1.1 General comments on microscopy instrumentation.

Bright field transmission and epi-fluorescence microscope images of H9c2 glutaraldehyde fixed cells stained with the well-characterized two-photon absorbing fluorene dye **A**, were collected on a Nikon Eclipse E600 upright microscope. Epi-fluorescent images of NT2 cells, glutaraldehyde fixed or as live cells under *in vitro* conditions containing hydrophilic fluorene derivatives (compound **13** or **14**), were imaged on an Olympus IX81-DSU (disk scanning unit). Additionally, epi-fluorecence images were also collected on a modified Olympus IX70 inverted microscope and

Fluoview 300 laser scanning confocal unit fitted with a mercury lamp for fluorophore excitation. The same Olympus IX70 inverted microscope, modified to accommodate a 10 W Verdi pumping a Ti:sapphire crystal of a Mira 900 (Coherent), was used for two-photon induced fluorescence excitation with subsequent image capture performed via two Hamamatsu PMT channels. Live cell fluorescence imaging was performed on cells cultured on 35 mm glass-bottom culture dishes (MatTek) or on a Bioptechs FCS2 closed system live-cell chamber coupled with an Instech P720 micro-perfusion peristaltic pump. Additional details of the both the linear microscopy systems and the modified Olympus IX70 inverted microscope to accommodate the near-IR laser system can be found in Appendix C.

6.1.2 Glutaraldehyde staining and fixation of H9c2 cells.

H9c2 rat cardiomyoblast cells (American type culture collection (ATCC) CRL-1446) were plated in a four-well Lab-Tek II chamber slide (Fisher Scientific) and kept in a humidified atmosphere of 5% CO_2 at 37 °C 24 hours prior to dye staining. The cells were in Dulbecco's modification of Eagle's medium (DMEM) (Mediatech, Inc.) supplemented with 10% fetal bovine serum (ATCC), 4-mM L-glutamine (Mediatech), and 100 μg/mL of penicillin-streptomycin (Mediatech) (complete medium). A glutaraldehyde fixation was followed as adapted from protocols presented by Bacallao and Stelzer [68]. Briefly, cells were washed with phosphate buffer saline (PBS, pH 7.2, Gibco) to remove growth medium. Cultures were fixed with 0.3 % glutaraldehyde (Fisher Scientific) solution in PBS at room temperature, and their cell membranes permeabilized with a 1 % Triton-X100 (Sigma) in PBS solution. The detergent was

removed with PBS washings, treated with freshly prepared solution of aqueous $NaBH_4$ solution (1 mg/mL, Aldrich), followed by a brief rinse with 0.1 % Triton-X100 in PBS (PBST). An aliquot of compound **A** (10 μL of 4.8 x 10^{-4} M) dissolved in anhydrous DMSO was delivered to the fixed cells in PBST solution. Details of the synthesis, linear and nonlinear characterization of compound **A** can be found in references 33. One of the wells did not receive any dye as a control. Cells were washed with PBS (x4) followed by ddH_2O, and mounted in ProLong Gold (Molecular Probes) mounting medium, cover slipped, and sealed.

6.1.3 Epi-fluorescence and 2PLSM images of fluorene A stained H9c2 cells.

Fluorene compound **A** is a well-characterized fluorophore that exhibits relatively high two-photon absorption cross-section in the excitation range of pulsed Ti:sapphire laser output. Figure 6.1 shows the structure of compound **A** along with pertinent photophysical data characterized in acetone. It is important to note, this compound was studied in a range of solvents of varying polarity, from hexanes to acetonitrile and acetone, and exhibits solvatochromic effects that influence its photophysical properties. Details of solvent effects on both its linear and nonlinear optical properties are presented in reference 12,33, and 51. Hence, the properties presented are indications of typical values to be expected from this highly photostable derivative [33d]. Furthermore, additional fluorene derivatives with much higher cross-sections, and, hence, action cross-sections, have also been prepared, and choice of fluorene **A** was selected as a proof-in-principle demonstration that fluorene derivatives can be used in microscopic imaging of biological samples.

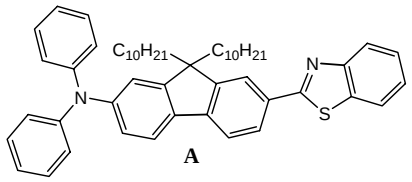

A

λ_{abs}	= 390 nm, λ_{em} = 492 nm; $\Delta\lambda_{St}$ = 101 nm
η_{fl}	≅ 0.6
τ	≅ 3 ns
ε_{380}	≅ 42 x 10^3 $M^{-1}cm^{-1}$
δ_{max}	≅ 202 GM (at ~780 nm)
$\delta\eta$	≅ 120 GM

Figure 6.1. Structure of a well-characterized two-photon absorbing fluorophore and its photophysical properties. λ_{abs}, λ_{em}, $\Delta\lambda_{St}$, ε = Linear absorption, steady-state fluorescence emission, Stokes shift, and molar absorptivity, respectively; η_{fl}, τ = fluorescence quantum yield and lifetime respectively; δ_{max} and $\delta\eta$ = two-photon cross-section and action cross-section, respectively.

The utility of fluorene **A**, and of additional fluorene-based derivatives, as an efficient two-photon absorbing biological fluorophore was demonstrated by staining glutaraldehyde fixed H9c2 rat cardiomyoblast cells. Bright field transmission and epi-fluorescence microscope images (DAPI filter set, 40x, NA 0.75) of the stained cells are shown in Figure 6.2 A and B, respectively. Furthermore, fluorene **A** did not undergo noticeable photobleaching during continuous exposure to the UV excitation light. No fluorescence was observed in the controls without any fluorophore (image not shown). Additionally, fluorescence was observed predominantly from the cytoplasmic region of the cells, with the nucleus clearly outlined, indicating potentially preferential staining with this fluorophore for cytoplasmic components.

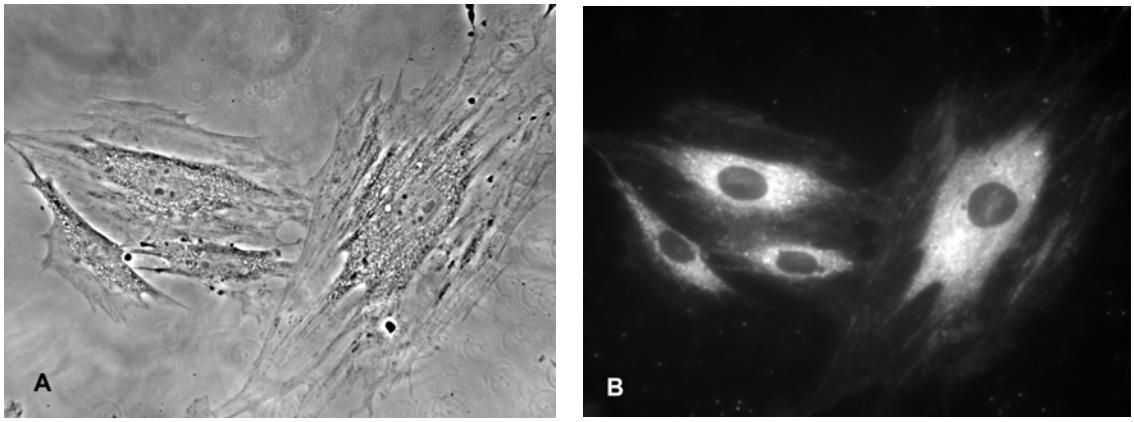

Figure 6.2. Bright field transmission (A) and epi-fluorescent (B) microscopy images (40x) of H9c2 cells stained with a two-photon absorbing dye **A**.

Two-photon excited fluorescence microscopy images of the same fluorene **A**-stained cells were collected on a modified Olympus IX70 inverted microscope and Fluoview 300 laser scanning confocal unit with a Ti:sapphire laser output from 740–830 nm (125 fs FWHM, 76 MHz repetition rate, ~25 mW, 40x, NA 0.85). The control cells that did not receive any fluorophore showed modest autofluorescence upon 800 nm fs excitation as shown in Figure 6.3-C, while the fluorophore-stained cells (Figure 6.3-D) revealed higher contrast and greater signal under the same excitation and power exposure as the control. Two-photon induced fluorescence was observed predominately from the cytoplasmic region, consistent with the images collected from epi-fluorescence images.

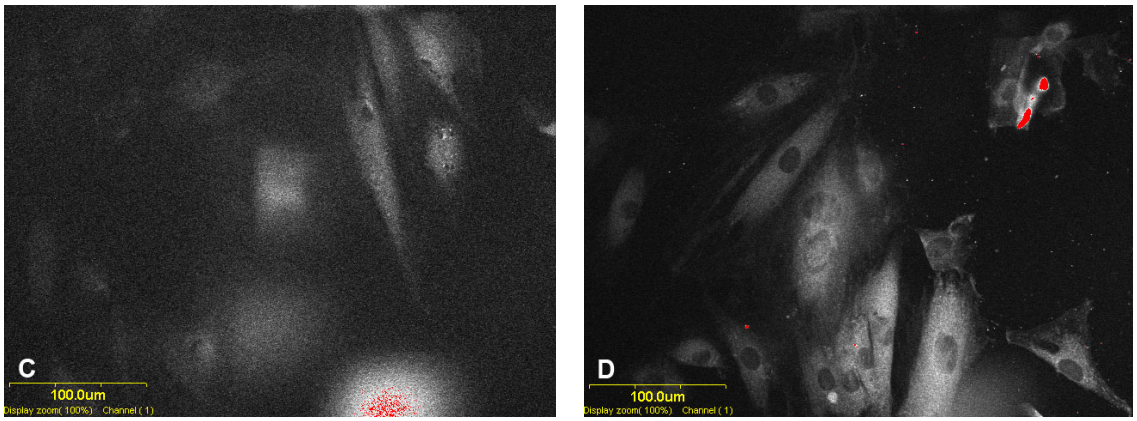

Figure 6.3. Two-photon induced fluorescence microscope images (40x) of C, control containing no fluorophore and exhibiting some autofluorescence and D, of cells stained with fluorene **A** upon 800 nm fs excitation. Red spots demark signal saturation.

A direct quadratic dependence of fluorescence intensity to excitation power to verify a two-photon absorption process was difficult to determine in the highly-scattering sample. Hence, assertion of multiphoton excited fluorescence was verified by imaging the same sample area and image plane using the same average power under mode-locked (ML) and non-mode locked (CW) conditions. A fluorescent image under ML conditions (Figure 6.4-E) was clearly generated, while no image was obtained under CW conditions (Figure 6.4-F), and while higher-order processes such as three-photon absorption may be involved, spectroscopic data suggest a two-photon process in the excitation range used (740-830 nm) would be dominant for compound **A**. No observed fluorescence under non-mode locked (CW) irreadition provides evidence for the absence of a simple linear absorption (one-photon) process. Hence, two-photon excited fluorescence images of H9c2 cells stained with fluorene **A** was demonstrated, providing strong motivation for the development of fluorene-based reactive reagents and probes for multiphoton bioimaging applications.

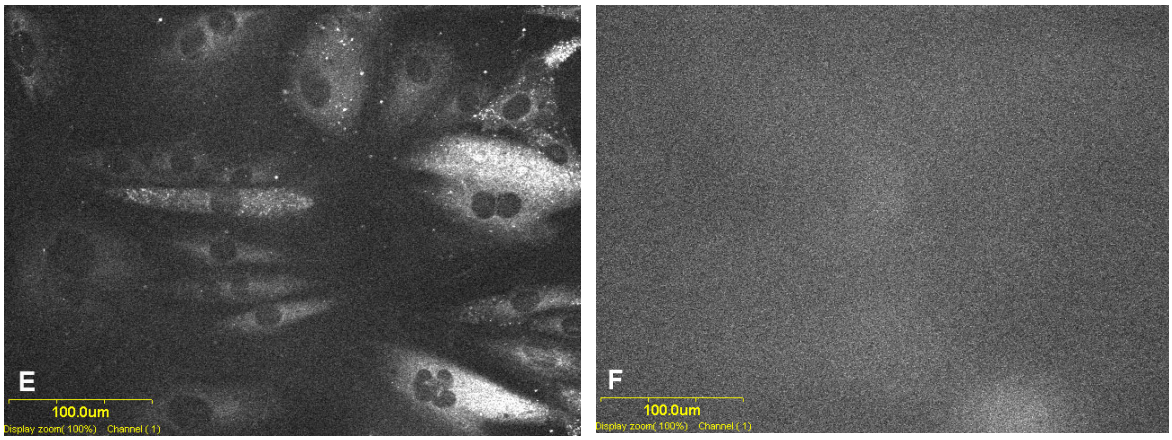

Figure 6.4. Two-photon induced fluorescence microscopy images (40x) of H9c2 cells stained with fluorene **A** under mode-locked (E) and non mode-locked Ti:sapphire irradiation conditions (F).

Development of fluorene-based fluorescent stains and reactive reagents for multiphoton bioimaging applications arises out of our systematic studies on structure-nonlinear optical property relationships for a wide range of fluorenyl derivatives. Demonstration of 2PM images of H9c2 cells stained with a well-characterized two-photon absorbing fluorophore **A**, albeit a hydrophobic derivative, lends credence to our efforts to further refine fluorene-based derivatives for bioimaging applications. Towards this end, the more hydrophilic fluorenyl derivatives, **13** and **14**, in two-photon induced fluorescence microscopy imaging were demonstrated. Furthermore, preliminary studies revealed hydrophilic fluorenyl derivatives incubated with NT2 cells exhibited relatively low cytotoxic effects. These hydrophilic fluorene derivatives are expected to exhibit similar photostabilities as those presented in Chapter 5. The fact they possess high fluorescence quantum yields, and high two-photon absorption cross-sections, and, therefore, action cross-sections, makes them ideal fluorescent contrast agents suitable for use over the tunability range of commercial Ti:sapphire lasers typically utilized in multiphoton imaging methods and techniques.

6.2 Cytotoxicity of Hydrophilic Fluorene Derivatives

The cytotoxic effect of hydrophilic fluorene derivatives on proliferating cells is a parameter of primary interest, particularly for any live-cell fluorescence imaging applications. The practical utility of these fluorescent compounds for any advanced live-cell imaging conditions would require assessing their effect on proliferating cells. Regardless of the number of desirable optical qualities a fluorophore may possess, if the fluorophore is highly toxic, particularly to a living system, it would obviously limit its utility in such bioimaging applications. Hence, an Alamar Blue (AB) reduction analysis was used to assess cytotoxic effects of two hydrophilic fluorene derivatives on proliferating NT2 (NTERA-2 cl.D1 [NT2/D1]) cells.

The Alamar Blue system is a relatively simple, rapid, and sensitive test, whereby 10% of the commercially available solution is added to the cell medium to assess for *in vitro* cell proliferation and cytotoxicity. The oxidized, blue, nonfluorescent, and nontoxic, Alamar Blue is reduced to a pink, fluorescent dye in the medium by cell activity. AB was identified as resazurin [69a], a compound used in the 'resazurin reduction test', whereby resazurin is reduced to fluorescent resorufin. It has been used for about 50 years to monitor bacterial and yeast contamination in biological fluids and milk [69b] before its use for assessing *in vitro* mammalian cell proliferation. A direct correlation between AB (or resazurin) reduction in the growth media and the proliferation of living cells, and its reliability to measure potency of potential toxicants can be measured either by colourimetry or fluorimetry. Fluorescence measurements are made by exciting the compound at 530-560 nm and measuring its emission at 590 nm, while

the resulting data are expressed as fluorescence emission intensity units as a function of incubation time.

Two hydrophilic fluorene compounds, **13** and **D**, were assessed for their toxic potency on proliferating NT2 cells by an external laboratory (Dr. Kiminobu Sugaya, UCF Biomolecular Science Center). The cells were treated with different concentrations of the compounds (0.1μM - 100 μM) dissolved in DMSO and were also treated with 10% AB solution. The fluorescence of reduced AB was then used to monitor NT2 cell proliferation in a dose-dependent response to fluorene compounds incubated with the cells. Results of the two hydrophilic fluorene compounds showed no apparent effect of these compounds on the growth of NT2 cells over a 48-hour time period (Figures 6.5 A and B). The observed fluorescence intensity of AB reduction by cells treated with various doses of the two fluorene compounds was similar to that observed for cells untreated with any fluorene compounds (control). This indicates these fluorene derivatives appear to have negligible effects on the cell proliferation activity of NT2 cells over a relatively wide concentration range.

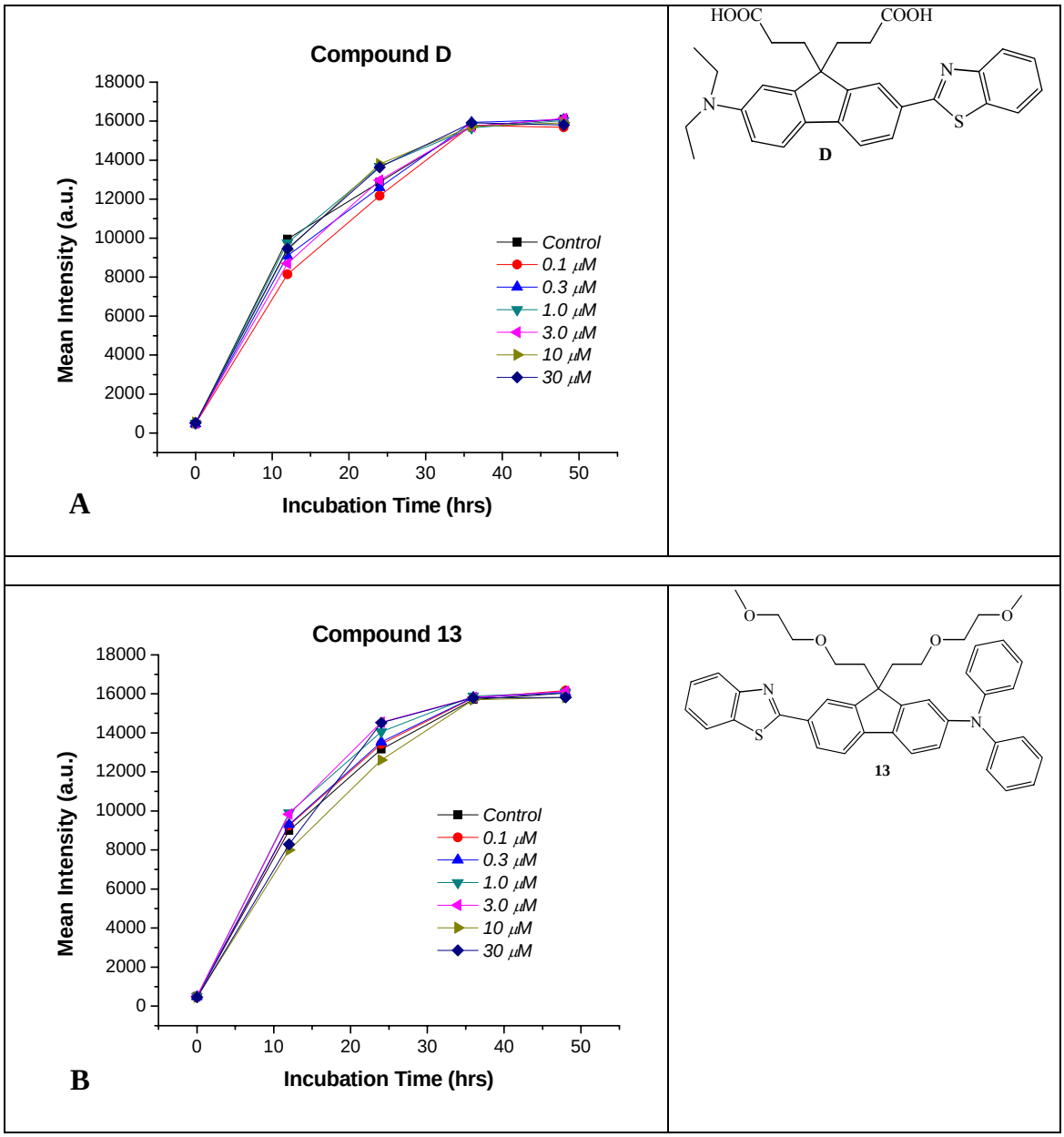

Figure 6.5. Cytotoxicity results of hydrophilic fluorene derivatives on proliferating NT2 cells. A) Water-soluble fluorene compound **D** and B) hydrophilic fluorene compound **13** incubated with NT2 cells treated with 10% AB solution were monitored via observation of fluorescence upon AB reduction.

6.3 2PA Hydrophilic Fluorene Compound in Linear- and 2PLSM imaging

The Alamar Blue reduction results of fluorene compounds introduced into proliferating NT2 cells are promising. The preliminary studies indicate these fluorene compounds are non-toxic over a wide concentration range. This bodes well for application of these, and perhaps additional fluorenyl based fluorophores, for live-cell fluorescence microscopy imaging. Demonstrated use of one of these hydrophilic compounds, **13**, in live-cell microscope imaging will be presented in the following section. This compound was effective as a fluorescent contrast agent in living cells under linear imaging conditions, but more importantly, was also effective for imaging living cells under long-term two-photon excitation conditions.

6.3.1 Confocal fluorescent microscopy images of live NT2 cells.

Hydrophilic fluorene compound **13** was determined to possess desirable optical properties for efficient fluorescence imaging applications. Preliminary cytotoxicity studies also indicated this compound has negligible effects on proliferating NT2 cells and is relatively benign during long incubation time, on the order of 48 h. Hence, it was used as a fluorescent contrast agent for live-cell imaging of NT2 cells cultured on 35 mm uncoated glass-bottom culture dish (MatTek). The cells were incubated with 30 μM of compound **13** dissolved in DMSO, and maintained in a humidified atmosphere at 37 °C and 5% CO_2 for 16 hours prior to imaging on an Olympus IX2-DSU (disk scanning unit). Fresh growth media was exchanged prior to performing confocal imaging to minimize contribution from excess fluorophore in the media. Compound **13** was clearly taken in by the NT2 cells as shown in Figure 6.6-A (40x, false-colored image). Compound **13**

was excited, and the resulting fluorescence was collected through a modified CFP filter (DAPI exciter Ex377/50 with CFP 458DM, Em483/32) filter set to accommodate the spectral profile of this dye.

The structure of **13** and a summary of its optical properties are listed below (Figure 6.6-B). The fluorescence appeared predominately in the cytoplasmic region as punctate structures, possibly exhibiting preferential staining for cytoplasmic organelles as the mitochondria. The possibility of compound **13** exhibiting preferential staining for organelles may extend its utility in fluorescence imaging of animal cells. To test for this potential preferential staining ability, the live NT2 cells were stained with a fluorescent stain for mitochondria. A solution of MitoTracker Red CMXRos (Molecular Probes), prepared in fresh DMSO, was incubated (1 μL of 0.94 mM) with NT2 cells already treated with compound **13** and maintained in a humidified atmosphere at 37 °C and 5% CO_2 for ~20 min. Fresh media was exchanged prior to confocal imaging. The mitochondria were immediately visible upon addition of the organelle-specific stain as can be seen from Figure 6.6-C. If fluorene dye **13** exhibited preferential staining for the same organelle, the overlayed fluorescent images collected from each of the separate channels would exhibit a combined color image. The MitoTracker Red fluorescence was imaged through a standard rhodamine filter set and the fluorescence from compound **13** through an independent, modified CFP filter set mentioned above. If the fluorescence from MitoTracker Red is dominant, than one would expect to observe a predominantly 'red' fluorescence and if the fluorescence from compound **13** is dominant, one would expect to observe predominantly a 'green' fluorescence. If the two fluorophores are present together, then the overlayed fluorescence collected from the 'red' and 'green'

would provide a combined color of a yellow-orange image, indicating a shared combination of each of the fluorophores contributing to the region of the overlayed fluorescence.

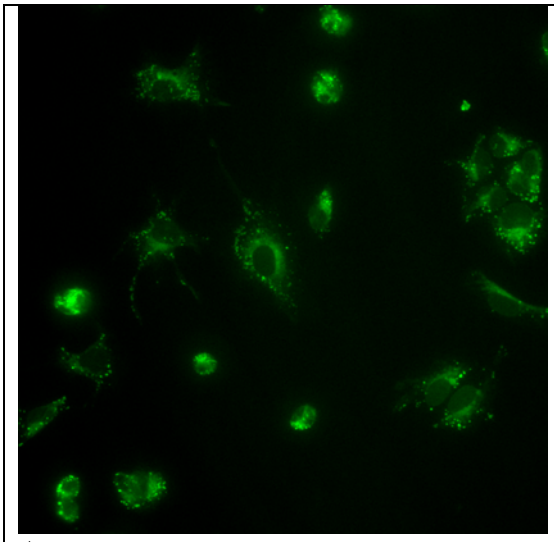

A. Live NT2 cells (40x) incubated with compound **13**.

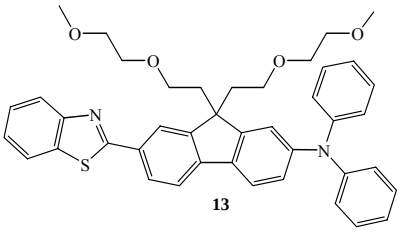

13

λ_{abs} = 395 nm, λ_{em} = 540 nm
$\Delta\lambda_{St}$ = 145 nm
η_{fl} ≅ 1.0
ε_{380} ≅ 40.6 x 10^3 $M^{-1}cm^{-1}$
δ_{max} ≅ 100 GM (790 nm)

B. Structure and optical properties of compound **13** (in DMSO).

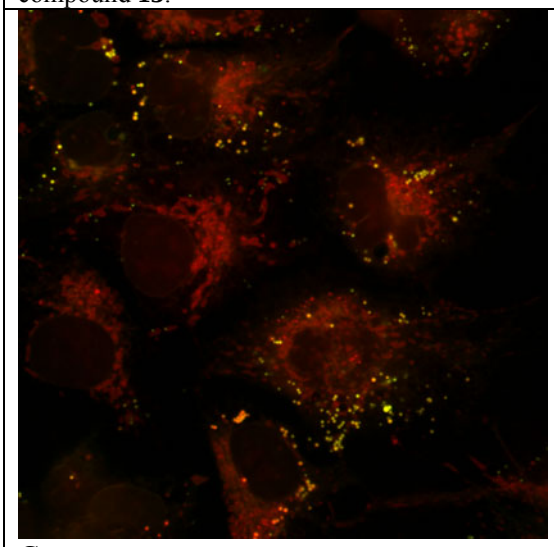

C. Live NT2 cells (60xOil) incubated with compound **13** + high MitoTracker Red.

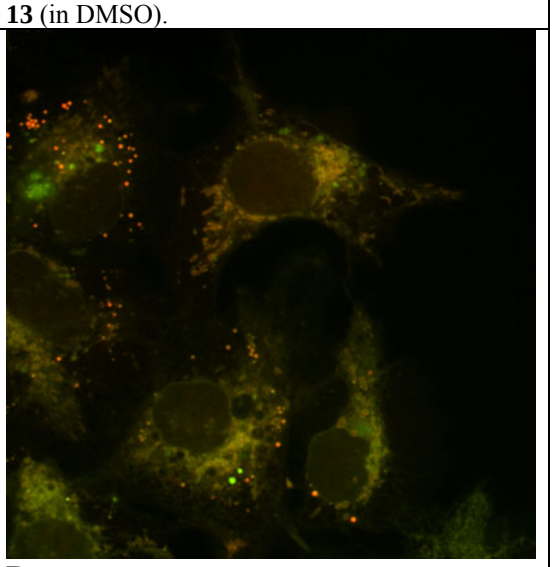

D. Live NT2 cells (60xOil) incubated with compound **13** + low MitoTracker Red.

Figure 6.6. Confocal microscopy images of NT2 cells incubated with a two-photon absorbing hydrophilic fluorene dye 13. A: Cells incubated with 30 mM of compound 13, whose structure is shown in B. C: Cells incubated compound **13** followed by introduction of a large concentration of a mitochondrial stain. D: Cells incubated with compound **13** and a reduced concentration of a mitochondrial stain.

The observed fluorescence from the overlayed images in Figures 6.6-C and D are interesting. Clearly, the overlayed image from Figure 6.6-C indicates a predominant red fluorescence, indicating MitoTracker Red is the dominant fluorophore, with few punctate regions of green and orange scattered throughout the image. Keeping in mind the cells were incubated with compound **13**, and the mitochondrial stain was introduced as an end-point stain for the organelle, one would expect to see a greater contribution of the two fluorophores if compound **13** exhibited preferential staining for mitochondria. A better representation of this expectation is shown in the confocal image shown in Figure 6.6-D, where the overlayed images resulted in a greater representation of the combined yellow-orange fluorescence. One may speculate that a possible reason for the predominately red fluorescence observed in Figure 6.6-C may be due to those cells uptaking greater amounts of the mitochondrial stain. This may have resulted when the organelle-specific stain was introduced into the cells at one region of the culture and not by the exchange of fresh media that diluted the stain. Hence, the area where the MitoTracker Red was directly loaded may have received a greater amount of the stain, relative to those cells located at the opposite site of stain introduction into the culture. Hence, compound **13** may exhibit preferential staining for the mitochondria of NT2 cells under *in vitro* conditions, as insinuated in Figure 6.6-D. This possible feature of the fluorene dye should be explored further to confirm this potential.

6.3.2 2PLSM images of NT2 cells.

Hydrophilic fluorene compound **13** was prepared as an efficient 2PA fluorescent compound for nonlinear bioimaging applications. Spectroscopic characterization of this

compound revealed it to possess key properties better optimized for two-photon induced fluorescence microscopy. The compound exhibited a fluorescence quantum yield (η_{fl}) of unity and a relatively high two-photon cross-section (δ), and, consequently, action cross-section ($\eta_{fl}\delta$) across a wide bandwidth of the near-IR under femtosecond excitation. For instance, the $\eta_{fl}\delta$ at 790 nm is ~ 100 GM units, practically an order of magnitude greater than typical fluorophores currently in use under similar nonlinear excitation conditions. Additionally, this fluorophore exhibits high two-photon absorptivity in the optimal output of the tunability range of commercial Ti:sapphire pulsed laser systems. These combined factors establish this compound as a prime candidate for two-photon induced fluorescence bioimaging.

The utility of compound **13** as an efficient 2PA fluorophore was demonstrated by two-photon induced fluorescence imaging of glutaraldehyde-fixed NT2 cells incubated with 30 μM for 16h. The NT2 cells were treated similarly as the H9c2 cells, excluding the Triton-X permeabilization, as the cells have been shown to readily uptake the fluorophore. Briefly, NT2 cells were plated into an 8-chamber glass slide (LabTek) and kept in a humidified atmosphere of 5% CO_2 at 37 °C for ~ 24 hour prior to fixing. Fluorene **13** solution dissolved in DMSO (30 μM) was then introduced into some of the wells 16 h prior to glutaraldehyde fixing; control wells received an equivalent volume of pure DMSO only (no dye). Fresh media was exchanged to reduce the concentration of free dye in the growth media, followed by brief washes with PBS solution. Cells were then fixed with 0.3 % glutaraldehyde solution in PBS at room temperature for ~ 20 min. followed by PBS washings. The cells were then mounted in ProLong Gold (Molecular Probes) mounting medium, cover slipped and sealed.

A two-photon induced fluorescence image of the fixed NT2 cells, incubated with compound **13** upon exposure to 800 nm excitation (160 fs, 10 mW, 76 MHz, 60x oil) using the modified Olympus IX70 microscope, is shown in Figure 6.7. No equivalent fluorescence was detected in the controls that did not contain the dye (images not shown) under the same irradiation conditions. Red spots in the image indicate signal saturation. The observed fluorescence appeared predominantly in the cytoplasmic region, similarly to that observed with the DSU confocal microscope under *in vitro* conditions. This reiterates the utility of this compound as an efficient 2PA fluorescent contrast agent for imaging fixed cells.

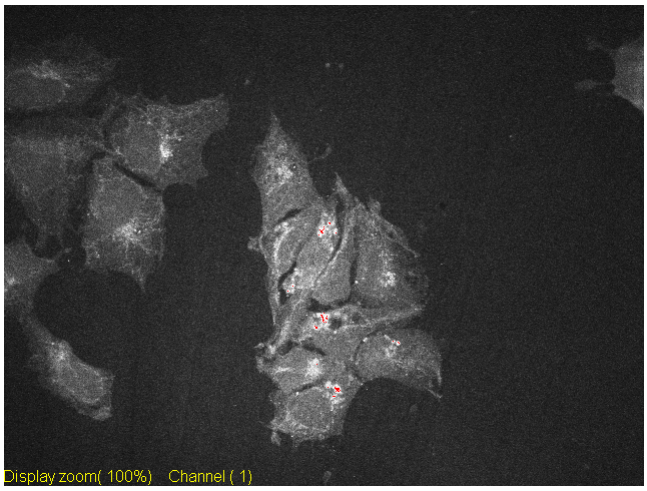

Figure 6.7. Two-photon induced fluorescence image of fixed NT2 cells (60x oil) stained with the hydrophilic fluorene compound **13**.

However, employing the full benefits of the optical properties this fluorophore exhibits resides in its application in *in vitro* conditions. Cytotoxicity studies have shown compound **13** to be non-toxic to proliferating NT2 cells over a 48 h time period. Hence, preliminary study of a long-term, live-cell imaging of the NT2 cells perfused with this dye was performed. Briefly, NT2 cells were plated onto a poly-d-lysine coated glass

cover slip (40 mm) ~ 24 hours prior to assembly into a Bioptechs FCS2 live-cell chamber system. The temperature of the heating base was set for 37 ºC and ~ 30 μM of compound **13** dissolved in DMSO was mixed into the growth media to be continuously perfused over the cells. The assembled FCS2 containing NT2 cells were then placed onto the modified Olympus IX70 stage and irradiated with 800 nm excitation (150 fs, ~ 30 mW, 76 MHz, 40x) at 10 min intervals for 17 hours. As can be seen in Figure 6.8, two-photon induced fluorescence from compound **13** was readily visible in the NT2 cells. The fluorophore appears to attach onto the cell surface during the initial time periods as indicated by the high fluorescence intensity observed over the cell bodies. The fluorescence pattern changes to a more punctate pattern throughout the cell (compare t3 vs. t33) indicating the fluorophore becomes internalized and compartmentalized within the cell over time. The fluorescence intensity appeared to be relatively intact over the time period, indicating the compound is photostable for imaging conditions of this duration. However, additional experiments need to verify the viability of cells subjected to these imaging conditions. For instance, the average power used for imaging these cells was higher than typical two-photon excitation conditions and a simple viability test, such as propidium iodide inclusion into the nucleus, should facilitate refining the application of compound **13** for live-cell, two-photon induced fluorescence imaging that reliably ensures the viability of cells under observation.

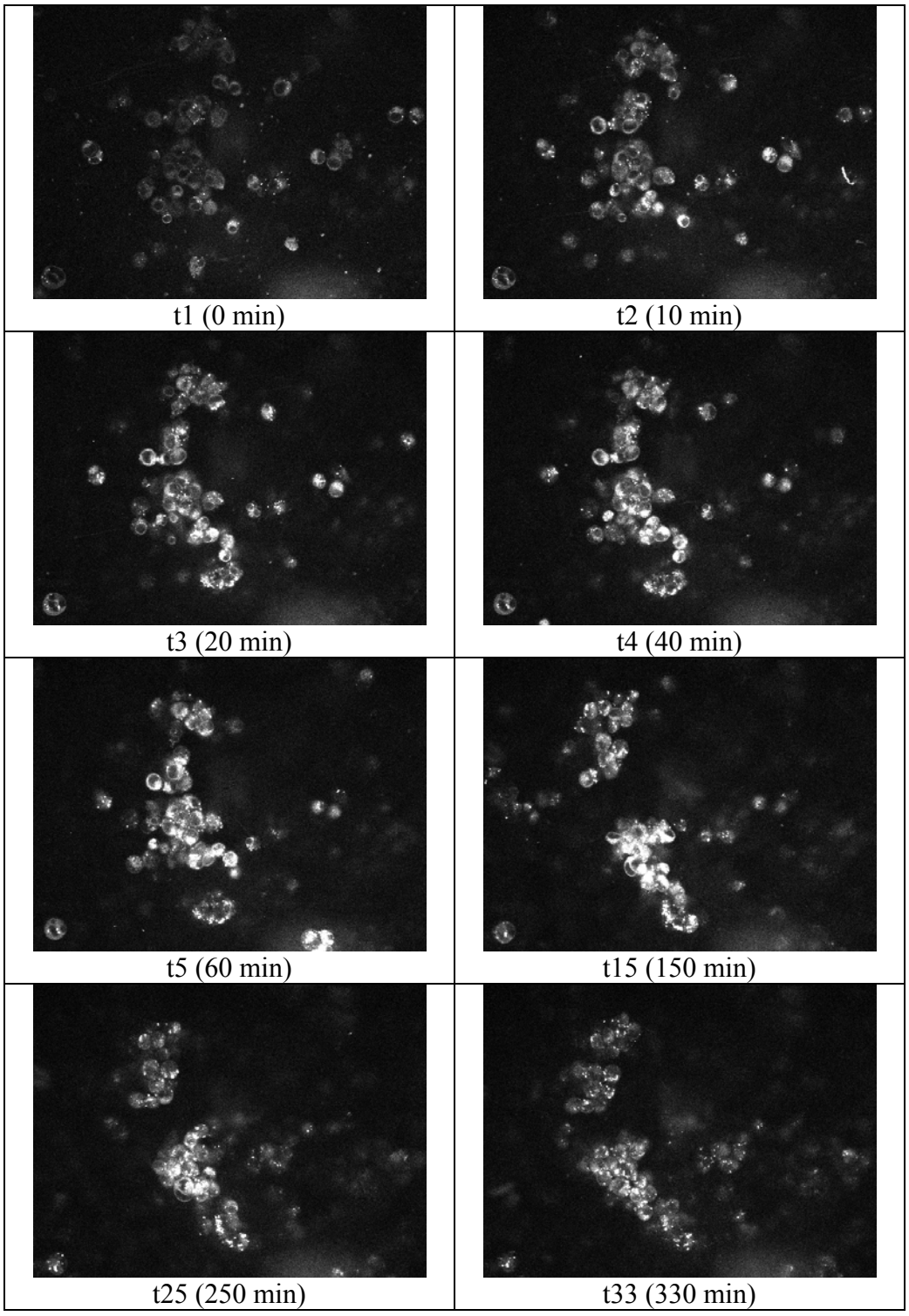

Figure 6.8. Two-photon induced fluorescence image of NT2 cells *in vitro* (40x) perfused with the hydrophilic fluorene compound **13** in growth media for 17 h. Images were captured every 10 min. Time interval is indicated with the total time following the first image capture indicated in parenthesis.

As a final note, fluorene compound **13** was shown to exhibite efficient 2P induced fluorescence in fixed NT2 cells upon exposure to a focused 140 fs scanning beam at 800 nm (76 MHz) of ~ 1 mW mean power. This is a relatively low power for observing two-photon induced fluorescence, as typical irradiation of fluorophores purported for bioimaging range from 5-10 mW [8]. The consequence of using low mean powers for efficient fluorescence bioimaging is particulary relevant under live-cell imaging conditions, where average powers > 5mW of femtosecond near-IR irradiation have been shown to be detrimental to cell vitality and proliferation [19]. Hence, careful controls need to be performed to verify that the irradiation conditions used for two-photon induced fluorescence imaging does not induce phototoxic effects, especially when long-term (on the order of hours) imaging of live specimens is of interest.

That fluorene compound **13** was shown to be sufficiently fluorescent with a low power of ~ 1 mW of the fs near-IR irradiation is a salient feature of this derivative. It provides strong motivation for further development of fluorene-based fluorophores for multiphoton fluorescence bioimaging. Prudent development of fluorene-based fluorophores for aqueous compatibility, integrated with specific reactive functionalities for covalent labeling onto biomolecules, is a worthy effort that is expected to yield high-performance, two-photon absorbing fluorophores, surpassing the performance of standard fluorophores in current use. The development of functional, organic, fluorophores with optical properties optimized for efficient nonlinear excitation are expected to push the frontier of live-cell bioimaging closer to a routine reality, where monitoring cellular processes and activities in real time will likely provide new information about life processes and interactions of living organisms.

CHAPTER 7: CONCLUSION

7.1 Synopsis

This dissertation focused on the synthesis, structural characterization, and photophysical properties of fluorene derivatives tailored for two-photon induced fluorescence microscopy applications. Target compounds were prepared based upon previous studies indicating some fluorene derivatives exhibit optical properties particularly suitable for two-photon excitation in the near-infrared wavelength region, a region of high transparency for biological tissue and cells. A synthetic methodology to increase the hydrophilicity of fluorene derivatives was incorporated into the construction of efficient two-photon absorbing fluorophores. This allowed for the isolation of two, highly efficient two-photon absorbing, fluorene derivatives as fluorescent contrast agents for two-photon induced fluorescence bioimaging of select animal cells. Efforts directed towards functionalizing fluorene compounds as reactive fluorescent reagents for covalent attachment onto biomolecules was initiated with the preparation and structural confirmation of key intermediates. Salient features of the fluorene derivatives prepared and studied in this dissertation are presented as the following:

Improved Hydrophilicity: Incorporation of ethylene-oxy substituents at the 9-position of the base fluorene ring chromophore provides an increase in its solubility in more polar solvents as DMSO, a water-miscible solvent. This increase in hydrophilicity was noticeable, as fluorene compounds, such as **13** and **14**, containing ethylene-oxy

substituents readily dissolved into DMSO, from which very high concentrations can be prepared on the order of 10^{-2} M. Fluorene compounds, such as **A**, containing linear alkyl substituents at the equivalent position were not as soluble in the more polar solvent. Incorporation of the hydrophilic substituents did not appear to perturb the electronic properties of the fluorene chromophore predominantly responsible for its optical properties. This was affirmed by the near identical UV-visible absorption, excitation, and steady-state fluorescence emission spectra collected on compounds **A** and **13** in the same solvent.

High Photostability: Photochemical stabilities of the dipolar fluorene compound **A** and symmetrical compound **B** were investigated under one- and two-photon excitation in solvents of disparate polarity. In nonpolar environments, the quantum yield of the photochemical reaction, Φ, for one-photon excitation was nearly the same as those of two-photon excitation for compounds **A** and **B**. The values of Φ in CH_2Cl_2 increased dramatically under two-photon excitation for fluorene **A**, while that of the symmetric fluorene **B** were similar to those of one-photon excitation. In general, these compounds are relatively photostable under both linear and two-photon excitation in organic solvents. One may question their photochemical stability in aqueous environments, and these experiments should be performed for the more hydrophilic fluorene compounds **13** and **14**. However, as the more hydrophobic analogues (fluorene compounds **A** and **B**) have been shown to exhibit excellent photostability in solvents of disparate polarity, one may expect the hydrophilic fluorene-based fluorophores to behave similarly. Certainly, the more pertinent photostability studies in DMSO or in aqueous environments will provide

better assessment of the proposed hydrophilic fluorene compounds for two-photon fluorescence bioimaging.

Low Cytotoxicity: The Alamar Blue reduction results of fluorene compounds introduced into proliferating NT2 cells are promising. The preliminary studies indicate fluorene compounds **13** and **D** are non-toxic over a wide concentration range. This bodes well for the utility of these and additional fluorene-based fluorophores, particularly for live-cell imaging applications. Utilization of the hydrophilic compound, **13**, in live-cell fluorescence microscopy imaging of NT2 cells was demonstrated. Furthermore, compound **13** appear to exhibit preferential staining of mitochondria in these cells.

Desirable Linear Spectral Properties: The fluorene derivatives prepared as fluorescent contrast agents exhibited desirable optical properties amenable for fluorescence imaging. The UV-visible absorption and fluorescence emission profiles of compounds **13** and **14** are well resolved, and are additionally characterized by their large Stokes shifts (Δ_{St}), of ~ 140 nm. Furthermore, their fluorescence quantum yields of unity in DMSO are the highest achievable for a fluorophore. These spectral properties, in conjunction with the expected high photostability, highlight their suitability as high-performance fluorescent agents in demanding imaging applications.

High Two-Photon Absorptivity: Hydrophilic fluorene compounds **13** and **14** have been shown to undergo efficient 2PA over a wide excitation wavelength range in the near-IR. Their two-photon absorption cross-section (δ) is ~100 GM units, practically an order of magnitude higher than many of the typical fluorophores used in two- and multi-photon fluorescence microscopy. Due to the relatively high δ value, efficient two-photon excitation followed by upconverted fluorescence was observed with compound **13** in

fixed NT2 cells using ~ 1 mW of 800 nm (~ 140 fs, 76 MHz) excitation wavelength. Fluorescent compounds with high δ values allow for the practical reduction of applying lower mean powers of femtosecond near-IR irradiation, minimizing the potential generation of phototoxic effects on living samples.

7.2 Future Work

Salient features of fluorene derivatives tailored for nonlinear fluorescent imaging garnered from this dissertation have been described. Results and conclusions from this effort reveal several potential avenues of research for continual development of fluorene derivatives, particularly for multiphoton fluorescence bioimaging applications. Some potential possibilities are listed below:

1. Alternative synthetic route to compound 20.

Future work should involve attempts at alternative synthetic routes to obtain functionalized fluorene compounds as reactive fluorescent agents. Full utility of fluorene-base fluorescent agents reside in preparing them as compounds integrated with reactive functionalities for specific targeting of biomolecules. Effort to secure an amine-reactive fluorenyl reagent (compound **20**) was met with an untimely synthetic challenge that prevented its isolation. Based upon the spectral properties revealed by the hydrophilic compounds **13** and **14**, it is expected that reactive, fluorene-based fluorescent compounds will be superior reagents for two- and multiphoton fluorescence bioimaging, an expectation that awaits worthy pursuit and development. An alternative route that

may yield the target compound **20** may be attempted by appending the *t*-BOC protected aminopropyl group as an end-group functionality as shown in Figure 7.1 below.

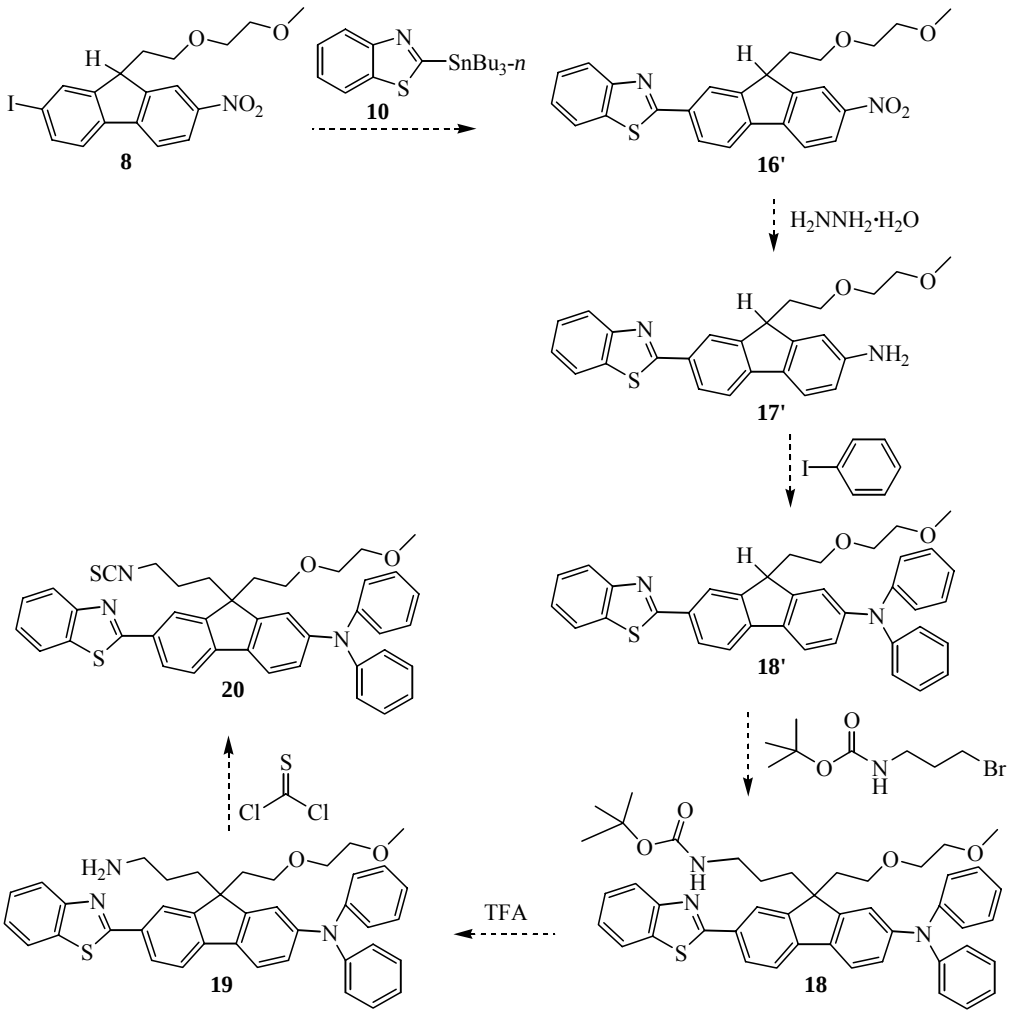

Figure 7.1. Alternative synthetic pathway to yield amine-reactive compound 20.

2. Alternative reactive groups.

Development of fluorene compounds as reactive reagents opens up the possibility of incorporating a wider range of bioconjugation techniques, such as dicyclohexylcarbodiimide (DCC) coupling chemistries. Alternative reactive

functionalities would extend the utility of fluorene-based compounds more germane to standard bioconjugation techniques. Hence, development of fluorene compounds containing succinimidyl esters as an alternative amine-reactive group, and alkyl halides or maleimides to react with thiols to form thioether conjugates, would extend the range of conjugate chemistries useful for fluorescence bioimaging.

3. Increase the ethylene-oxy chain-length

Increasing the ethylene-oxy (EO) chain length would expect to increase the hydrophilicity of fluorene derivatives. Given the relative ease with which the current ethylene-oxy chain length increased the solubility of fluorene compounds into the polar solvent DMSO, it will be a worthy endeavor to incorporate increasingly longer EO chain lengths into the fluorophore design strategy towards preparation of water-soluble fluorophores. Increasing the EO chain length may also facilitate the uptake of EO-containing fluorene derivatives into living systems, as was demonstrated with compound **13** incubated with proliferating NT2 cells.

4. Increase the conjugation length of fluorene fluorophore

Extensive investigation on the relationships between chemical structure and the two-photon absorbing properties of a series of fluorene derivatives were previously studied [12, 51]. The systematic alteration of these molecules gave rise to a myriad of structural designs which affects their nonlinear absorption. A tremendous enhancement of nonlinear absorption was noted in compounds whose conjugation length has been augmented by a styryl group, extending the π-conjugation length. Hence, future synthetic efforts should certainly be extended to include styryl units, particularly before an electron withdrawing end-group in a dipolar compound.

5. Refine cytotoxicity and photostability studies

The cytotoxicity studies should be refined to include a wider range of cell lines to investigate the effect of hydrophilic fluorene derivatives on a range of cell types. This would provide greater confidence of their use in a wide range of cell lines for long-term live-cell imaging applications. Additionally, inclusion of commonly used fluorophores, such as fluorescein, rhodamines, or Alexa Fluor (Molecular Probes) series, with the fluorene derivatives would allow for relative assessement of their cytotoxic potency against commonly used fluorophores.

Incorporation of these studies would undoubtedly yield fluorene derivatives possessing premium properties suitable for nonlinear, multiphoton fluorescence bioimaging. Highly fluorescent and photostable fluorene compounds containing reactive functional groups to target biomolecules utilizing mild bioconjugation conditions would be expected to outperform standard fluorophores currently in use. Two- and multiphoton fluorescence imaging provides major advantages for real-time imaging of dynamic processes occurring within the native environment of intact, living specimens. Future applications for muliphoton microscopy are broad and are expected to extend beyond basic research into the realm of noninvasive or endoscopic clinical and diagnostic work. Optimization of fluorescent probes and reagents with high two- and multiphoton absorption cross-sections are expected to be an integral part of this emerging technology.

APPENDIX A: STRUCTURES, ^{1}H, AND ^{13}C NMR SPECTRA (IN $CDCl_3$) OF FLUORENE DERIVATIVES.

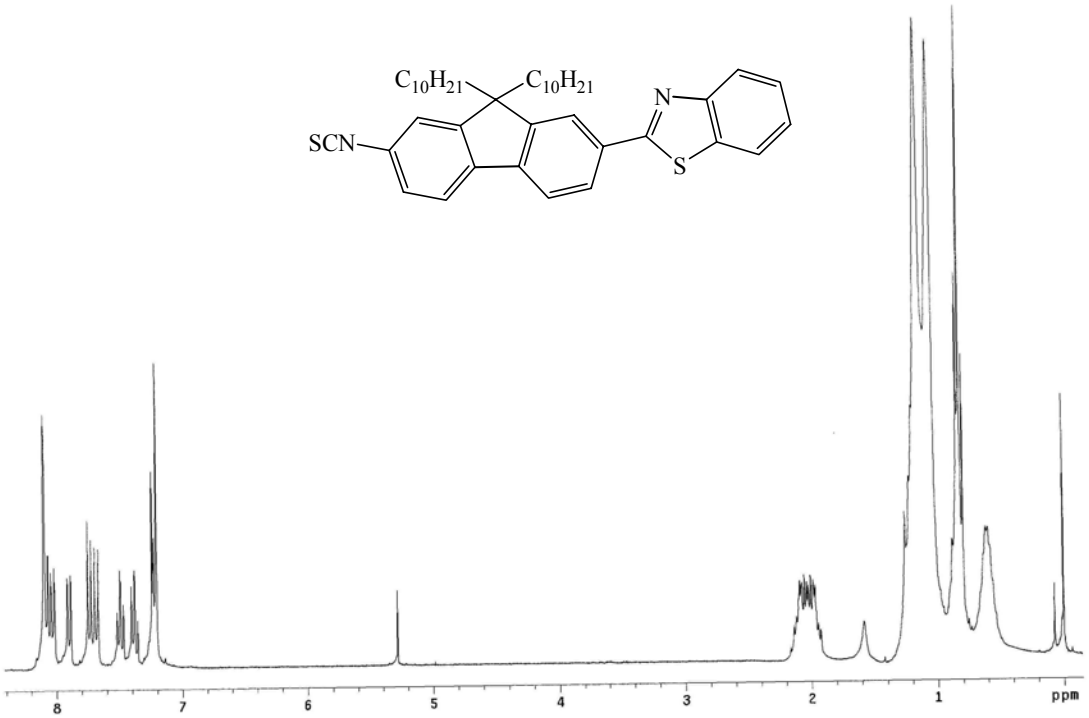

^{1}H NMR spectrum of Compound 2.

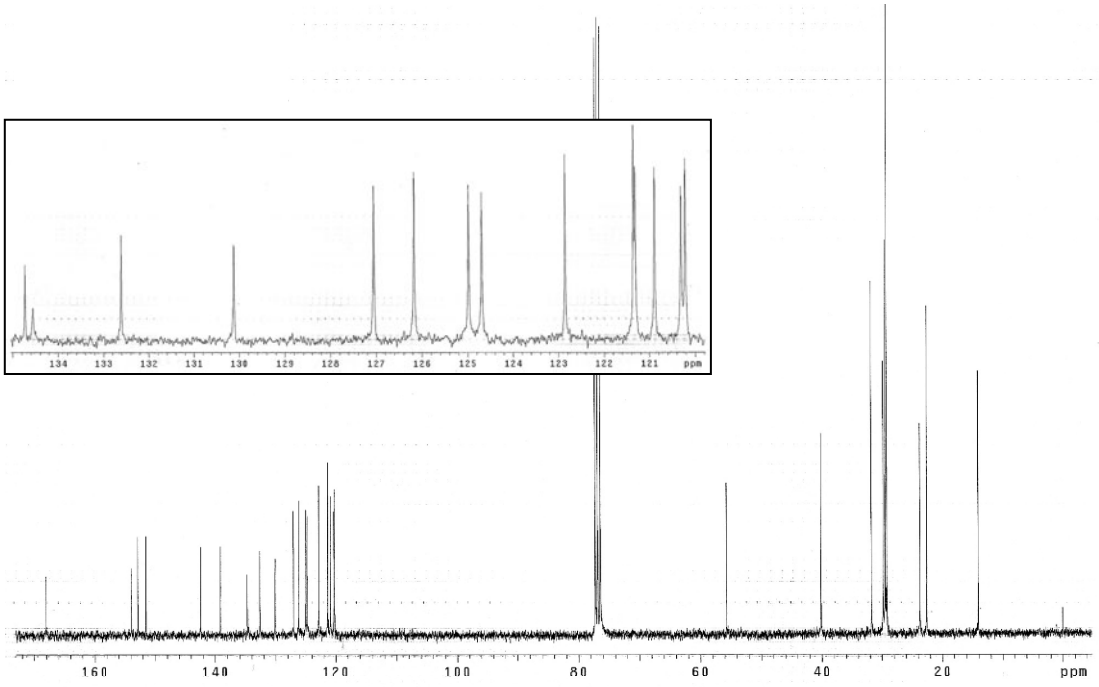

^{13}C NMR spectrum of Compound 2.

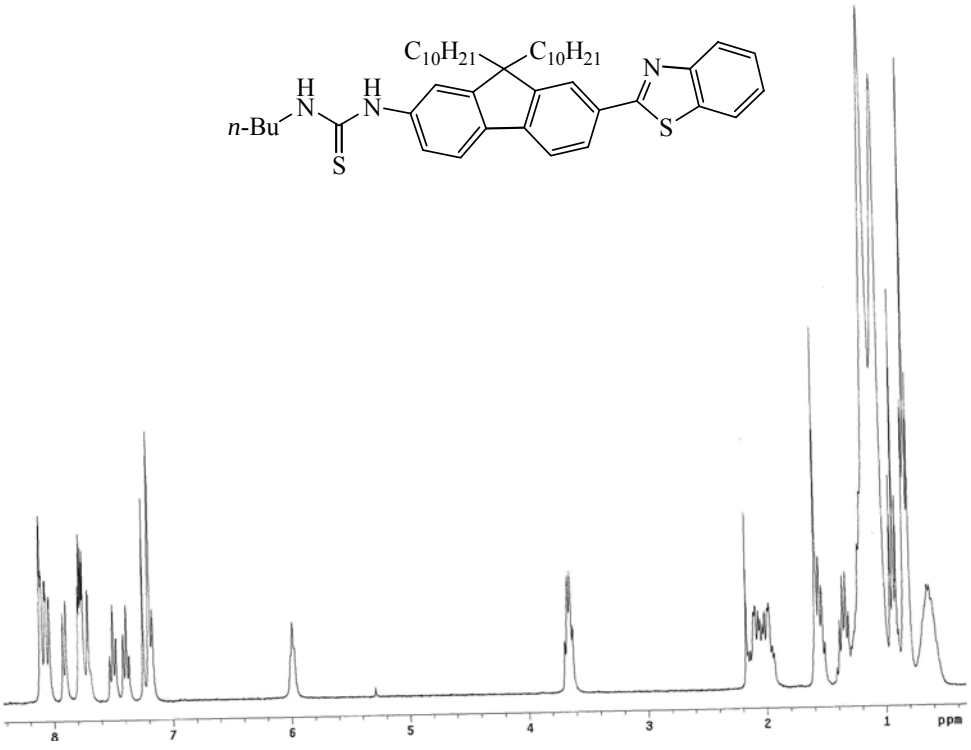

^{1}H NMR spectrum of Compound 3.

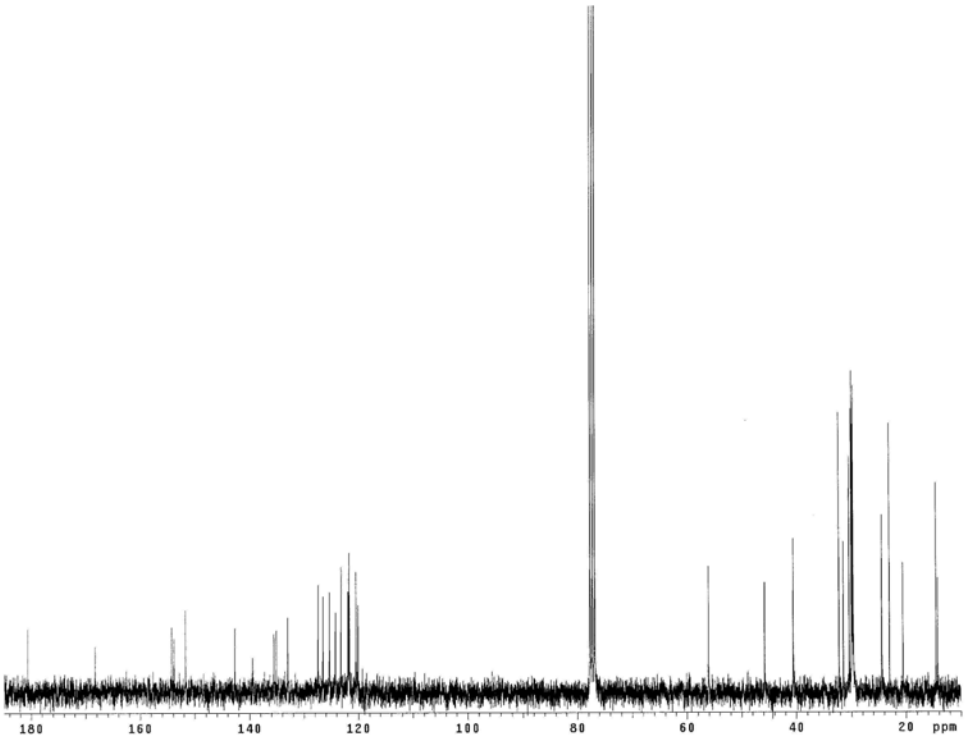

^{13}C NMR spectrum of Compound 3.

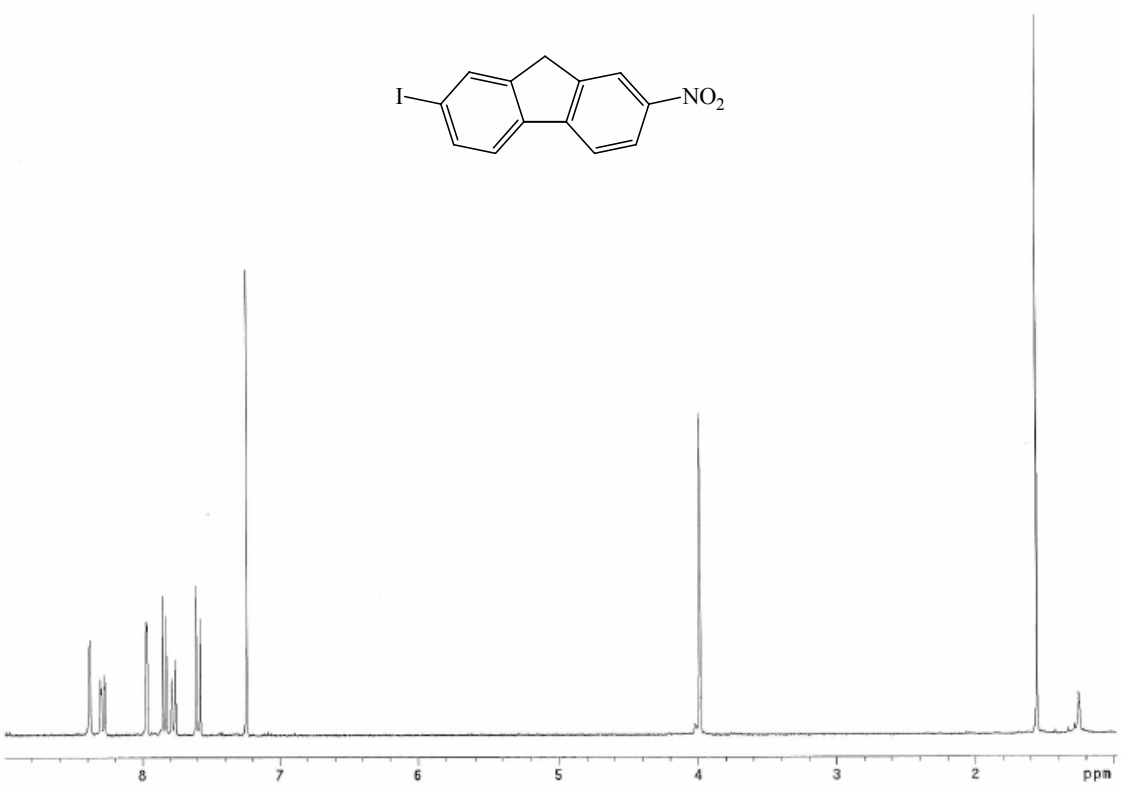

^{1}H NMR spectrum of Compound 7.

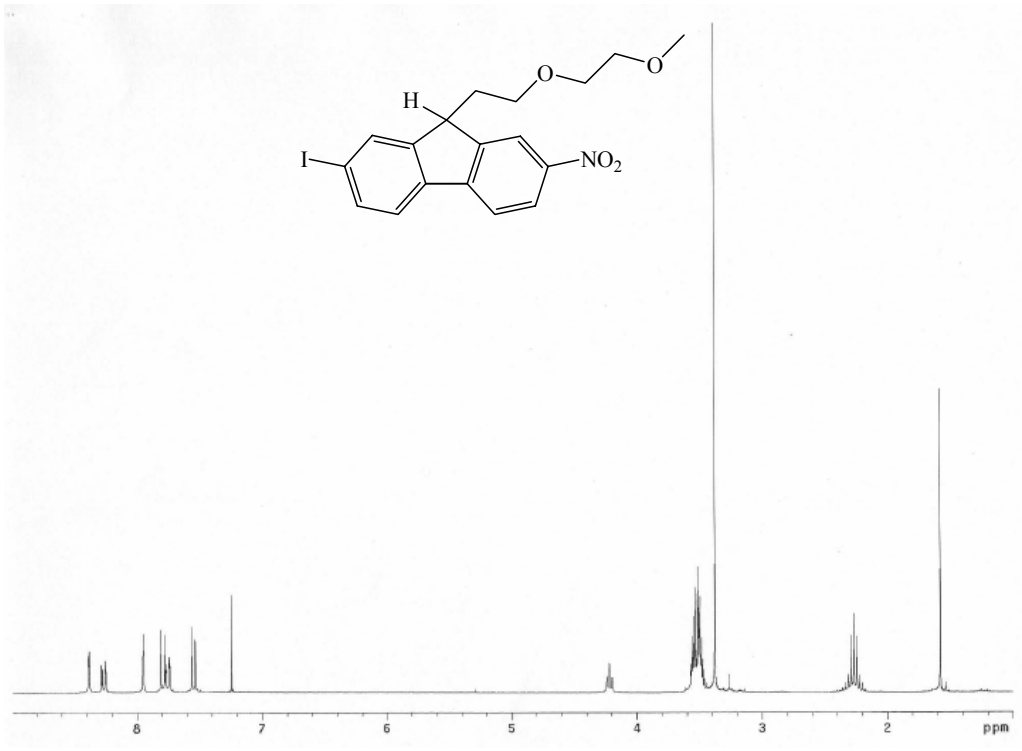

^{1}H NMR spectrum of Compound 8.

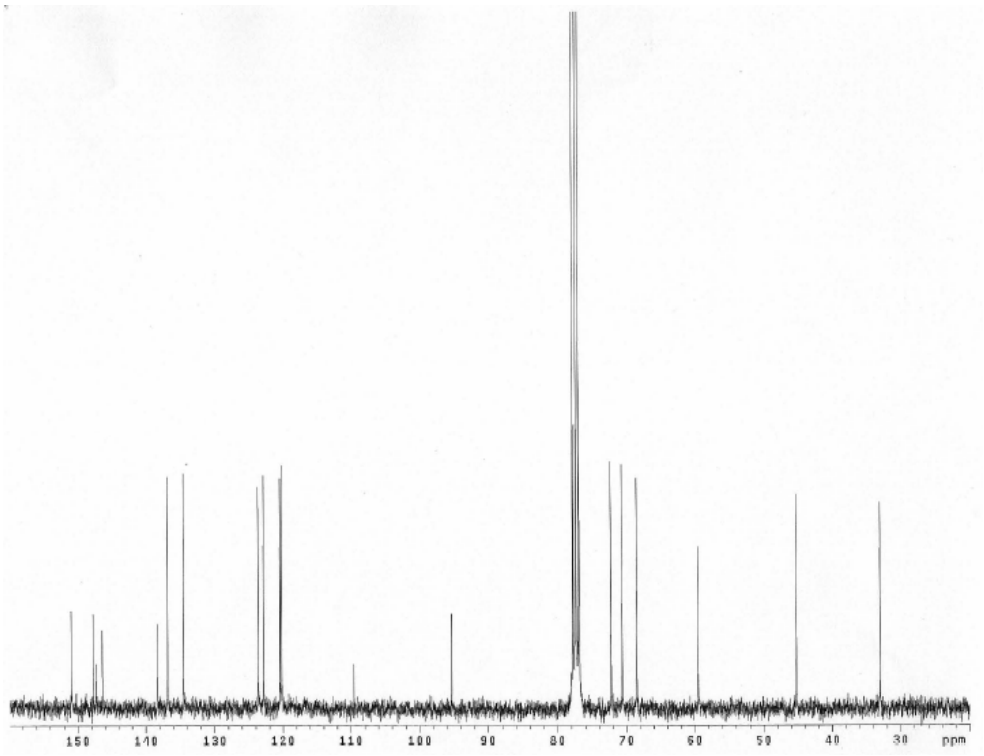

^{13}C NMR spectrum of Compound 8.

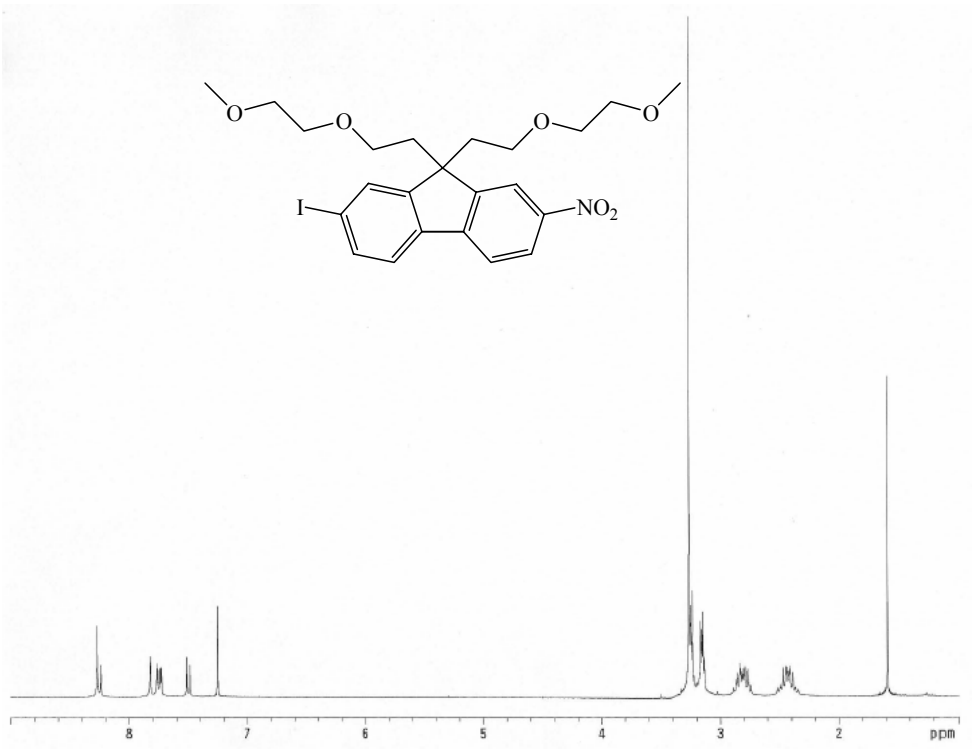

^{1}H NMR spectrum of Compound 9.

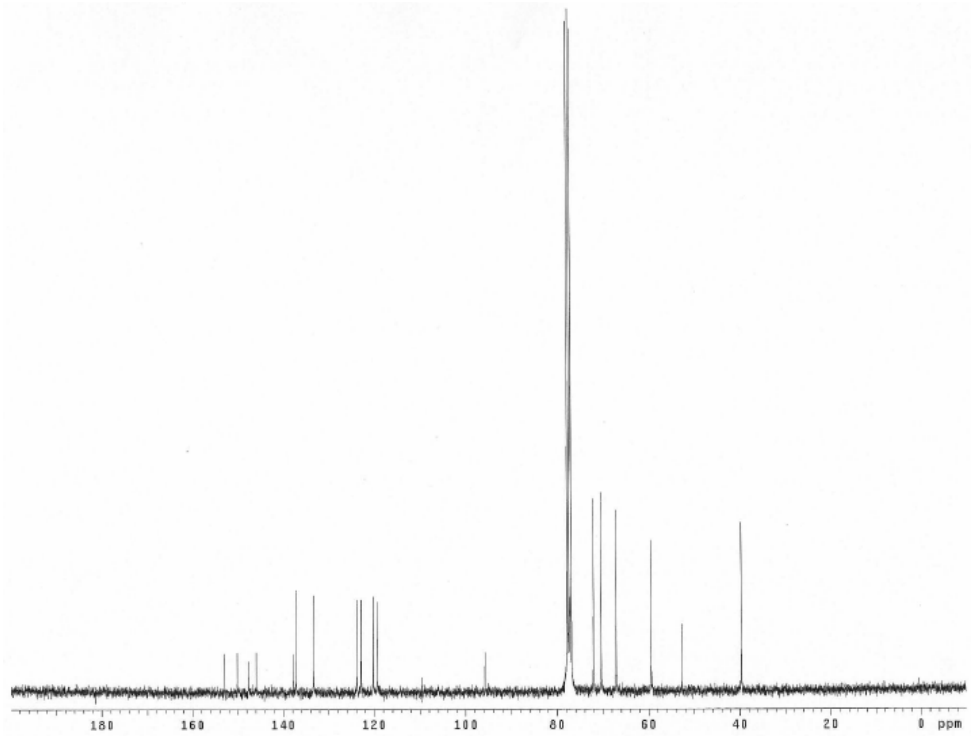

^{13}C NMR spectrum of Compound 9.

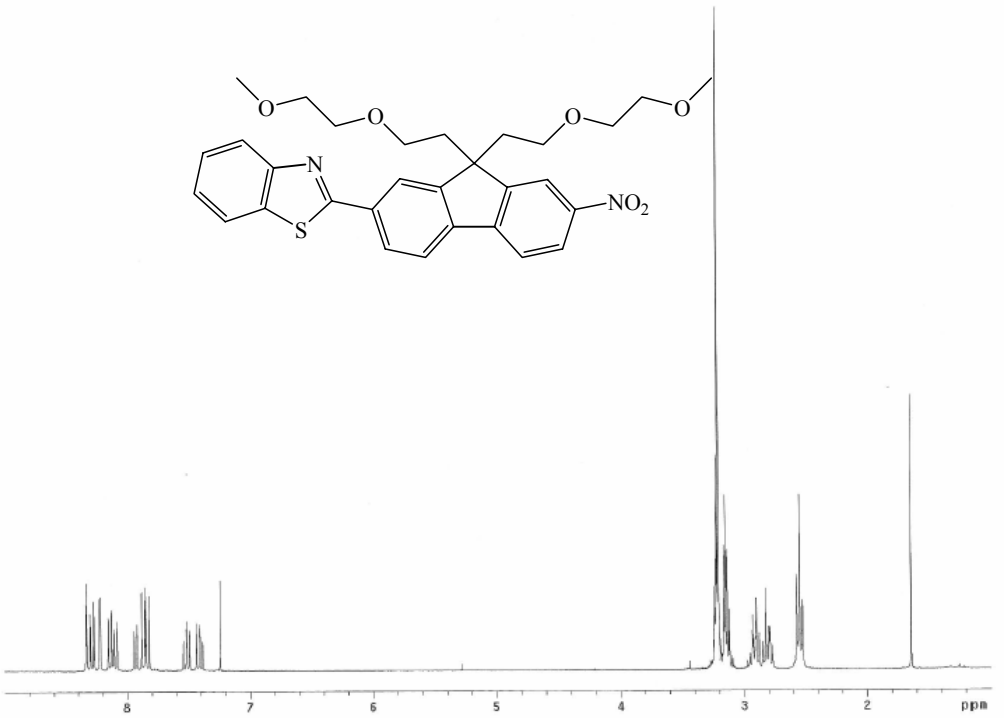

^{1}H NMR spectrum of Compound 11.

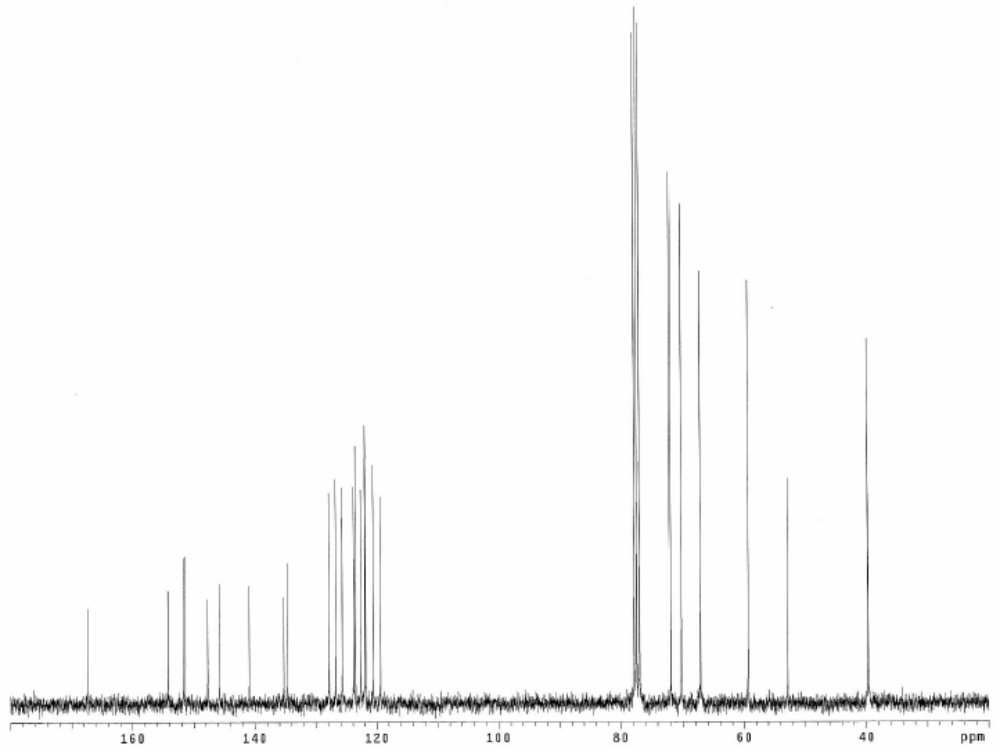

^{13}C NMR spectrum of Compound 11.

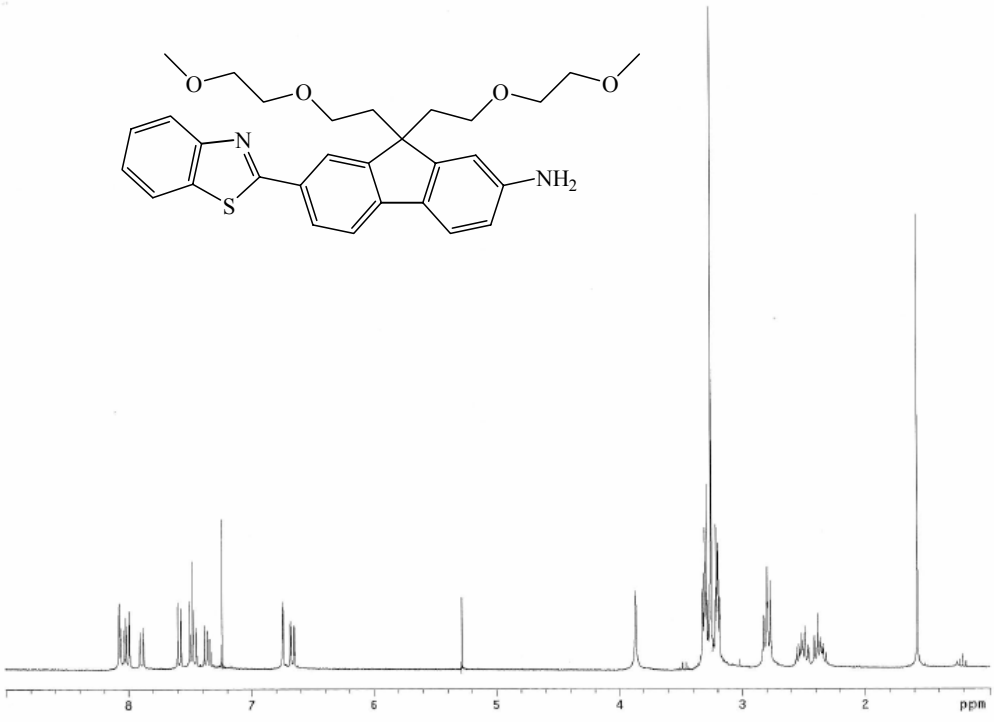

^{1}H NMR spectrum of Compound 12.

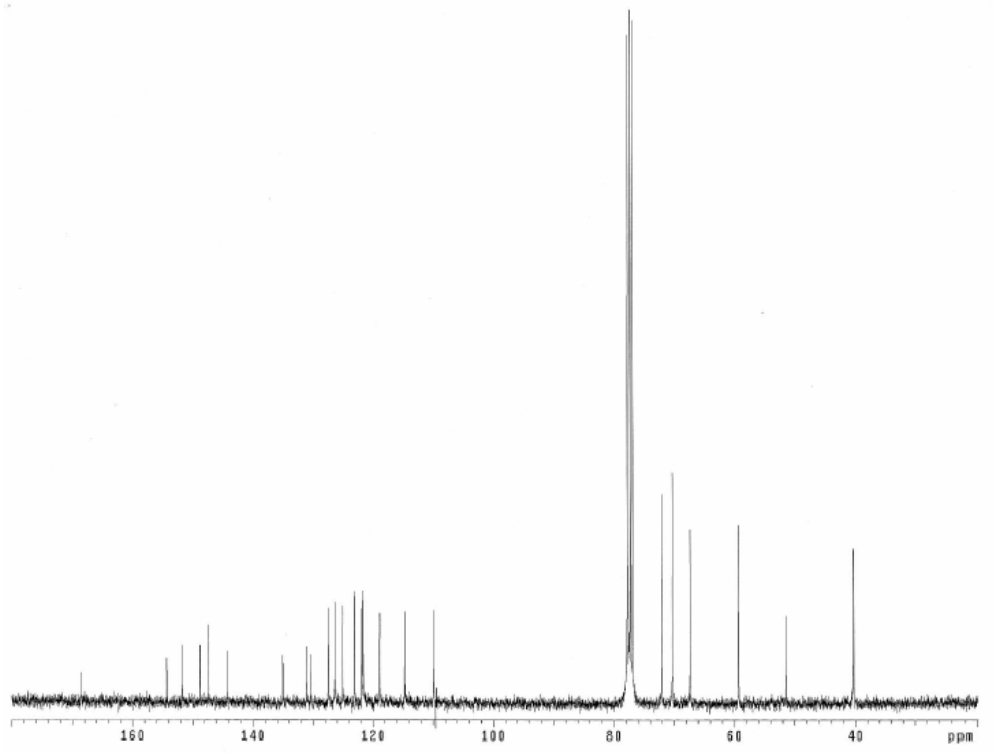

^{13}C NMR spectrum of Compound 12.

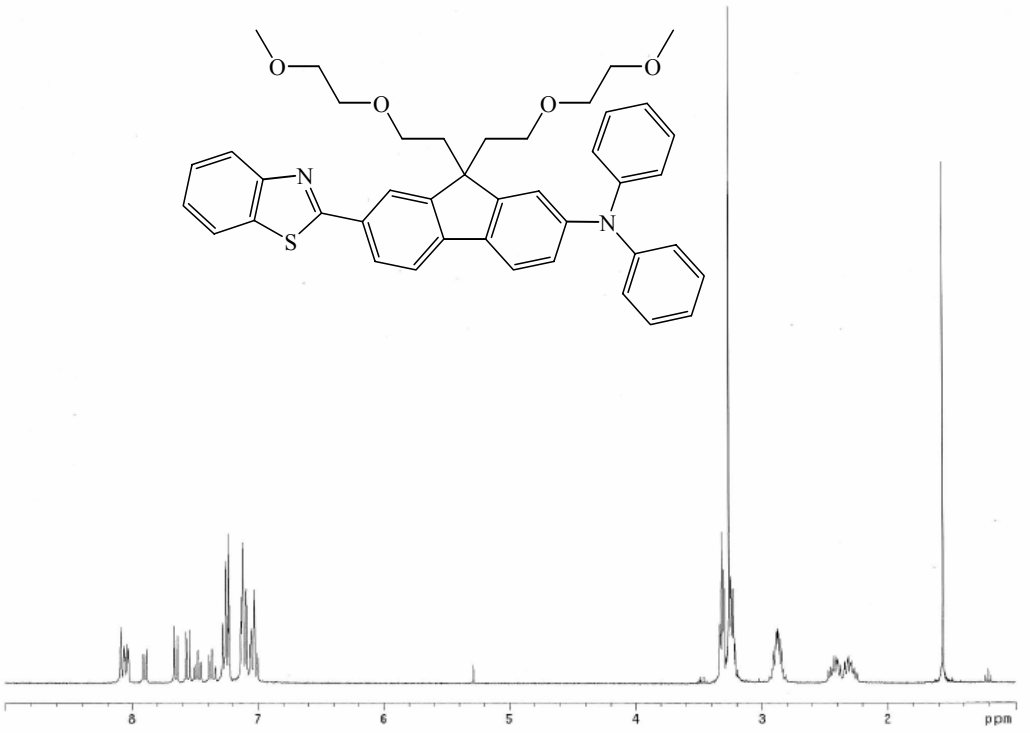

^{1}H NMR spectrum of Compound 13.

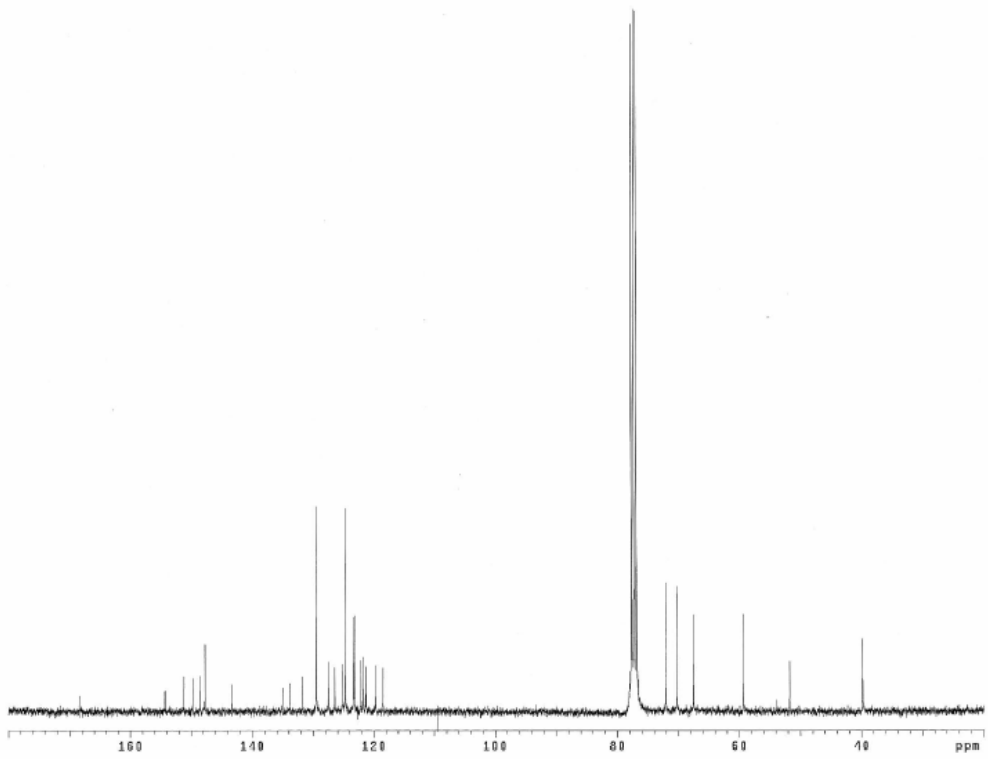

^{13}C NMR spectrum of Compound 13.

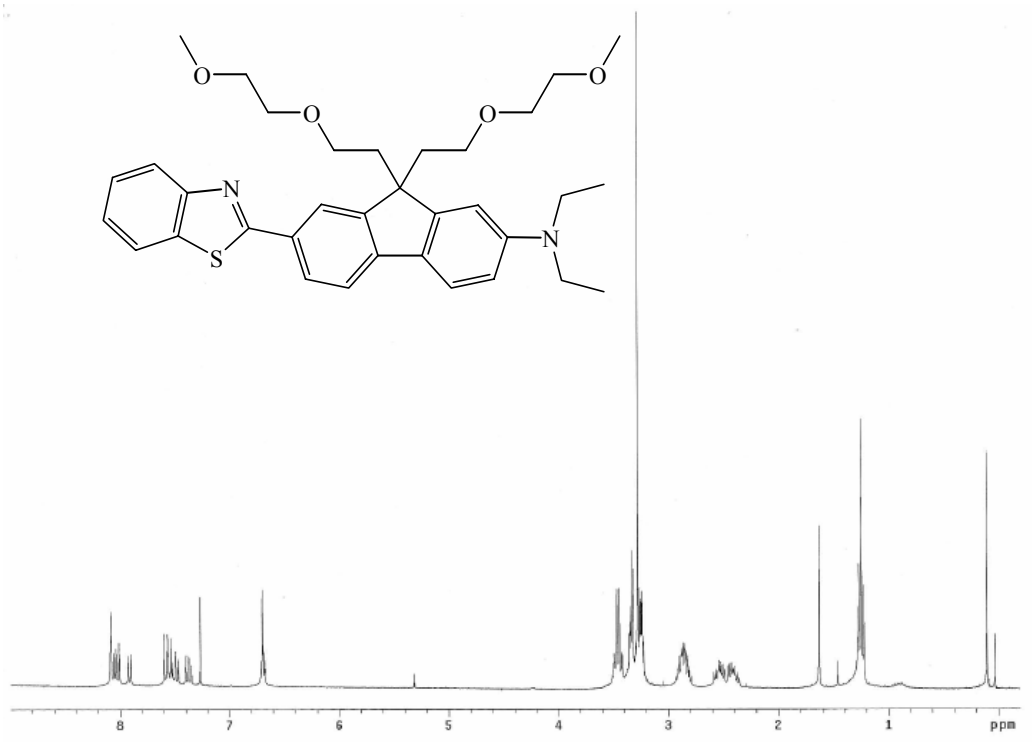

^{1}H NMR spectrum of Compound 14.

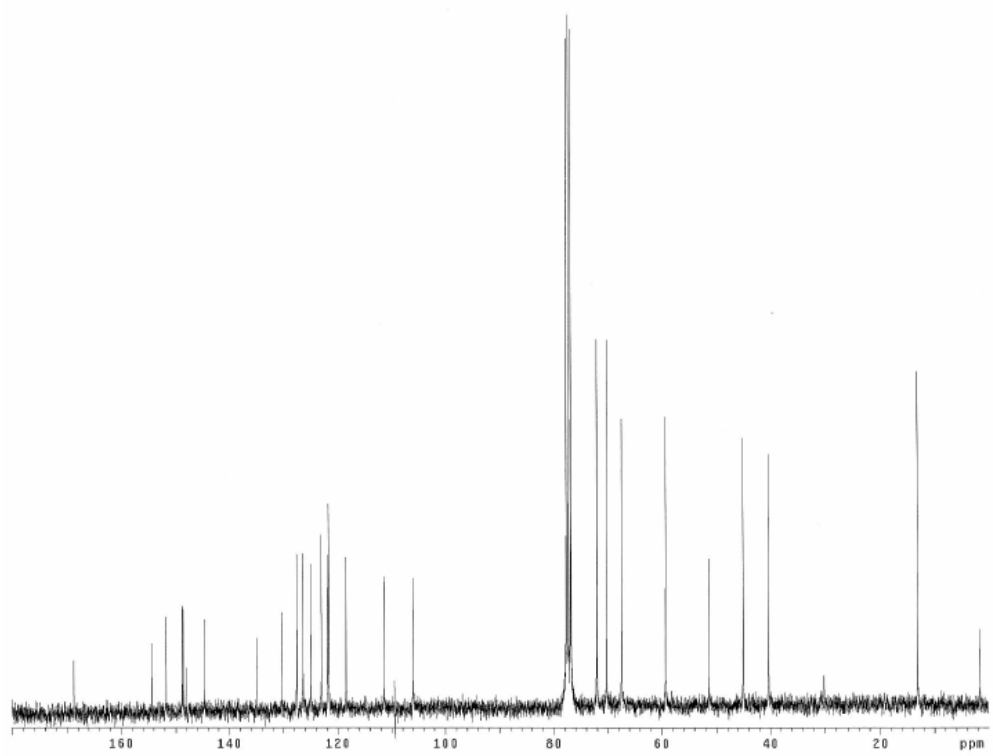

^{13}C NMR spectrum of Compound 14.

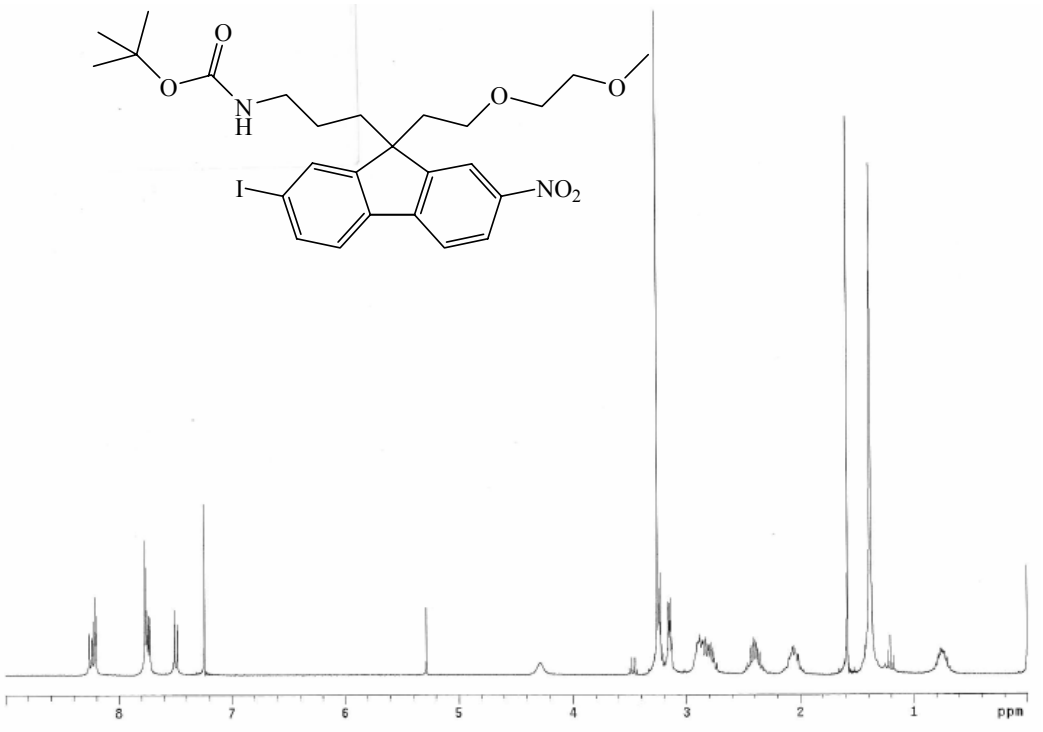

^{1}H NMR spectrum of Compound 15.

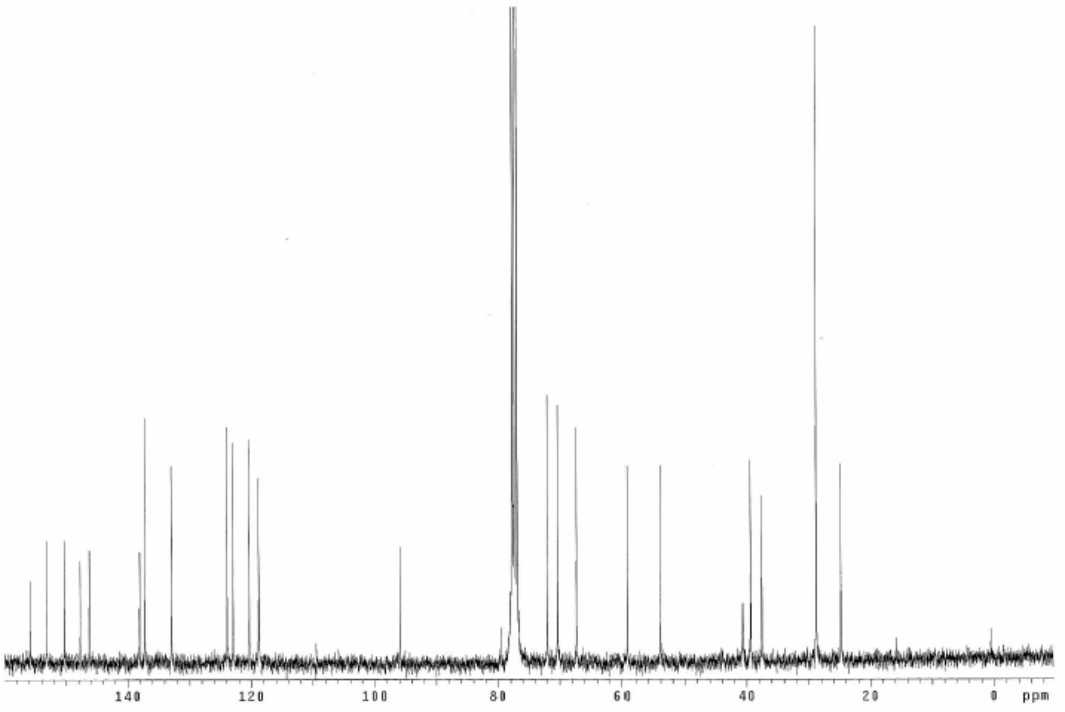

^{13}C NMR spectrum of Compound 15.

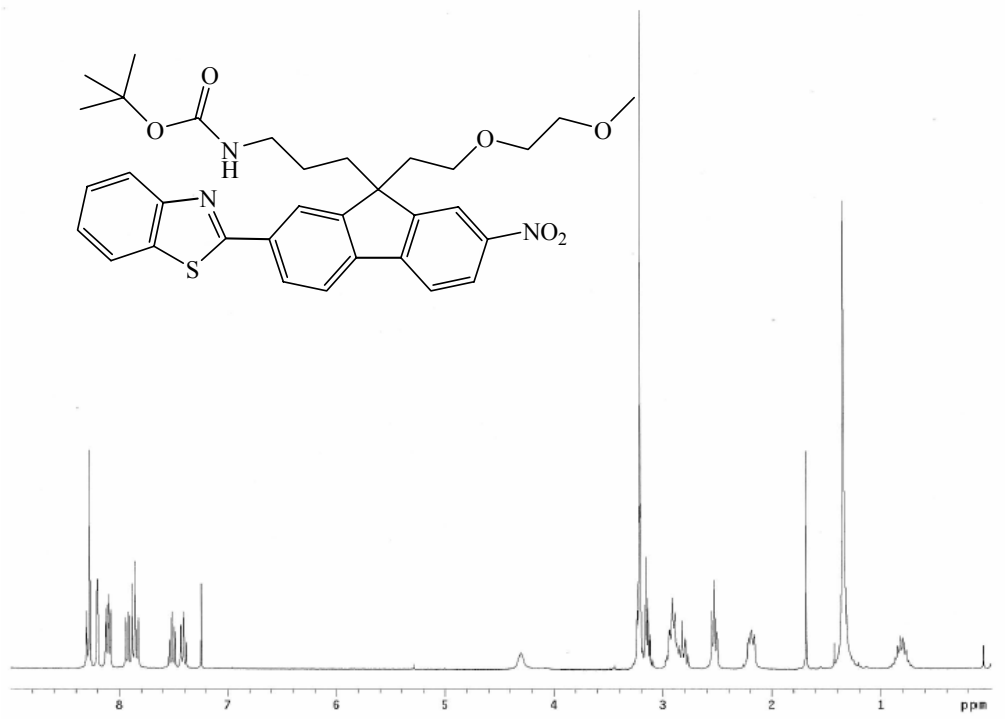

^{1}H NMR spectrum of Compound 16.

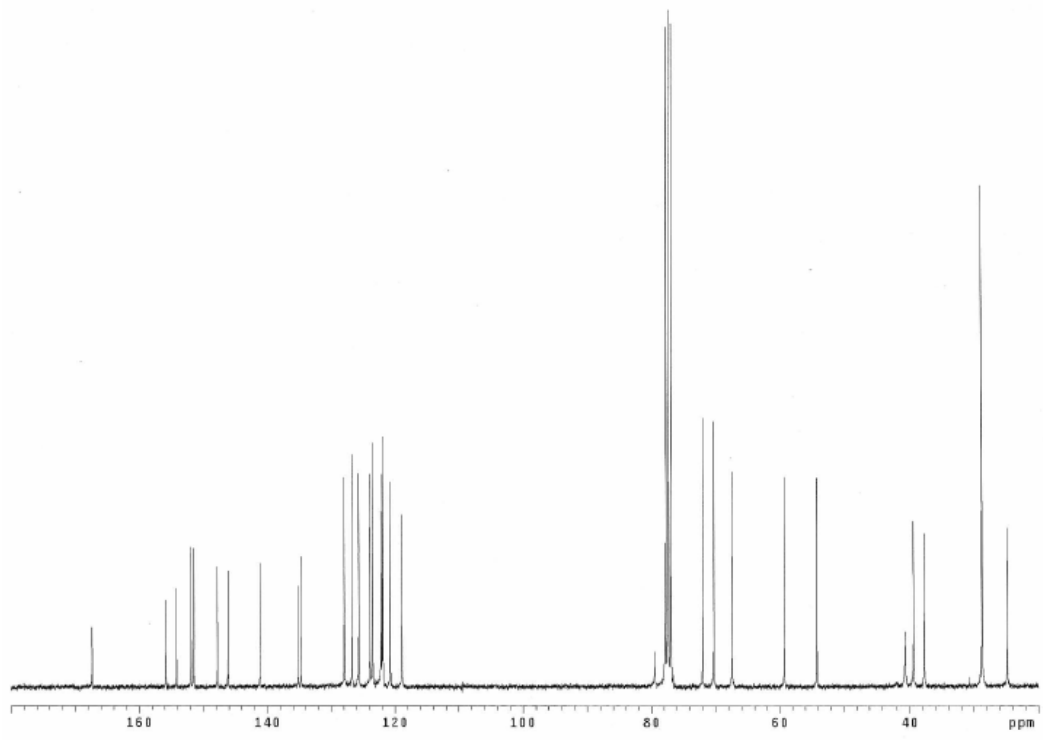

^{13}C NMR spectrum of Compound 16.

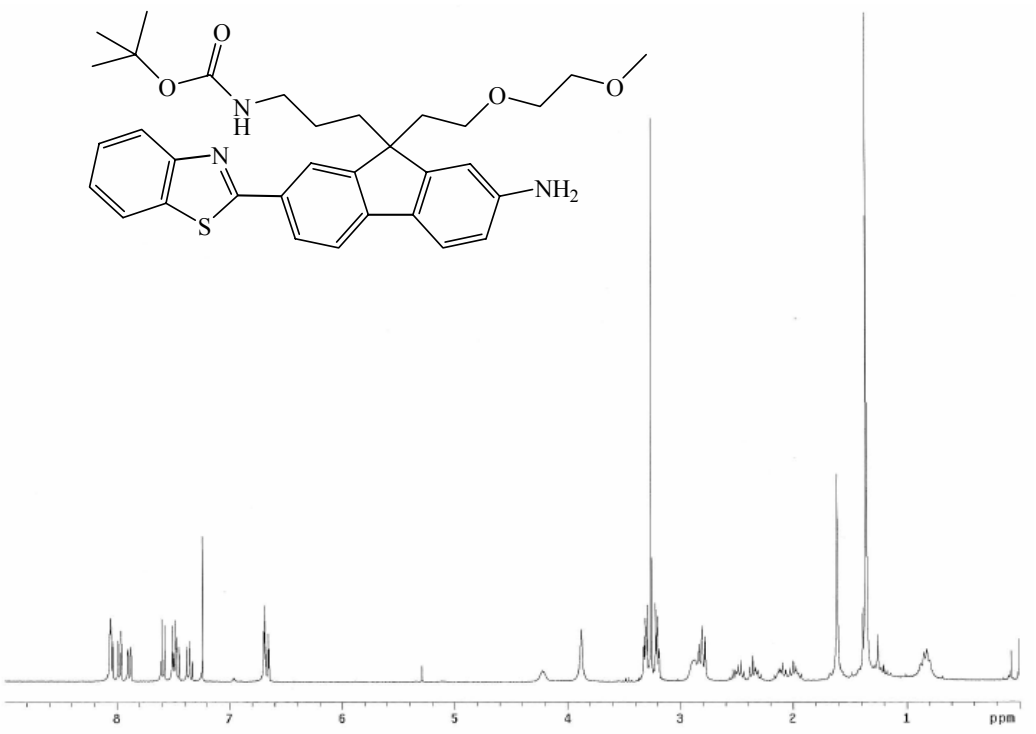

^{1}H NMR spectrum of Compound 17.

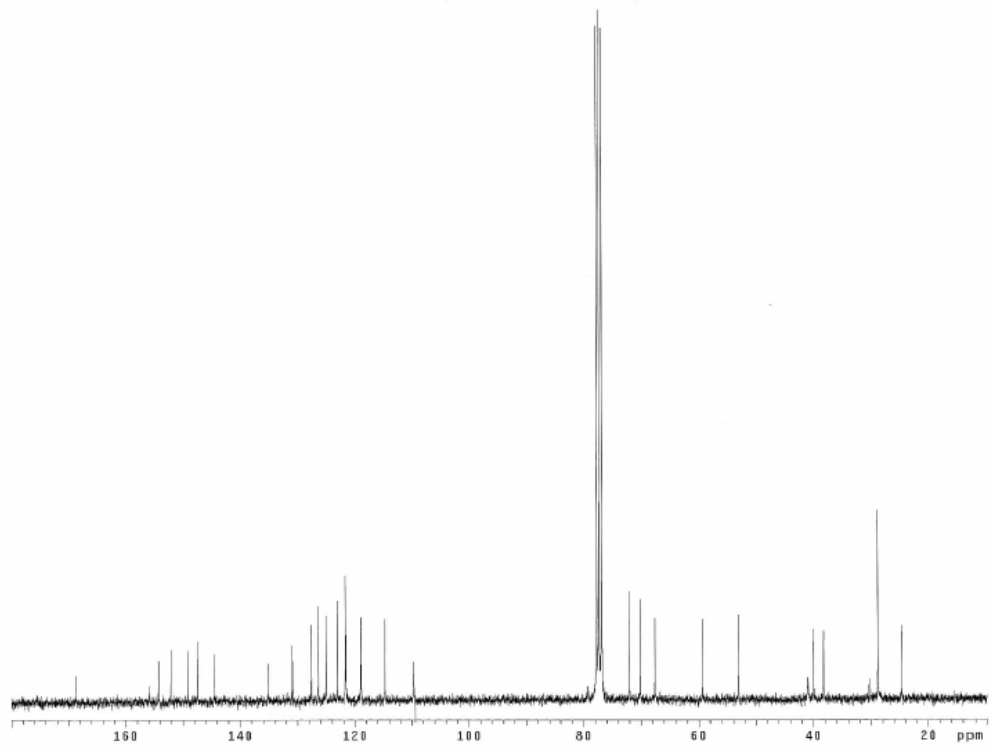

^{13}C NMR spectrum of Compound 17.

APPENDIX B: SPECTROSCOPIC TECHNIQUES AND METHODS

A.B.1: Linear Spectroscopic Techniques

The UV-visible absorption spectra were recorded on an Agilent 8453 spectrophotometer using standard 1 cm path length quartz cuvettes at room temperature. Identification of the absorption maximum of each compound was obtained from absorption spectra collected within the linear response of detection. Calculation of the molar absorptivity (ε) of the fluorene compounds were performed by preparing serial dilutions (minimum of three dilutions) in the range of 10^{-5} – 10^{-6} M from a concentrated stock solution in the range of 1.0 x 10^{-2} M. Average values of the absorption maximum obtained from the serial dilutions were used to report the molar absorptivity, ε, (units of $M^{-1}cm^{-1}$) of the compounds using the Beer-Lambert law, A = εbc, where A = absorbance, c = concentration of the sample in units of moles per liter (M), and l = path length in centimeters.

The seady-state fluorescence emission and excitation spectra were collected on a PTI Quantamaster spectrofluorimeter under 90 degree excitation in a T-format method [16] with a Xe lamp as the excitation source. Fluorescence quantum yield (η) calculations were determined using the same spectrofluorimeter and from the corrected fluorescence spectra using a standard method relative to Rhodamine 6G in ethanol (η = 0.94) and/or 9,10- diphenylanthracene (9,10-DPA) in cyclohexane (η = 0.95) [16]. All fluorescence measurements were performed in dilute solutions in the 10^{-6} M range to minimize reabsorption of the excitation light. Additional fluorescence measurements as the fluorescence lifetimes were obtained with a PTI Timemaster system with a strobe photomultiplier tube detector and a 600-picosecond laser pulse excitation (GL 302 dye laser, pumped by GL 3300 nitrogen laser with 10 Hz repetition rate). The time resolution

of this system was determined with the PTI Timemaster software and reached 0.1 ns. Fluorescence lifetime standards, *p*-terphenyl in ethanol (τ = 1.05 ns) and dimethyl-POPOP in ethanol (τ = 1.45 ns) were used to verify obtained lifetimes [16]. A more complete description of the steady-state and time-resolved fluorescence spectroscopic measurements obtained on fluorene derivatives may be found in references 33e and 33f.

A.B.2: Calcuations of the Degree of Labeling

The degree of labeling (DOL) for the model BSA-fluorene bioconjugate was estimated using average values from equations (1) and (5) below adopted from the Molecular Probes product brochure on Amine-Reactive Probes [http://probes.invitrogen.com/] and references 55, respectively. The protein concentration after conjugation was determined against a concentration calibration curve of free BSA in PBS (pH 7.2) solution, after taking into account the corrected absorbance of the dye at 280 nm. The correction factor, CF, accounts for the contribution of the dye to the absorbance at A_{280}. The CF value of the amine-reactive fluorene dye (**2**) was determined to be 0.09, and the $\varepsilon_{max(357)}$ of the free dye (at its absorption λ_{max} at 357 nm) in DMSO solution was 33,000. Typically, use of equation (5) afforded slightly elevated DOL values than that obtained from (1), but both were generally in good agreement with each other. In general, estimation of the DOL using (1) appears to suffice, assuming the molecular weight of the protein and its concentration is known.

$$DOL = \frac{A_{max} \times MW}{[protein] \times \varepsilon_{dye}} \quad (1)$$

MW = molecular weight of the protein

[protein] = protein concentration

ε_{dye} = extinction coeffieient of the dye at its absorbance maximum

A_{max} = absorption maximum for the dye

$$DOL = (A_{dye}/\varepsilon_{dye}) \times [\varepsilon_{280}/A_{280} - (A_{dye} \times CF)] \quad (2)$$

$$= \text{mol of dye/mol of protein}$$

A_{dye} = absorbance at peak wavelength

ε_{dye} = extinction coeffiecient of the dye (at same wavelength as Adye)

ε_{280} = extinction coefficient of the protein at 280 nm

CF = percentage correction factor (3)

$= A_{280}$ free dye/A_{max} free dye

$$A_{protein} = A_{280} - A_{max} \times CF \quad (4)$$

$$DOL = (A_{dye}/\varepsilon_{dye}) \times (\varepsilon_{280}/A_{protein}) \quad (5)$$

A.B.3: Two-Photon Spectroscopy

The primary nonlinear spectroscopic technique used to characterize the two-photon absorption behavior of the fluorene compounds in this dissertation was the two-photon induced fluorescence (2PF) method. In this process, a strong pump beam excites a material via 2PA and, provided the material is fluorescent, the strength of the two-photon induced fluorescence is monitored. One can determine the value of the 2PA cross-section, δ, for that particular pump wavelength and by varying the wavelength of the pump beam, while monitoring the two-photon induced fluorescence, the entire 2PA spectrum of the material is obtained. The 2PA behavior of the compound is compared, relative to that of a compound with a known 2PA cross section under the same

experimental condition. This method of two-photon induced fluorescence spectroscopy was initially implemented by Xu and Webb in 1996 [8d]. Details of the experimental setup used to determine the 2PA cross-section utilizing the 2PF method for the fluorene compounds studied in this dissertation is fully described in reference 12.

Another nonlinear spectroscopic method, the Z-scan [15b], was employed to verify the magnitude of the 2PA cross-section obtained from the 2PF method. In this techniuque, the transmittance of a single, focused, Gaussian beam through a nonlinear medium is monitored as a function of the sample position, z, measured with respect to the beam's waist. As the sample is translated along the axis of the focused beam, it passes through its waist where the irradiance is maximized. Provided the sample exhibits nonlinear absorption, the transmittance of the beam at this point should be a minimum. Fitting the transmission curve allows δ to be extracted [15b] and by repeating this experiment for various pump wavelengths, determination of the full 2PA spectrum can be made. The details of these experiments are beyond the scope of this study and full experimental descriptions of this and additional nonlinear spectroscopic techniques used to determine the 2PA cross-sections of the fluorene derivatives may be found in references 12 and 51.

APPENDIX C: MICROSCOPY IMAGING AND PROTOCOLS

A.C.1: Epi-Fluorescence and DSU Confocal Microscopy

Bright field transmission and epi-fluorescence microscope images of glutaraldehyde fixed H9c2 cells stained with a well-characterized two-photon absorbing dye **1**, were collected on a Nikon Eclipse E600 upright microscope using a standard FITC filter set. The NT2 cells were plated onto uncoated, 35 mm glass-bottom culture dishes (MatTek) incubated with compound **13** prior to their *in vitro* fluorescent imaging on an Olympus IX2-DSU (disk scanning unit) inverted confocal microscope. Fresh growth media was exchanged prior to performing confocal imaging to minimize contribution from excess fluorophore in the media. Typically, a 40x (NA = 0.6) or 60x (NA = 1.35) oil immersion objective was used and the image false-colored for ease of viewing. Compound **13** was excited (Hg lamp), and the resulting fluorescence was collected through a modified CFP filter (DAPI exciter Ex377/50 with CFP 458DM, Em483/32) filter set to accommodate the spectral profile of this dye. Images were collected on a Hamamatsu C9100-02 electron multiplier CCD camera.

A.C.2: Two-Photon Excited Laser Scanning Confocal Microscopy

Two-photon excited fluorescence microscopy images of the fixed H9c2 and live NT2 cells were performed on a modified Olympus IX 70 inverted microscope and Fluoview300 laser scanning confocal unit accommodating a 10 W Verdi (Coherent) pumping a Ti:sapphire crystal of a Mira 900 (Coherent). The system also accommodates an Argon ion laser (488 nm) for conventional laser scanning confocal imaging, as well as a mercury lamp for epi-fluorescent microscopy imaging. The general schematic of the system is shown below in figure A.C.2.1. Normal, epi-fluorescent images may be aquired via a cooled CCD camera (Retiga EX*i* from Q Imaging), while the confocal fluorescent images are collected via two Hamamatsu PMT

detectors. Some coatings on the interal optical components of the Fluoview laser scanning unit were modified to accommodate the near-IR wavelengths from the Ti:Sapphire laser. Additionally, a long-wavelength barrier filter was placed in front of the two PMTs to minimize the contributution of the high intensity, near-IR excitation wavelength to the two-photon induced fluorescence.

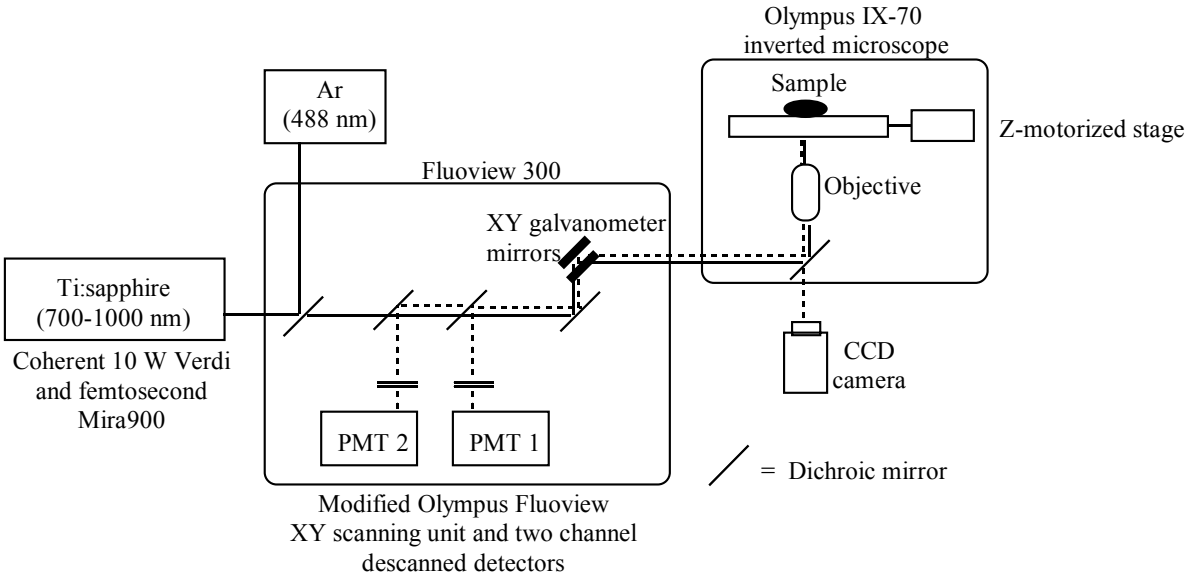

Figure A.C.1: General schematic of the modified Olympus IX70 inverted microscope with a Flouview300 laser scanning confocal unit accommodating a tunable Ti:sapphire femtosecond laser source.

Two-photon induced fluorescent images of the glutaraldehyde fixed cells incubated with fluorene derivatives were collected on the modified Olympus IX70 confocal system shown above. Two-photon induced fluorescence from the fluorophores was detected upon 760 – 880 nm fs excitation wavelengths. Typically, exposure to 800 nm excitation of 160 fs pulses, 10 mW average power, 76 MHz repetition rate, using either a 40x or 60x oil objectives were sufficient for fixed cells. The lowest average power used to collect the two-photon induced fluorescence from the fixed and stained cells was ~ 1.5 mW (at the sample).

The two-photon induced fluorescent live NT2 cell imaging were also collected on the Olympus IX70 system shown above. Typically, the NT2 cells were plated onto a poly-*d*-lysine coated glass cover slip (40 mm) ~ 24 hours prior to assembly into a Bioptechs FCS2 live-cell chamber system. The temperature of the heating base was set for 37 ºC and ~ 30 μM of compound **13** dissolved in DMSO was mixed into the growth media to be continuously perfused over the cells. The assembled FCS2 containing NT2 cells were then placed onto the modified Olympus IX70 stage and irradiated with 800 nm excitation (150 fs, ~ 30 mW, 76 MHz, 40x) at 10 min intervals for several hours, up to 17 hours. As a final note, fluorene compound **13** exhibited efficient 2P induced fluorescence in fixed NT2 cells upon exposure to a focused 140 fs scanning beam at 800 nm (76 MHz) of ~ 1 mW mean power. This is a relatively low power for observing two-photon induced fluorescence, as typical irradiation of fluorophores purported for bioimaging range from 5-10 mW [8]. The consequence of using low mean powers for efficient fluorescence bioimaging is particulary relevant under live-cell imaging conditions, where average powers > 5mW of femtosecond near-IR irradiation have been shown to be detrimental to cell vitality and proliferation [19]. Hence, careful controls need to be performed to verify that the irradiation conditions used for two-photon induced fluorescence imaging does not induce phototoxic effects, especially when long-term (on the order of hours) imaging of live specimens is of interest.

LIST OF REFERENCES

[1] Göppert-Mayer, M. "Elementary actions with two quantum leaps", *Ann. Phys.* **1931**, *9*, 273.

[2] Kaiser, W. and Garrett, C.G.B. "Two-photon excitation in CaF2:Eu2+", *Phys. Rev. Lett.* 1961, 7, 229.

[3] Hellwarth, R. and Christensen, P. "Nonlinear optical microscope examination of structures in polycrystalline ZaSe", *Opt. Commun.* **1974**, *12*, 318.

[4] Sehppard, C. and Kompfner, R. "Resonant scanning optical microscope", *Appl Opt* **1978**, *17*, 2879.

[5] Kleinschmidt, J.; Rentsch, S.; Tottleben, W.; Whilhelmi, B. "Measurement of strong nonlinear absorption in stilbene-chloroform solutions, explained by the superposition of two-photon absorption and one-photon absorption from the excited state" *Chem. Phys. Lett.* **1974**, *24*, 133.

[6] Denk, W.; Strickler, J.; Webb, W; Two-photon laser scanning fluorescence microscopy", *Science*, **1990**, *248*, 73.

[7] a) Denk, W.; Piston, D.W.; Webb, W.W. "Two-photon molecular excitation in laser-scanning microscopy", in *Handbook of Confocal Microscopy*, 2nd Edition. Pawley, J., Ed.; Plenum: New York, 445-458, 1995. b) Bhawalkar, J.D.; Shih, A.; Pan, S.J.; Liou, W.S.; Swiatkiewicz, J.; Reinhardt, B.A.; Prasad, P.N.; Cheng, P.C. "Two-photon laser scanning fluorescence microscopy--from a fluorophore and specimen perspective", *Bioimaging* **1996**, 4, 168. c) Diaspro, A. (Ed.) Two-photon microscopy-Part II. *Microsc. Res. Tec.* **2004**, *63*, 1-86.

[8] a) Xu, C. and Webb, W.W. "Measurement of two-photon excitation cross sections of molecular flurophres with data from 690 to 1050 nm", *J. Opt. Soc. Am. B.* **1996**, *13*, 481. b) Xu, C.; Williamns, R.M.; Zipfel, W.; Webb, W.W. "Multiphoton excitation cross-sections of molecular fluorophores", *Bioimaging* **1996**, *4*, 198. c) Xu. C.; Zipfel, W.; Shear, J.B.; Williams, R.M.; Webb, W.W. "Multiphoton fluorescence excitation: New spectral window for biological nonlinear microscopy", *Proc. Natl. Acad. Sci. USA* **1996**, *93*, 10763. d) Albota, M.A.; Xu, C.; Webb, W.W. "Two-photon fluorescence excitation cross sections of biomolecular probes from 690 to 960 nm", *Appl. Opt.* **1998**, *37*, 7352.

[9] a) Pettit, D.L.; Wang, S.S.H.; Gee, K.R.; Augustine, G.J. "Chemical two-photon uncaging: a novel approach to mapping glutamate receptors", *Neuron*, **1997**, *19*, 465. b) Wachter, E.A.; Partridge, W.P.; Fisher, W.G.; Dees, H.C.; Petersen, M.G. "Simultaneous two-photon excitation of photodynamic therapy agents", *Proc. SPIE*, **1998**, *3269*, 68.

[10] a) Brown, E.B.; Shear, J.B.; Adams, S.R.; Tsien, R.Y.; Webb, W.W. "Photolysis of caged calcium in femtoliter volumes using two-photon excitation", *Biophys. J.* **1999**, *76*, 489. b) Soeller, C.; Jacobs, M.D.; Donaldson, P.J.; Cannell, M.B.; Jones, K.T.; Ellis-Davies, G.C.R. "Application of two-photon flash photolysis to reveal intercellular communication and intracellular Ca2+ movements", *J. Biomed. Opt.* **2003**, *8*, 418. c) Wang, S.S.-H.; Khiroug, L.; Augustine, G.J. "Quantification of spread of cerebellar long-term depression with chemical two-photon uncaging of glutamate", *Proc. Natl. Acad. Sci. USA*, **2000**, *97*, 8635.

[11] a) Jacques, S.L.; Prahl, S.A. "Absorption spectra for biological tissues", *Oregon Graduate Institute*, http://omlc.ogi.edu/classroom/ece532/class3/muaspectra.html (1998). b)

Anderson, R.R. and Parrish, J. A. "The optics of human skin", *J. Invest. Derma.* **1981**, *77*, 13.

[13] a) Diaspro, A. "Introduction to Two-Photon Microscopy", *Microsc. Res. Tech.* **1999**, *47*, 163. b) So, P.T.C.; Kim, K.H.; Buehler, C.; Masters, B.B.; Hsu, L.; Dong, C-Y. "Basic Principles of Multiphoton Exciation Microscopy". Periasamy, A. (Ed.), in *Methods in Cellular Imaging*, Oxford: New York, 2001.

[14] a) Birge, R.R. and Pierce, B.M., "A theoretical analysis of the two-photon properties of linear polyenes and the visual chromophores", *J. Chem. Phys*. **1979**, *70*, 165. b) Birge, R.R., "One-photon and Two-Photon Excitation Spectroscopy". Kliger, D.S. (Ed.), in *Ultrasensitive Laser Spectroscopy*, Academic Press: New York, 109-174, 1983. c) McClain, W.M., "Excited state symmetry assignment through polarized two-photon absorption studies of fluids", *J. Chem. Phys*. **1971**, *55*, 2789. d) Friedrich, D.M. and McClain, W.M. "Two-photon molecular electronic spectroscopy", *Ann. Rev. Phys. Chem*. **1980**, *31*, 559. e) Wirth, M.J.; Koskelo, A.; Sanders, M.J. "Molecular symmetry and two-photon spectroscopy", *Appl. Spect*. **1981**, *35*, 14. f) Mortensen, O.S and Svendsen, E.N. "Initial and final molecular states as "virtual states" in two-photon processes", *J. Chem. Phys.* **1981**, *74*, 3185. g) Dick, B. and Hohlneicher, G. "Importance of initial and final states as intermediate states in two-photon spectroscopy of polar molecules", *J. Chem. Phys*. **1982**, *76*, 5755.

[15] a) Twarowski, A.J. and Kliger, D.S., "Multiphoton absorption spectra using thermal blooming", *Chem. Phys*. **1977**, *20*, 259. b) Sheik-Bahae, M.; Said, A.A.; Wei, T.; Hagan, D.; Van Stryland, E.W. "Sensitive measurement of optical nonlinearities using a single

beam", *IEEE J. Quantum Electron.* **1990**, *26*, 760. c) Hermann, J.P. and Ducuing, J. "Absolute measurement of two-photon cross sections", *Phys. Rev. A* **1972**, *5*, 2557.

[16] Lakowicz, J.R. in *Principles of fluorescence spectroscopy*, 2nd ed. Kluwer Academic/Plenum: New York, 1999.

[17] a) Bestvater, F.; Spiess, E.; Stobrawa, G.; Hacker, M.; Feurer, T.; Porwol, T.; Berchner-Pfannschmidt, U.; Wotzlaw, C.; Acker, H. "Two-photon fluorescence absorption and emission spectra of dyes relevant for cell imaging", *J. Micros.* **2002**, *208*, 108. b) Neu, T.R.; Kuhlicke, U.; Lawrence, J.R. "Assessment of fluorochromes for two-photon laser scanning microscopy of biofilms", *Appl. Environ. Microbiol.* **2002**, *68*, 901.

[18] Coherent Inc. http://www.cohr.com/downloads/MIRA900.pdf

[19] a) Konig, K.; So, P.T.C.; Mantulin, W.W.; Gratton, E. "Cellular response to near-infrared femtosecond laser pulses in two-photon microscopes", *Opt. Lett*. **1997**, *22*, 135. b) Konig, K.; Becker, T.W.; Fischer, P.; Riemann, I..; Halbhuber, K-J. "Pulse-length dependence of cellular response to intense near-infrared laser pulses in mulitphoton microscopy", *Opt. Lett*. **1999**, *24*, 113. c) Tirlapur, U.K.; Konig, K.; Peuckert, C.; Krieg, R.; Halbhuber, K-J. "Femtosecond near-infrared laser pulses elicit generation of reactive oxygen species in mammalian cells leading to apoptosis-like death", *Exp. Cell Res*. **2001**, *263*, 88.

[20] a) Lakowicz, J. R., and Gryczynski, I., "Tryptophan fluorescence intensity and anisotropy decays of human serum albumin resulting from one-photon and two-photon excitation", *Biophys. Chem*. **1992**, *45*, 1. b) Lackowicz, J.R.; Kierdaszuk, B.; Callis, P.; Malak, H.; Gryczynski, I. "Fluorescence anisotropy of tyrosine using one-and two-photon exciation", *Biophys. Chem*. **1995**, *56*, 263.

[21] a) Kierdaszuk, B.; Malak, H.; Gryczynski, I.; Callis, P.; Lakowicz, J.R. "Fluorescence of reduced nicotinamides using one- and two-photon excitation", *Biophys. Chem*. **1996**, *62*, 1. b) Piston, D.W.; Master, B.R.; Webb, W.W.; "Three-dimensionally resolved NAD(P)H cellular metabolic redox imaging of the in situ cornea with two-photon excitation laser scanning microscopy", *J. Micros.* **1995**, *178*, 20.

[22] Shear, J.B.; Xu, C.; Webb, W.W. "Multiphoton-excited visible emission by serotonin solution", *Photochem. Photobiol*. **1997**, *65*, 931.

[23] a) Tsien, R.Y. and Waggoner, A. "Flurophores for confocal microscopy, in Handbook of biological confocal microscopy" in *Handbook of Confocal Microscopy*, 2nd Edition. Pawley, J.B, Ed.; Plenum: New York, 267-279, 1995. b) Song, L.; Varma, C.A.G.O.; Verhoeven, J.W.; Tanke, H.J.; "Influence of the triplet excited state on the photobleaching kinetics of fluorescein in microscopy", *Biophys. J*. **1996**, *70*, 2959. c) Song, L.; Hennink, E.J.; Young, I.T.; Tanke, H.J. "Photobleaching kinetics of fluorescein in quantitative fluorescence microscopy", *Biophys. J*. **1995**, *68*, 2588.

[24] a) Patterson, G.H. and Piston, D.W. "Photobleaching in two-photon excitation microscopy", *Biophys. J*. **2000**, *78*, 2159. b) Dittrich, P.S. and Schwillle, P. "Photobleaching and stabilization of fluorophores used for single-molecule analysis with one- and two-photon excitation", *Appl. Phys. B: Lasers and Optics*, **2001**, *73*, 829.

[25] Chalfie, M.; Yuan, T.; Ghia, E.; Ward, W.W.; Prasher, D.C., "Green fluorescent protein as a marker for gene expression", *Science*, **1994**, *263*, 802

[26] a) Tsien, R.Y. "The green fluorescent protein", *Annu. Rev. Biochem*. **1998**, *67*, 509. b) Baird, G.S.; Zacharias, D.A.; Tsien, R.Y. "Circular permutation and receptor insertion

within green fluorescent proteins", *Proc. Natl. Acad. Sci. USA*, **1999**, *96*, 11241. c) Shaner, N.C.; Campbell, R.E.; Steinbach, P.A.; Giepmans, B.N.G.; Palmer, A.E.; Tsien, R.Y., "Improved monomeric red, orange and yellow fluorescent proteins derived from *Discosoma* sp. red fluorescent protein", *Nat. Biotech*. **2004**, *22*, 1567.

[27] a) Potter, S.M., Wang, C-M., Garrity, P.A., Fraser, S.E. "Intravital imaging of green fluorescent protein using two-photon laser-scanning microscopy", *Gene*, **1996**, *173*, 25. b) Blab, G.A.; Lommerse, P.H.M.; Cognet, L.; Harms, G.S.; Schmidt, T. "Two-photon excitation action cross-sections of the autofluorescent proteins", *Chem. Phys. Lett.* **2001**, *350*, 71. c) Spiess, E.; Bestvater, F.; Heckel-Pompey, A.; Toth, K.; Hacker, M.; Stobrawa, G.; Feurer, T.; Wotzlaw, C.; Berchner-Pfannschmidt, U.; Porwol, T.; Acker, H. "Two-photon excitation and emission spectra of the green fluorescent protein variants ECFP, EGFP and EYFP", *J. Microsc.* **2005**, *217*, 200.

[28] Gryczynski, I.; Piszczek, G.; Lakowicz, J.R.; Lagarias, J.C. "Two-photon excitation of a phytofluor protein", *J. Photochem. Photobiol. A: Chemistry*, **2002**, *150*, 13.

[29] a) Chan, W.C.W.; Nie, S. "Quantum dot bioconjugates for ultrasensitive nonisotropic detection", *Science*, **1998**, *218*, 2016. b) Gao, X.; Chan, W.C.W.; Nie, S., "Quantum-dot nanocrystals for ultrasensitive biological labeling and multicolor optical encoding", *J. Biomed. Opt*. **2002**, *7*, 532. c) Larson, D.R.; Zipfel, W.R.; Williams, R.M.; Clark, S.W.; Bruchez, M.P.; Wise, F.W.; Webb, W.W. "Water-soluble quantum dots for multiphoton fluorescence imaging in vivo", *Science*, **2003**, *300*, 1434. d) Sukhanova, A.; Devy, J.; Venteo, L.; Kaplan, H.; Artemyev, M.; Oleinikov, V.; Klinov, D.; Pluot, M.; Cohen,

J.H.M.; Nabiev, I. “Biocompatible fluorescent nanocrystals for immunolabeling of membrane proteins and cells”, *Anal. Biochem.* **2004**, *324*, 60.

[30] Nikesh, V.V.; Dharmadhikari, A.; Ono, H.; Nozaki, S.; Kumar, G.R.; Mahamuni, S. “Optical nonlinearity of monodispersed, capped ZnS quantum particles”, *Appl. Phys. Lett.* **2004**, *84*, 4602.

[31] Haugland, R.P. *Handbook of Fluorescent Probes and Research Chemicals*, 9th Ed. Eugene: Molecular Probes, Inc., 2002.

[32] Carl Zeiss interactive fluorophore database: http://www.zeiss.de/C12567BE0045 ACF1/Contents-Frame/3A1AE3EEC72195D8C1256DA500364F61.

[33] a) Belfield, K.D.; Morales, A.R.; Kang, B-S; Hales, J.M.; Hagan, D.J.; Van Stryland, E.W.; Chapela, V.M.; Percino, J. “Synthesis, characterization and optical properties of two-photon absorbing fluorene derivatives”, *Chem. Mater.* **2004**, *16*, 4634. b) Belfield, K.D.; Morales, A.R.; Hales, J.M.; Hagan, D.J.; Van Stryland, E.W.; Chapela, V.M.; Percino, J. “Linear and two-photon photophysical properties of a series of symmetrical diphenylaminofluorenes”, *Chem. Mater.* **2004**, *16*, 2267. c) Belfield, K.D.; Bondar, M.V.; Przhonska, O.V.; Schafer, K.J. “Photostability of a series of two-photon absorbing fluorene derivatives”, *J. Photochem. Photobiol. A: Chemistry*, **2004**, *162*, 489. d) Belfield, K.D.; Bondar, M.V.; Przhonska, O.V.; Schafer, K.J. ”Photochemical properties of (7-benzothiazol-2-yl-9,9-didecylfluoren-2-yl)diphenylamine under one- and two-photon excitation”, *J. Photochem. Photobiol. A: Chemistry*, **2004**, *162*, 569. e) Belfield, K.D.; Bondar, M.V.; Przhonska, O.V.; Schafer, K.J. “Steady-state spectroscopic and fluorescence lifetime measurements of new two-photon absorbing fluorene derivatives”, *J. Fluores.*

2002, *12*, 449. f) Belfield, K.D.; Bondar, M.V.; Przhonska, O.V.; Schafer, K.J.; Mourad, W. "Spectral properties of several fluorene derivatives with potential as two-photon fluorescent dyes", *J. Luminescence* **2002**, *97*, 141. g) Belfield, K.D.; Schafer, K.J.; Mourad, W.; Reinhardt, B.A. "Synthesis of new two-photon absorbing fluorene derivatives via Cu-mediated Ullmann condensation", *J. Org. Chem.* **2000**, *65*, 4475. h) Belfield, K.D.; Hagan, D.J.; Van Stryland, E.W.; Schafer, K.J.; Negres, R.A. "New two-photon absorbing fluorene derivatives: Synthesis and nonlinear optical characterization", *Org. Lett.* **1999**, *1*, 1575. i) Belfield,K.D.; Schafer, K.J. "A new photosensitive polymeric material for WORM optical data storage using multichannel two-photon fluorescence readout", *Chem. Mater.* **2002**, *14*, 3656.

[34] Mongin, O.; Porres, L.; Moreaux,.; Mertz, J.; Blanchard-Desce, M. "Synthesis and photophysical properties of new conjugated fluorophores designed for two-photon-excited fluorescence", *Org. Lett.* **2002**, *4*, 719.

[35] a) Reinhardt, B.A.; Brott, L.L.; Clarson, S.J.; Dillard, A.G.; Bhatt, J.C.; Kannan, R.;Yuan, L.; He, G.S.; Prasad, P.N. "Highly active two-photon dyes: design, synthesis, and characterization toward application", *Chem. Mater.* **1998**, *10*, 1863. b) Kannan, R.; He, G.S.; Lin, T-C.; Prasad, P.N.; Vaia, R.A.; Tan, L-S. "Toward highly active two-photon absorbing liquids. Synthesis and characterization of 1,3,5-triazine-based octupolar molecules", *Chem. Mater*. **2004**, *16*, 185. c) Baur, J.W.; Alexander Jr., M.D.; Banach, M.; Denny, L.R.; Reinhardt, B.A.; Vaia, R.A.; Fleitz, P.A.; Kirkpatrick, S.M. "Molecular environment effects on two-photon-absorbing heterocyclic chromophores", *Chem. Mater*. **1999**, *11*, 2899.

[36] Cheng, P.C.; Pan, S.J.; Kim, K-S.; Liou, W.S.; Park, M.S. "Highly efficient upconverters for multiphoton fluorescence microscopy", *J. Microsc.* **1998**, *189*, 199.

[37] Abbotto, A.; Beverina, L.; Bozio, R.; Facchetti, A.; Ferrante, C.; Panani, G.A.; Pedron, D.; Signorini, R. "Novel heterocycle-based two-photon absorbing dyes", *Org. Lett.* **2002**, *4*, 1495.

[38] Woo, H.Y.; Hong, J.W.; Liu, B.; Mikhailovsky, A.; Korystov, D.; Bazan, G.C. "Water-soluble [2.2]paracyclophane chromophores with large two-photon action cross sections", *J. Am. Chem. Soc.* **2005**, *123*, 820.

[39] Margineanu, A.; Hofkens, J.; Cotlet, M.; Habuchi, S.; Stefan, A.; Qu, J.; Kohl, C.; Mullen, K.; Vercammen, J.; Engelborghs, Y.; Gensch, T.; De Schryver, F.C. "Photophysics of a water-soluble rylene dye: comparison with other fluorescent molecules for biological applications", *J. Phys. Chem. B* **2004**, *108*, 12242.

[40] Pond, S.J.K.; Tsutsumi, O., Rumi, M.; Kwon, O.; Zojer, E.; Bredas, J-L.; Marder, S.R.; Perry, J.W. "Metal-ion sensing fluorophores with large two-photon absorption cross sections: Aza-crown ether substituted donor-acceptor-donor distyrylbenzenes", *J. Am. Chem. Soc.* **2004**, *126*, 9291.

[41] Kim, H.M.; Jeong, M-Y.; Ahn, H.C.; Jeon, S-J.; Cho, B.R. "Two-photon sensor for metal ions derived from azacrown ether", *J. Org. Chem.* **2004**, *69*, 5749.

[42] a) Miyawaki, A.; Griesbeck, O.; Heim, R.; Tsien, R.Y. "Dynamic and quantitative Ca^{2+} measurements using improved chameleons", *Proc. Nat. Acad. Sci. (USA)*, **1999**, *96*, 2135. b) Adams, S.R.; Lev-Ram, V.; Tsien, R. Y. "A new caged Ca^{2+}, azid-1, is far more photosensitive than nitrobenzyl-based chelators", *Chem. Biol.*, **1997**, *4*, 867.

[43] Taki, M.; Wolford, J.L.; O'Halloran, T.V. "Emission ratiometric imaging of intracellular Zinc: design of a benzoxazole fluorescent sensor and its application in two-photon microscopy", *J. Am. Chem. Soc.* **2004**, *126*, 712.

[44] Chang, C.J.; Nolan, E.M.; Jaworski, J.; Okamoto, K-I.; Hayashi, Y.; Sheng, M.; Lippard, L.J. "ZP8, a neuronal zinc sensor with improved dynamic range; imaging zinc in hippocampal slices with two-photon microscopy", *Inorg. Chem.* **2004**, *43*, 6774.

[45] Charier, S.; Ruel, O.; Baudin, J-B.; Alcor, D.; Alleman, J-F.; Meglio, A.; Jullien, L. An efficient fluorescent probe for ratiometric pH measurements in aqueous solutions", *Angew. Chem. Int. Ed.* **2004**, *43*, 4785.

[46] Werts, M.H.V.; Gmouh, S.; Mongin, O.; Pons, H.; Blanchard-Desce, M. "Strong modulation of two-photon excited fluorescence of quadripolar dyes by (de)protonation", *J. Am. Chem. Soc.* **2004**, *126*, 16294.

[47] Piszczek, G.; Maliwal, B.P.; Gryczynski, I.; Dattelbaum, J.; Lakowicz, J.R. "Multiphoton ligand-enhanced excitation of Lanthanides", *J. Fluoresc.* **2001**, *11*, 101.

[48] Ohulchanskyy, T.Y.; Pudavar, H.E.; Yarmoluk, S.M.; Yashchuk, V.M.; Bergey,E.J.; Prasad, P.N. "A monomethine cyanine dye cyan 40 for two-photon-excited fluorescence detection of nucleic acids and their visualization in live cells", *Photochem. Photobiol.* **2003**, *77*, 138.

[49] a) Meltola, N.J.; Wahlroos, R.; Soini, A.E. "Hydrophilic labeling reagents of dipyrrylmethene-BF2 dyes for two-photon excited fluorometry: syntheses and photophysical characterization", *J. Fluoresc.* **2004**, *14*, 635. b) Meltola, N.J.; Soini, A.E.;

Hanninen, P.E. “Syntheses of novel dipyrrylmethene-BF2 dyes and their performance as labels in two-photon excited fluoroimmunoassay”, *J. Fluoresc.* **2004**, *14*, 129.

[50] a) Albota, M.; Beljonne, D.; Bredas, J-L.; Ehrlich, J.E.; Fu, J-Y.; Heikal, A.A.; Hess, S.E.; Kogej, T.; Levin M.D.; Marder, S.R.; McCord-Maughon, D.; Perry, J.W.; Rockel, H.; Rumi, M.; Subramaniam, G.; Webb, W.W.; Wu, X-L.; Xu, C. “Design of organic molecules with large two-photon absorption cross sections”, *Science,* **1998**, *281,* 1653. b) Rumi, M.; Ehrlich, J.E.; Heikal, A.A.; Perry, J.W.; Barlow, S.; Hu, Z.; McCord-Maughon, D.; Parker, T.C.; Rockel, H.; Thayumanavan, S.; Parder, S.R.; Beijonne, D.; Bredas, J-L. “Structure-property relationships for two-photon absorbing chromophores: Bis-donor diphenylpolyene and bis(styryl)benzene derivatives”, *J. Am. Chem. Soc.* **2000**, *122*, 9500.

[51] Hales, J.M.; Hagan, D.J.; Van Stryland, E.W.; Schafer, K.J.; Morales, A.R.; Belfield, K.D.; Pacher, P.; Kwon, O.; Zojer, E.; Bredas, J-L. “Resonant enhancement of two-photon absorption in substituted fluorene molecules”, *J. Chem. Phys.* **2004**, *121*, 3152.

[52] Katan, C.; Terenziani, F.; Mongin, O.; Werts, M.H.V.; Porres, L.; Pons, T.; Mertz, J.; Tretiak, S.; Blanchard-Desce, M. “Effects of (Multi)branching of dipolar chromophores on photophysical properties and two-photon aborption”, *J. Phys. Chem. A* **2005**, *109*, 3024.

[53] Yao, S.; Belfield, K.D. “Synthesis of two-photon absorbing unsymmetrical branched chromophores through direct tris(bromomethylation) of fluorene”, *J. Org. Chem*. **2005**, *70*, 5126.

[54] Garin, J.; Melendez, E.; Merchan, F.L.; Merino, P.; Orduna, J.; Tejere, T. “Synthesis of unsymmetrical diheteroarylbenzenes: benzazole and quinazoline derivatives,” *J. Hererocyclic Chem.* **1991**, *28*, 359.

[55] Haugland, R.P. In *Methods in Molecular Biology: Monoclonal antibody protocols*, V. 45; chap. 22, Davis, William C. Ed. Humana Press: Totoway New Jersey 1995, pp. 205-214.

[56] Bewley, T.A. "A novel procedure for determining protein concentrations from absorption spectra of enzyme digests," *Anal. Biochem.* **1982**, *123*, 55.

[57] Schafer, K.J.; Belfield, K.D.; Yao, S.; Frederiksen, P.K.; Hales, J.M.; Kolattukudy, P.E., "Fluorene-based fluorescent probes with high two-photon action cross-sections for biological multiphoton imaging applications", *J. Biomed. Opt.* **2005**, in press

[58] Hermanson, G.T. In *Bioconjugate Techniques*, Academic Press: San Diego, 1996.

[59] Kosugi, M.; Koshiba, M.; Atoh, A.; Sano, H.; Migita, T. *Bull. Chem. Soc. Jpn*. **1986**, *59*, 677.

[60] Hark, R.R.; Hauze, D.B.; Petrovskaia, O.; Joullie, M.M.; Jaouhari, R..; McComiskey, P. *Tet. Lett.* **1994**, *35*, 7719.

[61] Fletcher, T.L.; Taylor, M.E.; Dahl, A.W. "Derivatives of fluorene. I. N-Substituted 2-aminofluorene and 2-aminofluorenone", *J. Org. Chem.* **1955**, *20*, 1021-1025.

[62] Moeini-Nombel,L.; Matsuzawa, S. "Effect of solvents and a substituent group on photooxidation of fluorene**",** *J. Photochem. Photobiol. A: Chem.* **1998**, *119*, 15.

[63] Barbas, J.T.; Sigman, M.E.; Arce, R.; Dabestani, R.J. "Spectroscopy and photochemistry of fluorene at a silica gel/air interface", *J. Photochem. Photobiol. A: Chem*. **1997**, *109,* 229.

[64] Wood, P.D.; Johnston, L.J. "Photoionization and Photosensitized Electron-Transfer Reactions of Psoralens and Coumarins", *J. Phys. Chem. A* **1998**, *102*, 5585.

[65] Kao, F-J.; Wang, Y-M.; Chen, J-C.; Cheng, P-C.; Chen, R-W.; Lin, B-L. "Photobleaching under single photon and multi-photon excitation: chloroplasts in protoplasts from Arabidopsis", *Opt. Commun*. **2002**, *201*, 85.

[66] Belfield, K.D.; Bondar, M.V.; Morales, A.R.; Yavuz, O.; Przhonska, O.V. "A new blue light-emitting oligofluorene glass: Synthesis, characterization and photophysical properties", *J. Phys. Org. Chem.,* **2003**, *16*.

[67] Belfield, K.D.; Bondar, M.V.; Liu, Y.; Przhonska, O.V. "Photophysical and photochemical properties of 5,7-dimethoxycoumarin under one- and two-photon excitation", *J. Phys. Org. Chem*., **2003**, *16*, 69.

[68] Bacallao, R. and Stelzer, E.H.K. "Preservation of biological specimens for observation in a confocal fluorescence microscope and operational principles of confocal fluorescence microscopy", *Meth. Cell Biol.* 31 (Vesicular Transp., Pt. A), 437-52 (1989).

[69] a) O'Brien, J.; Wilson, I.; Orton, T.; Pognan, F. "Investigation of the Alamar Blue (resazurin) fluorescent dye for the assessment of mammalian cell cytotoxicity", *Eur. J. Biochem*. **2000**, *267*, 5421. b) Erb, R.E.; and Ehlers, M.H. "Resazurin reducing time as an indicator of bovine semen fertilizing capacity", *J. Dairy Sci.* **1950**, *12*, 853.